POLITECNICO DI TORINO

Collegio di Ingegneria Chimica e dei Materiali

Corso di Laurea Magistrale
in Ingegneria Chimica e dei Processi Sostenibili

Tesi di Laurea Magistrale

Natural zeolites for energy-related applications

Relatore/i

prof. Marco Piumetti
prof. Samir Bensaid
prof.ssa Debora Fino

Candidato

Bianca Ziantoni

28 Novembre 2023

Riassunto in italiano

Una delle principali cause del surriscaldamento globale può essere attribuita all'effetto serra, dovuto all'incremento di concentrazione di anidride carbonica in atmosfera. Questa deriva principalmente dalla combustione dei tradizionali combustibili fossili, la più importante fonte energetica al livello mondiale. Per ovviare a questo problema negli ultimi anni si sta investendo molto sulla ricerca sia per la produzione di energia da fonti rinnovabili sia per il recupero energetico da processi industriali. Inoltre, bisogna sottolineare che circa il 50 % della domanda energetica europea è per sistemi di riscaldamento e/o raffreddamento, il 35 % della quale è destinata al settore domestico per scaldare acqua e ambienti. Dunque, occorre focalizzarsi su una produzione di energia termica più sostenibile. Tuttavia, tra le varie fonti di energia, quella termica risulta difficile da stoccare nel lungo termine, per via delle numerose perdite di calore che generalmente si registrano, e la sua conversione in lavoro utile non è né banale né economicamente vantaggiosa. Per poter sfruttare al meglio anche questo tipo di energia, sono stati condotti numerosi studi volti alla ricerca di materiali alternativi che potessero garantire lo stoccaggio a lungo termine di energia termica di origine solare oppure proveniente dai gas di scarico industriali. In questo contesto si collocano le zeoliti, accattivanti perché in grado di stoccare e rilasciare energia termica mediante cicli di idratazione e disidratazione. Le zeoliti, anche conosciute come setacci molecolari, sono una famiglia di alluminosilicati microporosi, la cui struttura base è costituita dalla ripetizione di unità tetraedriche di tipo TO_4 (dove T indica la presenza di un atomo di silicio o alluminio). Molto importante nelle zeoliti è il rapporto Si/Al. Infatti, mentre un alto quantitativo di silicio garantisce un'elevata stabilità termica, l'alluminio invece influenza il carattere idrofilo del materiale. Un alto rapporto Si/Al dunque indica la presenza di una zeolite stabile termicamente ma tendenzialmente idrofoba.

Grazie alle loro numerose proprietà , tra cui l'elevata stabilità termica, l'alta igroscopicità ,selettività e capacità di scambio ionico questi alluminosilicati trovano largo impiego in numerose applicazioni , dalla catalisi al trattamento delle acque reflue , dalla bonifica di terreni agricoli all'impiego come additivi nei mangimi , fino ad essere adoperate in settori non convenzionali come quello medico (dove sono sfruttate per le, loro proprietà disintossicanti, antinfiammatorie e antiossidanti), negli imballaggi alimentari o ancora nel drug delivery. Tra i campi di applicazione non tradizionali rientra l'utilizzo delle zeoliti nei sistemi TES (Thermal Energy Storage) per l'accumulo e il successivo rilascio di energia termica. Ciò è possibile grazie alla capacità delle zeoliti di adsorbire e desorbire ciclicamente acqua. Più precisamente, l'adsorbimento di vapor d'acqua comporta il rilascio del calore necessario per rompere il legame debole con la molecola d'acqua, lo stesso che poi dovrà essere fornito per la disidratazione. In questa tesi è stato analizzato il ruolo della Clinoptilolite per stoccaggio e rilascio di energia termica. Si tratta di una zeolite naturale appartenente al gruppo delle heulanditi (HEU), avente una struttura monoclina con tre diversi canali (A, B, C), delimitati da anelli a 8 (canale A e C) o 10 atomi (canale B). A differenza dell'heulandite, la clinoptilolite risulta avere un rapporto Si/Al >4 e dunque non si degrada a temperature elevate. Dal momento che, come precedentemente accennato, il processo di carica (desorbimento) e scarica (adsorbimento) del materiale si basa su una fase di idratazione e una di disidratazione, ci si è focalizzati sull'analisi dell'affinità della clinoptilolite con acqua. L'obiettivo di questa tesi è stato dimostrare la fattibilità dell'impiego di una zeolite naturale per questo scopo energetico, in sostituzione della più comunemente usata zeolite sintetica 13 X.A titolo di esempio può essere citato il sistema ibrido di riscaldamento termico (pompa di calore), dotato di caldaia a zeolite (la zeolite adoperata è appunto la 13X) disegnato e commercializzato dalla Zeotherm.

La clinoptilolite è largamente disponibile al livello globale, non è nociva per l'uomo, non è inquinante ma soprattutto è molto più economica rispetto alla 13 X, il cui processo di sintesi è dispendioso al livello energetico ed economico. Dai dati presenti in letteratura si evince infatti che il costo della clinoptilolite (200€/ton) è di un ordine di grandezza inferiore rispetto a quello della 13 X(2000€/ton)

Siccome è noto in letteratura che, per incrementare la capacità di adsorbimento di acqua della clinoptilolite, la si può funzionalizzare mediante scambio ionico con cationi di diversa dimensione e raggio ionico, in fase sperimentale questa zeolite è stata studiata sia nella sua forma originale (senza funzionalizzazioni) sia nella forma modificata con sodio mediante scambio ionico. Questo confronto è stato fatto proprio perché il contenuto di acqua dipende da vari fattori, tra cui la natura e la dimensione dei cationi nella struttura, dimensione e forma dei canali, condizioni operative quali temperatura, pressione e umidità. Infatti, mentre nella zeolite non funzionalizzata le molecole d'acqua presenti tendono a legare tra loro piuttosto che a legarsi alla superficie zeolitica, favorendo così la formazione di clusters di acqua , la presenza di cationi esterni dovrebbe facilitare il legame tra molecole d'acqua alla superficie dell'adsorbente dal momento che il catione prima attrae la molecola d'acqua (polare) grazie alla presenza di un campo elettrico a lungo raggio, successivamente con essa forma un legame ed infine le molecole d'acqua subiscono un riarrangiamento che permette loro di muoversi verso l'interfaccia catione-framework, massimizzando così l'interazione fisica con la zeolite.

Dunque, durante le attività sperimentali, lo scambio ionico è stato effettuato seguendo due diverse procedure, una avente NaCl come precursore (da cui si è ottenuto il campione Na-Clino1) e una basata invece sull'impiego di $NaNO_3$ come precursore (da qui il campione Na-Clino2).Questa seconda procedura è stata testata in quanto prevedeva un pretrattamento con allo scopo di incrementare la presenza di ioni ammonio i quali, secondo quanto riportato in letteratura, comportano un maggior scambio ionico e dunque un maggior quantitativo di sodio.

Alla fine della fase di sintesi sono stati ottenuti 4 campioni: la clinoptilolite naturale (anche detta Clino T.Q, *talis et qualis*), Na-Clino1, Na-Clino2 e la 13X, usata come campione di riferimento. Successivamente sono state effettuate una serie di caratterizzazioni fisico-chimiche, quali fisisorbimento con azoto a -196°C per valutare l'area superficiale e la dimensione dei pori, un'analisi di Diffrazione ai raggi X (XRD) per lo studio della struttura cristallina, un'analisi EDX (energy-dispersive x-ray) per valutare la composizione elementare dei campioni. Per quanto riguarda il fisisorbimento con N_2 a -196°C è stato trovato un riscontro con quanto già presente in letteratura. Infatti, i campioni di zeolite naturale (Clino T.Q, Na-Clino1 e Na-Clino2) per quanto riguarda l'isoterma di adsorbimento, presentano un loop di isteresi di tipo H3, secondo la classificazione IUPAC, tipica dei materiali porosi. Analizzando inoltre i valori di area superficiale specifica (SSA) e il diametro dei pori si è potuto osservare che, anche se le zeoliti rientrano nella categoria di materiali microporosi, presentano un diametro dei pori nel range dei mesopori (2-50 nm). Le isoterme di adsorbimento sono riportate nel seguente grafico:

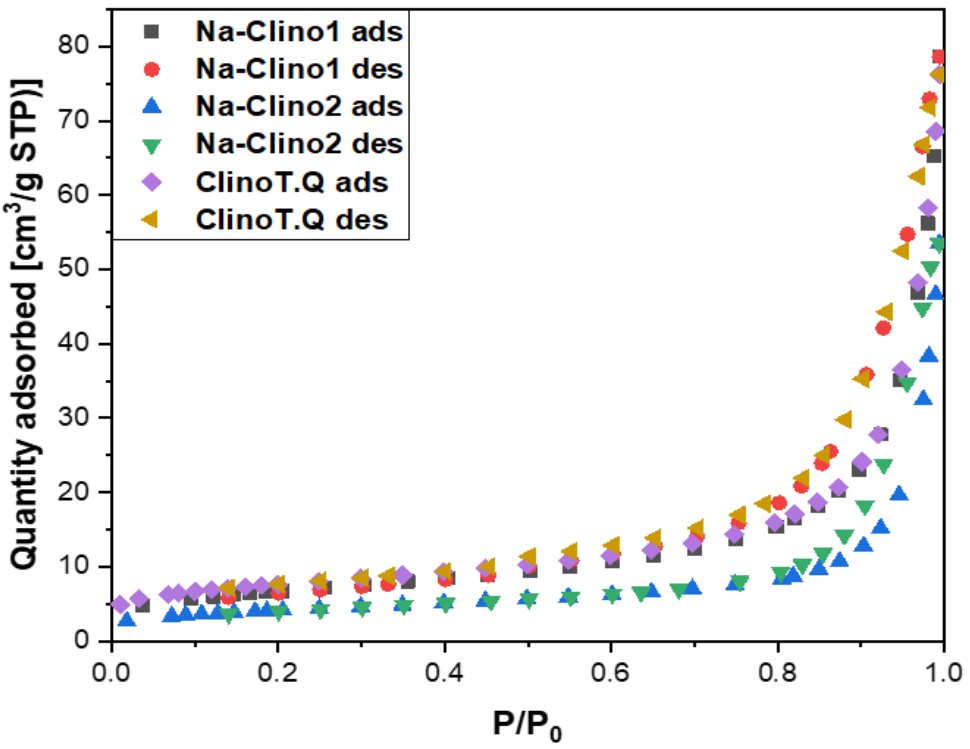

Figura I: isoterme di adsorbimento dei campioni Clino T.Q; Na-Clino1 e Na-Clino2

Anche i risultati dell'analisi XRD sono stati indicizzati mediante il software Highscore Plus hanno trovato un ulteriore riscontro nei codici identificativi di riferimento (ref code) riportati in letteratura e, per quanto riguarda i campioni Na-Clino1 e Na-Clino2, i diffrattogrammi ottenuti hanno confermato la corretta esecuzione dello scambio ionico.

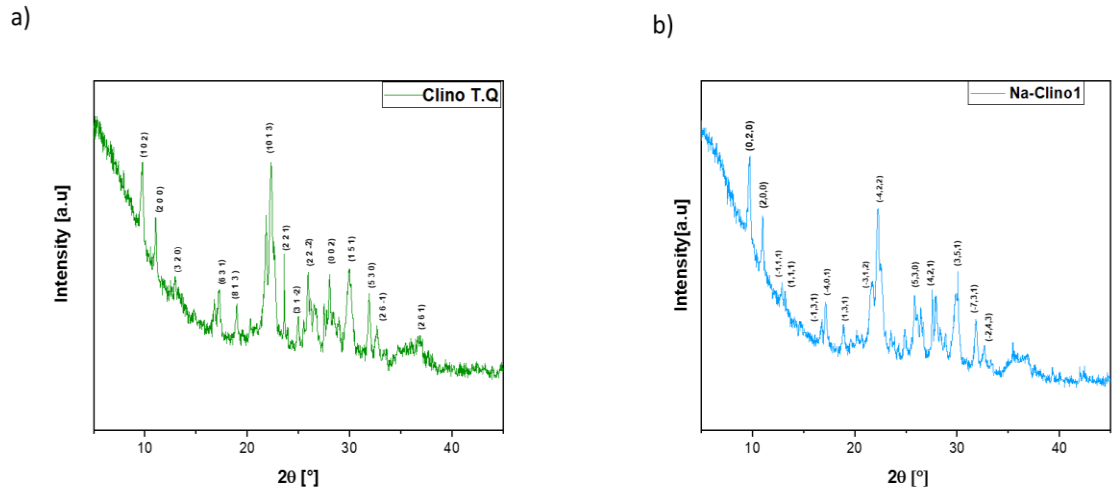

Figura II: Diffrattogrammi dall'analisi XRD per i campioni:a) Clino T.Q (Ref. Code 00-139-1383), b) Na-Clino1(Ref.Code 96-900-1393)

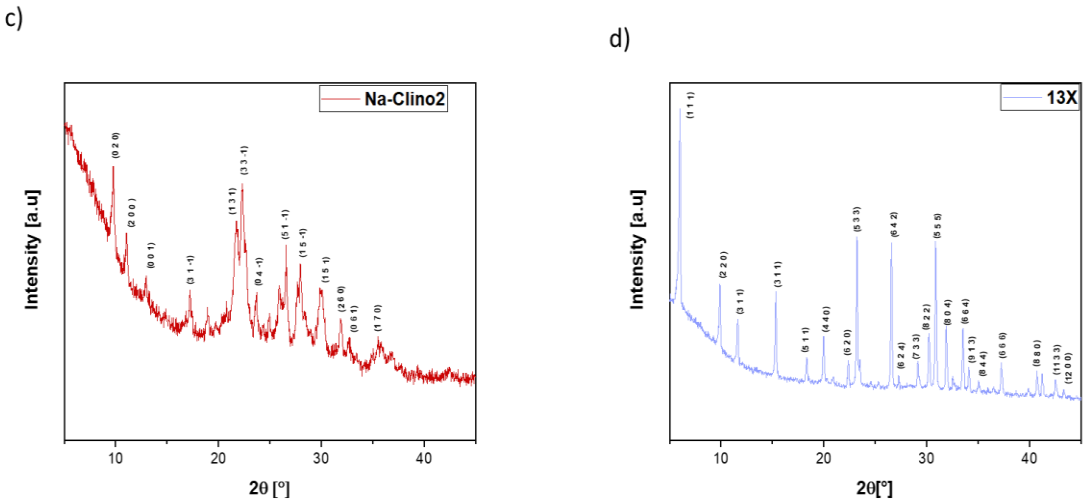

Figura III: Diffrattogrammi dall'analisi XRD per i campioni: c) Na-Clino2 (Ref. Code 96-900-1393), d)13X (Ref Code 00-100-8756)

È stata inoltre effettuata un'analisi XRD in operando per verificare eventuali cambiamenti della struttura zeolitica a seguito di riscaldamento ad alta temperatura. Dal momento che la stabilità termica del materiale dipende principalmente dal rapporto Si/Al il quale rimane invariato a seguito dello scambio ionico, come dimostrato dall'analisi EDX effettuata in parallelo, la misura XRD in operando è stata effettuata sul campione di Clino T.Q e su quello di 13X per confronto. I risultati hanno dimostrato come fino a 400°C la struttura zeolitica rimanga praticamente inalterata dal momento che non è stata riscontrata la scomparsa di alcun picco. Dopo i 400°C, aumentando la temperatura, si assiste a lievi scostamenti e /o diminuzioni di intensità di alcuni picchi, dovuti a leggere modifiche della struttura cristallina. Complessivamente, dunque, sia la zeolite naturale che quella sintetica hanno dimostrato una buona stabilità termica e a seguito di questa analisi è stata scelta la temperatura di pretrattamento di 400°C usata poi nei test di adsorbimento in impianto con azoto umido.

Dall'EDX è stato appreso che il contenuto di sodio nel campione Na-Clino2 (6.6% wt) è il doppio di quello nell'Na-Clino1(3,3% wt) ed è sei volte quello della Clino T.Q (0.7%wt). Invece il contenuto di silicio e quello di alluminio è rimasto praticamente invariato, così come la percentuale di ossigeno. Invece la quantità di calcio è passata diminuita passando dall1.7 wt% nella clinoT.Q allo 0.4 wt% e 0.5 wt% nei campioni Na-Clino1 e Na-Clino2, rispettivamente.

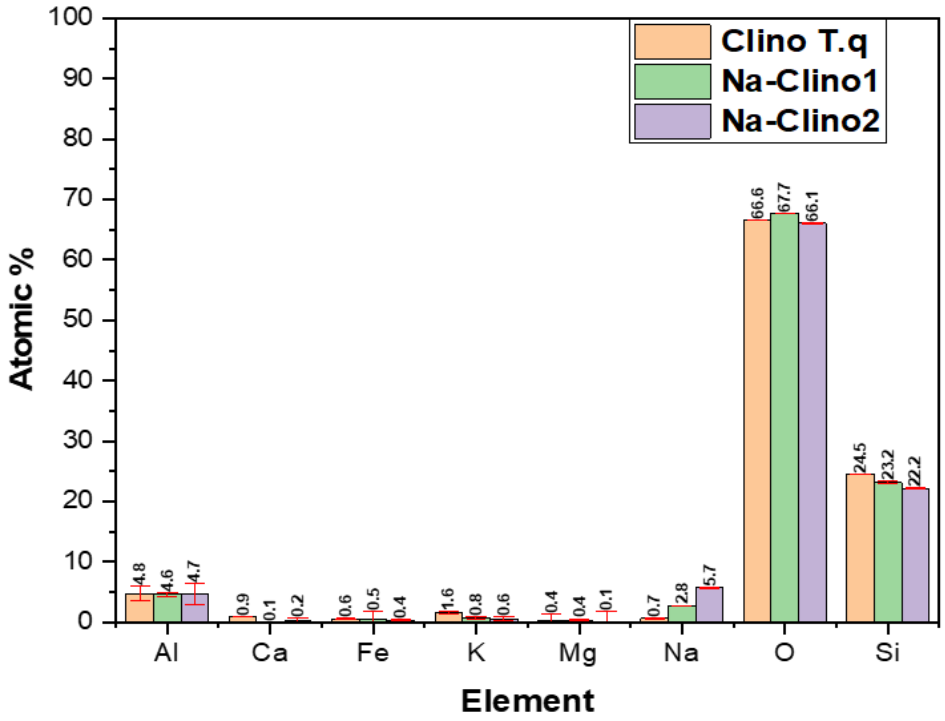

Figura IV: risultati dell'analisi EDX

In aggiunta a ciò, per comprendere fino a fondo la distribuzione dei vari elementi costituenti sulla superficie dei tre campioni in esame, è stata fatta una mappa EDX degli stessi, dalla quale è risultato che ciascun componente (incluso il sodio aggiunto mediante scambio ionico in Na-Clino1 e Na-Clino2) risulta omogeneamente disperso al livello superficiale.

È stata poi condotta un'analisi termogravimetrica (TGA) per valutare la percentuale di acqua persa da ciascun campione durante la disidratazione e un'analisi calorimetrica (DSC = Differential Scanning Calorimetry), prima con i campioni asciutti per valutare il calore specifico(cp), poi con gli stessi campioni in condizione di saturazione per stimare l'entalpia di desorbimento(ΔH). Mentre per la DSC il range di temperatura investigato è stato tra i 50°C e i 350°C, per quanto riguarda la TGA è stata studiata la perdita di acqua da parte di ogni campione in un range termico più esteso, tra i 25°C e i 700°C. Ciò è stato fatto perché è noto da letteratura che esistono tre tipologie di acqua desorbita, a seconda dell'intervallo di temperatura osservato. Più precisamente mentre a basse temperature (tra i 50°C e i 150°C) si perde l'acqua debolmente fisisorbita sulla superficie zeolitica (weekly bond water),, tra i 150°C e i 250°C si perde invece l'acqua presente all'interno delle cavità zeolitiche e quella legata ai cationi extraframework e infine tra a partire dai 450°C si perde la cosiddetta acqua di struttura, con conseguente distruzione del framework zeolitico. Dalla TGA è stato riscontrato che quantità di acqua persa durante il riscaldamento varia nei campioni nel seguente ordine decrescente: 13X>ClinoT.Q>Na-Clino1>Na-Clino2. Tramite la derivata prima della curva relativa alla TGA è stata ottenuta la curva DTG che ha permesso di comprendere la tipologia di acqua persa in ciasun campione. Infatti dalla curva DTG relativa alla Clino T.Q si nota un picco tra i 25°C e i 150°C in cui viene registrata una perdita di acqua del campione del 9%, in per la Na-Clino1 tale picco appare spostato tra i 25°C e i 225°C e viene invece riscontrata una perdita di acqua dell'8%. Per quanto riguarda invece il campione Na-Clino 2 si ha una perdita di acqua inferiore (circa il 4%) tra i 25°C e i 175°C. Infine, la 13X perde circa il 20% di acqua in un range termico

compreso tra i 25°C e i 300°C. Dall'analisi, tuttavia, non è risultata una perdita di acqua di struttura fino a 700°C, ulteriore prova della stabilità termica di tutti i campioni analizzati. La quantità di acqua adsorbita/ desorbita da ciascun campione e quantificata dalla TGA ha permesso in un secondo momento di effettuare i bilanci energetici.

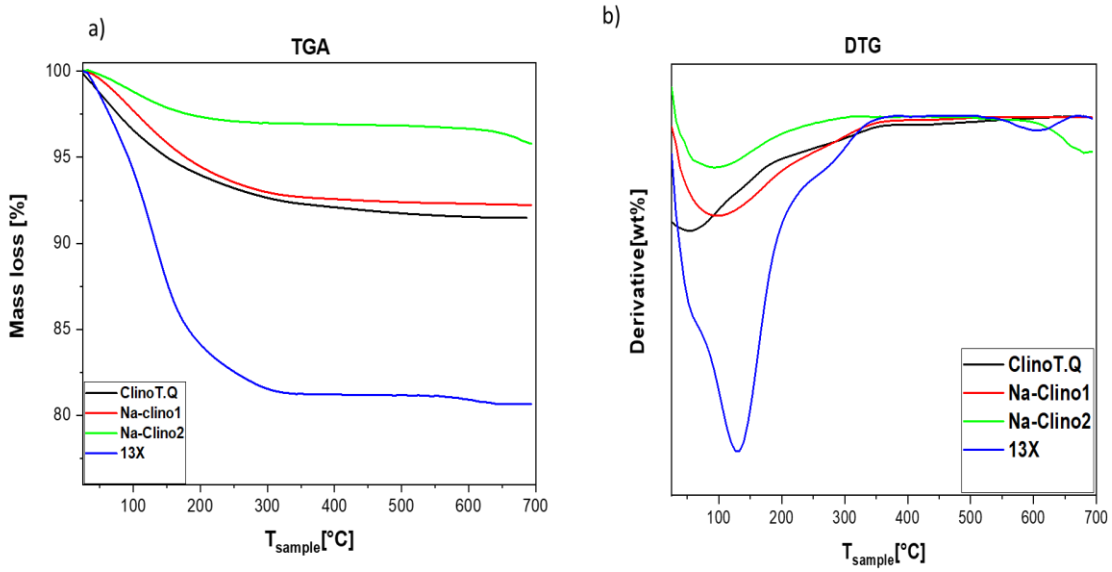

Figura V: curva a) TGA e b) DTG relativa ai campioni analizzati

I grafici relativi alla DSC trovano un riscontro nei risultati ottenuti dalla TGA/DTG e mostrano per tutti i campioni un picco endotermico tra i 41 e i 232 °C (con eccezione per la 13X il cui picco varia tra i 39 e i 229°C), corrispondente all'eliminazione dell'acqua fisicamente adsorbita alla zeolite, secondo quanto precedentemente affermato. Valori crescenti di entalpia sono stati registrati nell'ordine Na-Clino2 <Na-Clino1 <ClinoT.Q<13X.Per quanto riguarda invece il calore specifico, questo assume valori crescenti nell'ordine 13X<ClinoT.Q<Na-Clino2<Na-Clino1. Possiamo notare un andamento decrescente del in funzione della temperatura fino a T=125°C, probabilmente dovuto al desorbimento dell'acqua debolmente legata.

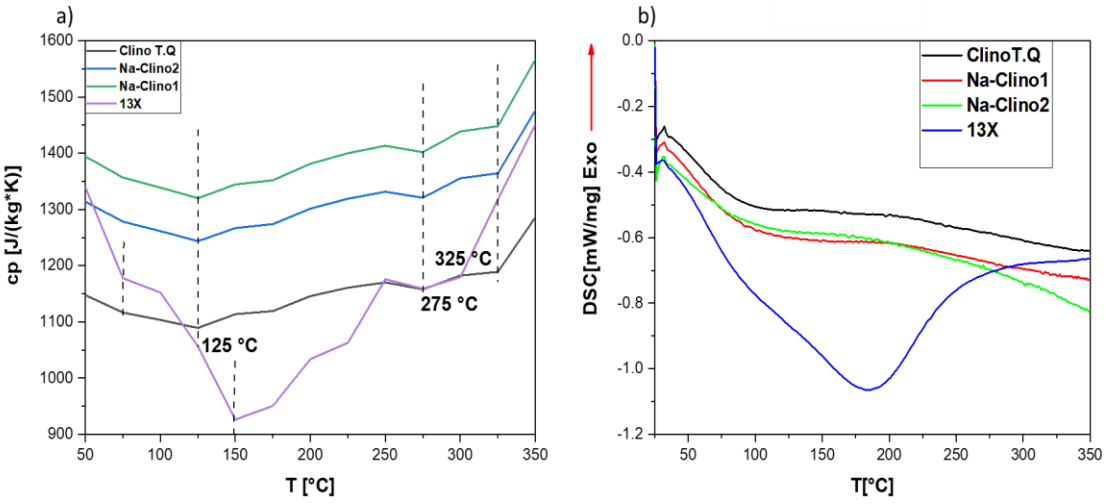

Figura VI: risultati della DSC a) per il calore specifico (cp) e b) per l'entalpia

In aggiunta a ciò, è stata sfruttata la spettroscopia a infrarossi FT(Fourier-Trasform) -IR (infrared) per studiare l'affinità con acqua mediante invii di acqua a pressioni parziali crescenti, seguiti da espansioni graduali. Gli spettri acquisiti hanno rilevato un incremento di intensità dei picchi sia nella banda tra i 3750 cm^{-1} e i 3100 cm^{-1}(relativa allo stretching dei gruppi -OH) sia in quella relativa al bending dei gruppi -OH, caratterizzata da un picco a 1630 cm^{-1} relativo alla deformazione vibrazionale dell'acqua adsorbita. Analizzando l'intensità di questo ultimo picco in funzione della pressione di equilibrio per i tre campioni di zeolite naturale. è stata riscontrata a basse pressioni un'affinità migliore verso l'acqua per quanto riguarda la Clino T.Q mentre andando a medie pressioni è possibile notare l'effetto dello scambio ionico sull'adsorbimento di acqua, in quanto l'intensità del picco risulta essere maggiore per il campione Na-Clino1 rispetto alla clinoptilolite naturale. Questo comportamento viene spiegato in letteratura considerando la cinetica del processo di adsorbimento da parte di una zeolite funzionalizzata mediante scambio ionico. È noto, infatti, che tale processo consta di due fasi caratterizzate da due cinetiche differenti. Più precisamente, durante il primo step, cineticamente lento, il catione extra-framework legato alla superficie zeolitica crea un campo elettrico che attrae le molecole d'acqua polari e ad esse si lega. Segue il secondo step, cineticamente più veloce, in cui si assiste a un riarrangiamento strutturale delle molecole d'acqua in modo tale che queste siano il più possibile fisicamente a contatto con la superficie della zeolite. In questo modo l'affinità, intesa come capacità di adsorbimento delle molecole d'acqua, risulta maggiore. A fronte di questa spiegazione è possibile dedurre che a basse pressioni prevale il primo step e dunque Na-Clino1 mostra performance peggiori. Tuttavia, aumentando ulteriormente la pressione è stato notato che la Clino T.Q torna ad avere una maggiore affinità e per spiegare questo comportamento è stato ipotizzato un effetto inibente da parte dei cationi di sodio ad elevate pressioni. Inoltre, dai risultati sperimentali appare anche chiaro che è importante la modulazione della quantità di cationi extra-framework presenti sulla superficie dal momento che il loro eccesso potrebbe comportare un minor adsorbimento di acqua per via di un effetto inibente. Infatti, l'Na-Clino 2 non solo ha mostrato un'affinità peggiore ma è stato l'unico campione per cui il desorbimento di acqua è avvenuto per semplice espansione (negli altri casi invece è stata dimostrata la necessità di desorbire mediante trattamento termico). Complessivamente, il confronto riguardo l'affinità con l'acqua (espressa in termini di intensità del picco nella regione -OH bending in funzione della pressione di linea) per i diversi campioni è riportato nella figura sottostante.

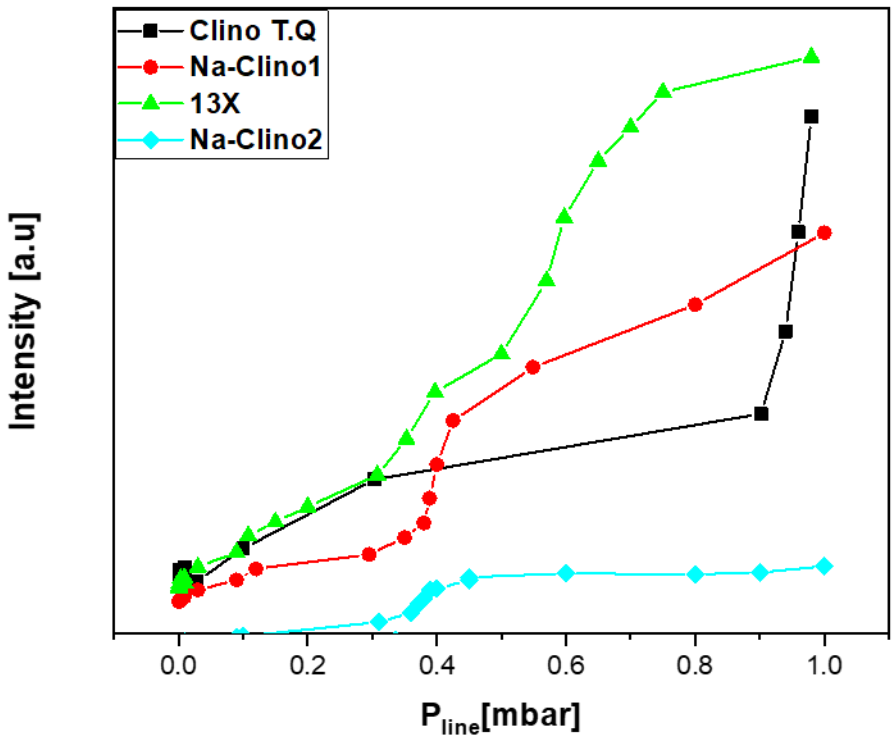

Figura VII: Intensità dei picchi nella regione -OH bending (1631-1650 cm^{-1}) in funzione della pressione di linea.

Infine, si deve aggiungere che, rispetto agli altri due campioni scambiati con sodio, per la clinoT.Q sono state osservate performance migliori anche nei test di adsorbimento in impianto, atti a simulare il processo di scarica di una zeolite nei sistemi STES. Questi test sono stati effettuati a pressione atmosferica, inviando in un reattore ad U una corrente di azoto al 10% di umidità relativa (RH=10%). Nel reattore di vetro, del diametro di 4 mm, riscaldato da un forno a 50°C, è stato inserito un supporto in lana di quarzo su cui è stato successivamente posto il letto catalitico, di altezza variabile a seconda della quantità e della tipologia di campione testato. A contatto il letto è stata posta una termocoppia, per rilevare l'incremento di temperatura a seguito del riscaldamento. Più precisamente la corrente umida all'interno del reattore entra in contatto con il letto di zeolite su cui avviene il processo esotermico di adsorbimento, esce dal reattore ed infine, prima di giungere all'analizzatore passa attraverso un drexel posto in uscita su cui avviene la condensazione della quota parte di umidità residua. Sono stati eseguiti 4 test, uno per ciascun campione a disposizione, e in tutti i casi le prove sono state effettuate a parità di massa (500 mg di pellet di dimensione compresa tra i 212 µm e i 250 µm) per comprendere meglio l'influenza della temperatura di trattamento (50°C in tutti i casi) e dell'altezza del letto catalitico.

Prima di eseguire il test di adsorbimento a 50°C, tutti i campioni testati sono stati pretrattati con una corrente costituita da 100 ml/min di N_2(in condizioni dry) a 400°C per 1h. Lo scopo del pretrattamento è stato infatti quello di simulare la fase di carica della zeolite nel sistema STES, in cui tutta l'acqua presente (tranne quella di struttura) viene desorbita. I risultati di questo test hanno mostrato un incremento di temperatura di 9°C nella Clino T.Q, paragonabile a quello di 10°C ottenuto con la 13 X, valore maggiore rispetto a quello di Na-Clino 1(ΔT=7.5°C) e di Na-Clino2(ΔT=1°C).

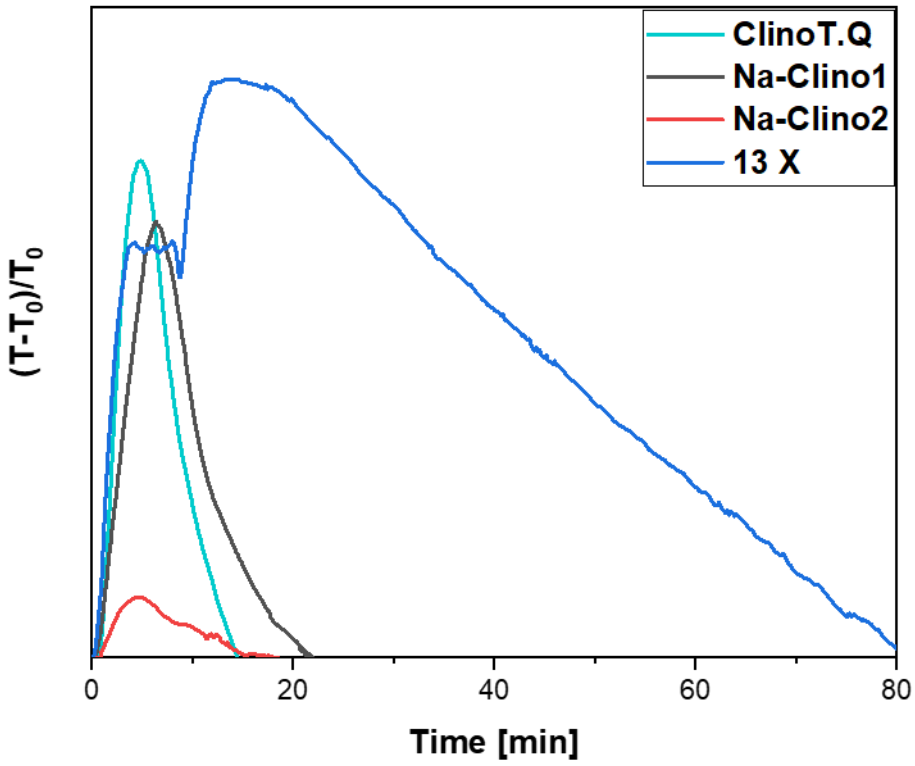

Figura VIII: confronto tra i ΔT di ciascun campione ottenuti nei test di adsorbimento di azoto umido.

Occorre però sottolineare che si tratta di un'indagine condotta a basse pressioni, in cui potrebbe dunque non essere apprezzabile l'effetto benefico del sodio. Una differenza sostanziale tra la Clino T.Q e la 13X risiede sicuramente nella cinetica del processo: mentre infatti la clino T.Q mostra il ΔT sopra citato in circa 15 minuti, dopodiché torna alla sua temperatura iniziale di 50°C, la durata del test con la 13 X invece è di circa 80 minuti : Ciò viene spiegato in letteratura con la maggior capacità di adsorbimento da parte della zeolite commerciale in questione, la quale impiega più tempo perché adsorbe un maggior quantitativo di acqua, Inoltre l'adsorbimento di acqua sulla 13 X viene realizzato in due step, a seconda del tipo di pori che vengono coinvolti nel processo di adsorbimento e complessivamente si rileva un miglior mantenimento dell'alta temperature. Quindi sono state effettuate delle prove di ottimizzazione sul campione più performante tra quelli naturali, ossia la Clino T.Q, per vedere se si potesse apprezzare un maggiore incremento di temperatura variando la massa (e dunque l'altezza del letto), la temperatura di test o la forma di catalizzatore e lasciando invariata la corrente in ingresso di azoto e il tipo di pretrattamento. Più precisamente si è provato dapprima a ridurre la massa di catalizzatore effettuando delle prove con 100 mg di pellets (anziché 500 mg) con un test a 50°C, per vedere se la massa di catalizzatore e dunque l'altezza del letto, potesse dare origine a dei cammini preferenziali e dunque a delle perdite di carico. Tuttavia, si è potuto apprezzare soltanto un ΔT di 5°C. Successivamente è stata effettuata una prova lasciando invariata la quantità di Clino T.Q (500 mg) ma abbassando la temperatura di test da 50 a 30°C, per favorire in tal maniera la natura esotermica del processo di adsorbimento. Tuttavia, anche in questo caso è stato rilevato un ΔT di soli 5°C. Per dimostrare infine come un incremento della temperatura di test andasse a scapito del processo di adsorbimento sono stati effettuati due ulteriori test (sempre con 500 mg di campione) a 100°C e 150°C rispettivamente. Come

previsto, l'incrementi di temperatura è stato minimo a 100°C (ΔT=3°C) e non significicativo a 150°C. Infine è stato effettuato un test con 100 mg di Clinoptilolite in polvere e non in pellet e anche in questo caso non è stato possibile ottimizzare il processo. Dunque, è stato appurato che i risultati ottenuti sono quelli con 500 mg di pellets ad una temperatura di test a 50°C.

La parte finale della tesi è stata invece incentrata sull'analisi e valutazione dei Key Performance Indicators o KPIs, ossia quei parametri che consentono di valutare e confrontare l'efficienza di materiali diversi tenendo conto sia dei costi che delle performance al livello energetico. Tra i KPIs più importanti per questo studio rientrano sicuramente la capacità di stoccaggio energetico (ESC) ossia la capacità di stoccaggio per unità di massa, la densità di stoccaggio energetica (ESD) ovvero la capacità di stoccaggio energetico per unità di volume, la temperatura di carica della zeolite, il costo e la durabilità del materiale. Per quanto riguarda la temperatura di attivazione della zeolite, siccome i sistemi TES per applicazioni domestiche normalmente sono collegati a collettori solari che forniscono il calore necessario ai cicli di carica/scarica, servirebbero zeoliti con temperatura di attivazione al di sotto dei 160°C e dunque, solo le zeoliti commerciali (13 X) risulterebbero adatte a questo scopo. Le zeoliti naturali hanno una temperatura di attivazione intorno ai 350°C (per questo motivo nei test spettroscopici FT-IR così come in quelli di adsorbimento è stata scelta una temperatura di pretrattamento di 400°C) e dunque si prestano ad essere utilizzare in sistemi TES che sfruttano i gas di scarico industriali, uscenti dagli impianti a temperature elevate. Per quanto riguarda il costo invece, come già precedentemente accennato, le zeoliti naturali risultano essere più vantaggiose di quelle sintetiche. Infine, ci si è focalizzati sul calcolo della ESD a partire dalla densità energetica (ED) ipotizzando un sistema adiabatico e e sfruttando le seguenti formule:

$$E = \sum_i m_i cp_i \, \Delta T \quad \text{(I)}$$

$$ED = \frac{E}{m_{sample} / \rho_{sample}} \quad \text{(II)}$$

$$ESD = \frac{41kJ/mol}{18} \cdot \rho + ED \quad \text{(III)}$$

In cui con m [kg] si indica la massa di tutti i componenti presenti nel sistema (nel nostro caso acqua e zeolite in esame), ciascuno dei quali viene moltiplicato per il proprio calore specifico e infine il ΔT[K] è rappresenta l'incremento di temperatura osservato durante i test di adsorbimento con la corrente di azoto umida (RH=10%). Occorre sottolineare che la massa d'acqua è stata stimata mediante la TGA, anche se per una misura più rigorosa sono necessarie misure in camera climatica, in cui la perdita di acqua viene relazionata anche alla variazione di umidità, il cp [J/K/Kg] della zeolite è stato calcolato invece mediante DSC, con ρ[Kg/m^3] si intende invece la densità volumetrica del letto catalitico e il valore 41kI/mol fa riferimento all'entalpia di vaporizzazione del vapor d'acqua Una volta valutata l'ESD si può ricavare l'ESC [kJ/kg] attraverso la seguente relazione:

$$ESC = ESD/\rho \quad \text{(IV)}$$

In cui ρ rappresenta la densità volumetrica[kg/m^3] del letto catalitico preso in esame.

Infine, è possibile calcolare la SCC, il KPI chiave che ha reso possibile un confronto complessivo tra i vari campioni presi in esame

$$SCC = \frac{€/tonn}{ESC \cdot 1000} \cdot 3600 \quad \text{(V)}$$

I risultati ottenuti dai bilanci hanno evidenziato valori di SCC crescenti nell'ordine ClinoT.Q <Na-Clino1<Na-Clino2<13X, sottolineando ancora una volta come la Clinoptilolite possa

essere una valida alternativa alla commerciale 13 X in quanto il costo per kWh risulta nettamente inferiore (13-20 €/kwh) rispetto a quello della 13X(111-167 €/kwh)

In conclusione, analizzando complessivamente tutti i risultati ottenuti dalle prove sperimentali, si può affermare che lo scambio ionico con sodio si è rivelato efficace nel caso del campione Na-Clino1 per quanto concerne l'incremento dell'affinità con l'acqua a medie pressioni, come ha dimostrato l'analisi FT-IR. Tuttavia, a basse e alte pressioni la ClinoT.Q si è rivelato essere il campione migliore tra quelli naturali. In definitiva, la funzionalizzazione mediante scambio ionico non ha rivelato un miglioramento apprezzabile dell'efficienza del materiale , Infine, le scarse performance di Na-Clino 2 possono essere spiegate ipotizzando un effetto inibente del sodio, presente in quantità eccessiva all'interno della struttura zeolitica .Dunque, dal momento che la clinoptilolite in forma "originale" è largamente disponibile in natura, è economica, non pericolosa e può essere utilizzata tal quale, senza lunghi processi di funzionalizzazione (la sintesi del campione Na-Clino 2 ha richiesto circa 2 settimane e quella dell'Na-Clino 1 3 giorni) e ha mostrato una performance complessiva inferiore ma comunque paragonabile a quella della zeolite commerciale, può essere considerata una valida alternativa alla 13 X nei sistemi TES. Ulteriori studi, tuttavia, risultano necessari per poterne ottimizzare l'efficienza in modo tale da poterla sfruttare su larga scala.

Index

Πάθει μάθος
(Eschilo, Agamennone)

1. Introduction

One of the major causes of global warming is the increase of carbon dioxide (CO_2) emissions which is considered the most important greenhouse gas. It is released in the atmosphere from human activities, as a product from the combustion of traditional fossil fuels, even though it can also derive from intensive livestock breeding or agriculture. It is well known that fossil fuels are recognized as the main source of energy for the planet. In this regard it should be emphasized that half of the European energy demand is destined to the heating and cooling sector. Furthermore, 35% of this percentage is necessary for the domestic sector, to heat water and spaces but also to cook and to cool spaces. The other half of European energy demand is usually required by industries and /or other services (Davidson and Monteleone, 2022; de Gennaro *et al.*, 2022a; Aghemo *et al.*, 2023) .In addition all the environmental problems linked to the use of fossil fuels, there are also economic problems related to the frequent price fluctuations, depending on the geopolitical situation of the market seller country , as well as the health problems regarding the correlation between fossil fuels' emissions and the increase of health diseases (i.e tumors) and the incidence of mortality.

To overcome this problem a lot of money have been invested to find alternative ways to produce and store thermal energy in a more sustainable way which could involve the exploitation of renewable sources. Among all types of energy, thermal one is quite challenging to store in the long term because of the huge amount of thermal losses associated, not to mention that it results challenging to convert into useful work because of the cost effectiveness and feasibility of the process. Consequently, in these last decades a lot of research has been conducted to realize a transition from conventional fossil fuels to renewable sources. As long as thermal energy production is concerned, the main renewable source investigated was the solar one. As a drawback, the main disadvantage of using solar collectors relies in its strong dependence on the seasons. In other words, thermal energy from solar collectors is fully available only if the driven heating system is equipped with an efficient seasonal storage(Jänchen *et al.*, 2004). The ideal thermal storage technology should be capable of collecting and storing during summer the heat necessary in wintertime, with little or no significant heat losses and should be able to satisfy energy peaks. In this contest zeolites play a key role as sustainable alternatives for the storage and release of thermal energy. Indeed, zeolites fall into the category of solid sorbents which can be utilized in sorption thermal energy storage (STES) systems. STES fall into the category of thermochemical storage systems (TCES) which exploit sorption and desorption cycles to store heat in the long-term period. This system is based on the interaction between a sorbent (in this case the zeolite) and a sorbate (in this thesis the sorbate is water vapor). In TCES systems the endothermic charging process consists in providing heat to the system so that the adsorbent is separated from the adsorbate without thermal losses. On the other hand, discharging phase occurs when heat is required by the system and consequently the adsorbent and adsorbate are put again into contact so that sorbent evaporation is possible. This step is exothermic and releases the heat needed (Jänchen *et al.*, 2004; Lavagna *et al.*, 2020).It can be added that STES systems can be opened or closed, depending on the specific application. Open cycles are cheap and easier to realize since water vapor present in the atmosphere is captured to produce heat for space heating, but it is strictly reliant on the relative humidity (RH) of the surrounding environment. Closed systems on the other hand are more efficient but also more expensive since the desorption process leads to the isolation of both sorbent and sorbate from the surrounding environment by putting them in two different tanks. Until these two components remain separated heat is stored, but when adsorption step is required, the heat of evaporation from the surrounding environment is provided to the sorbate which evaporates and enters into contact with the sorbent, thereby producing the heat required. Regarding zeolites, they should be competitive if only their energetic performance was taken into consideration(Aghemo *et al.*,

2023). However, TES systems currently on the market involve the use of synthetic zeolites, especially commercial 13 X, whose synthesis process is energy demanding and not cost effective. To overcome these limits, natural zeolites have been studied to replace synthetic ones in energy-related application. In nature more than 50 natural zeolites are largely available, cost effective and, apart from some exceptions such as erionite, they are not dangerous either for mankind or environment. However, their composition and chemical properties are strongly connected to their origin, and, despite their hydration and dehydration properties, they have only been marginally investigated on a laboratory scale.

Hence the aim of this thesis is to investigate the potential role of natural zeolite Clinoptilolite in TES systems and to compare its performance with the one of synthetic 13 X. Moreover, ionic exchange with sodium has been performed in order to analyze the effect of a specific extra-framework cation on the adsorption capacity towards water. More precisely, the first section is dedicated to a state of the art about zeolites, their structure, their properties, the difference between natural and synthetic zeolites and the main fields of application. Later it is presented an overview about TES systems, followed by a description of the main advantages and disadvantages of replacing synthetic zeolites with natural ones to store thermal energy. Hence ionic exchange is analyzed as a possible strategy to increase clinoptilolite's efficiency in energy-related applications.Then the following chapters are dedicated to the experimental section (description of materials and methods, results and discussion), followed by thermodynamic considerations and cost analysis. Finally, conclusions and future perspectives can be found in the last chapter.

2. Zeolites

Zeolites can be defined as a family of open-framework aluminosilicate minerals that possess orderly distributed micropores in molecular dimensions. The term zeolite derives from two Greek terms, **ζέω** which means "to boil" and **λίθος**, which has the meaning of stone. Their discovery can be attributed to a Swedish mineralogist, Freiherr Axel Friedrick Cronsted and it dates back to 1756.

The structural unit of a zeolite is a corner-sharing TO_4 tetrahedron, where "T" usually indicates the presence of tetrahedrally coordinated Si, Al or P. It should be emphasized that all the different frameworks of zeolites are built on the variety of possible connections between these tetrahedra(Weitkamp, 2000).

Even though natural zeolites have been known for 250 years and throughout the decades scientists have been identified up to 50 species of natural zeolites, it was only in 1950s that, thanks to the introduction of the synthetic ones, zeolites have begun to be exploited in the industrial sector.

The aluminosilicate material originates from a structural modification of volcanic ash in an aqueous environment, occurred millions of years ago. This category of materials also comprises alkali or alkaline earth metals as well as hydrated natural silicas. More precisely, the process which leads to the conversion of aluminosilicates and feldspar into zeolites is known as zeolitization process.

2.1 Structure and main properties

As anticipated, zeolites are characterized by the interconnection of structural building units, mainly AlO_4 and SiO_4 tetrahedra, which are linked together through a common oxygen atom, thereby resulting in a well-defined, three- dimensional framework. This is a direct consequence of the fact that the net formulae of the tetrahedral units are respectively AlO_4^- and SiO_2 because Si belongs to the fourth group in the periodic table while Al belongs to the third one. The result is the creation of a network of channels and cavities, usually occupied by water molecules and other cations, with the aim of balancing the positive charge defect of the aluminum-containing tetrahedra(Weitkamp, 2000).

The chemical composition of a zeolite can be summarized as it follows(Weitkamp, 2000):

$$A_{y/m}{}^{m+}\left[(SiO_2)_x \cdot (AlO_2{}^-)_y\right] \cdot zH_2O \qquad (2.1)$$

Where:

- A is the cation with the charge m
- (x+y) is the number of tetrahedra per crystallographic unit cell
- x/y is the silicon- aluminum ratio (also known as Si/Al)
- z is the number of water molecules

What makes zeolites really appealing for industrial applications is the multiplicity of properties which characterize them, such as ion exchange capacity, adsorptive properties together with shape selectivity, catalytic activity, and the ability to host nanocomponents within them.

Since the above-mentioned properties are strictly reliant on the aluminosilicate's structure, structural analysis plays a key role in characterizing and understanding the type of material(McCusker and Baerlocher, 2001).

Firstly, it should be noted that information on the type of framework allows a clarification of the main characteristics of zeolites. As a matter of fact, the framework describes the topology of atoms belonging to the tetrahedral unit, arranged as symmetrically as possible, without reference to chemical composition. It unambiguously defines the size and shape of the pores, the size of the channels interconnecting the cavities of the tetrahedral structure, the volume and conformation of the cages, as well as indicating which cations can bind to the sites inside. However, other factors such as the chemical composition, the type of post-synthesis treatment and the species present within the channels may influence the properties of the zeolite itself(McCusker and Baerlocher, 2001).

It must be kept in mind that many zeolites, especially synthetic ones, consist of a periodic repetition of individual crystalline units that are analyzed by a combination of different analytical techniques, including absorption tests, NMR analysis, electron microscopy and diffraction, just to mention some of them.

The classification of zeolites currently accepted by the scientific community has been drafted by Meyer and Olson in1970s (MEIER and OLSON, 1974) . Differently from the structure, the framework type simply describes the type of connection between the T atoms of the tetrahedral unit while symmetry, composition and cell size are not considered. Consequently, several zeolites can be classified under a single designation.

More precisely, a three-letter code (usually derived from the name of the zeolite or the type of base material) is assigned to each type of framework by the *National Zeolite Association* commission on the guideline of the rules defined by the classification system of the *IUPAC Commission on Zeolites* (Treacy and Higgins, no date; McCusker, Liebau and Engelhardt, 2001).

.

Moreover, the type of framework can be categorized according to the degree of pore openings and the size of the channel system. The opening of the channels depends on the size of the ring that delimits the pore, called an n-ring where n denotes the number of T atoms in the ring. It can be noted that an 8-ring is characteristic of a pore with a low degree of openness, a 10-ring has a medium degree of openness, while a 12-ring describes a pore with a high degree of openness,(McCusker and Baerlocher, 2001).

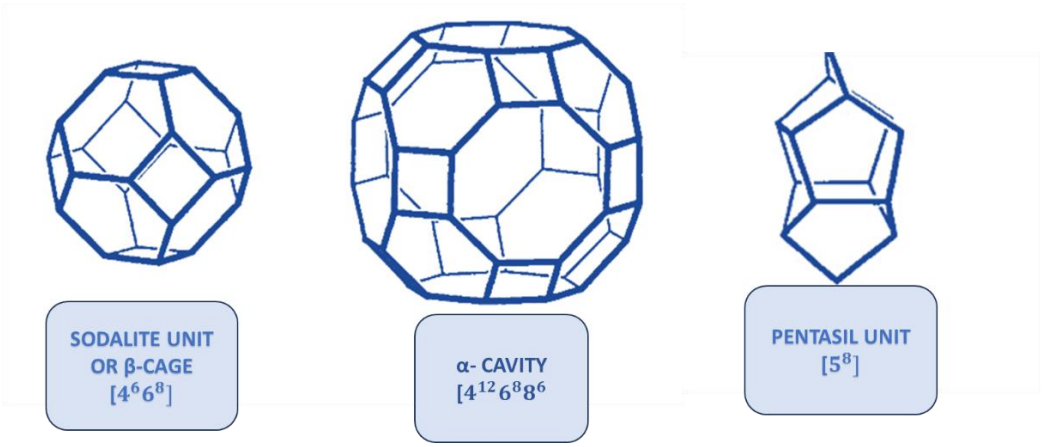

Figure 2.1: zeolites framework type of sodalite unit, α-cavity and pentasil unit. Illustration taken from(McCusker and Baerlocher, 2001) with modifications.

Since the main structural features (cages, channels, chains, sheets) are repeated identically in different types of frameworks, some units such as the α-cage, β-cage, pentasil unit, single and double gooseneck tree chains, and the 4.8 ^{2} sheets, in the **figure 2.2** (this spelling indicates the presence of one 4-atom ring and two 8-atom rings, where the number of amount of atom rings is indicated by the single quote marks) have become commonly used. Sometimes these are known in terms of the n rings defining each face, as shown in the **figure 2.1.** As an example, the sodalite unit, a truncated octahedron whose surface is characterized by 6 rings with 4 atoms and 8 rings with 6 atoms is referred to as a cage 4^6 6^8.

As with three-dimensional structures, a similar nomenclature is used for 2D lattices and cages connected at three points. In this case, the nomenclature with n-atom rings is used as shown in the **figure 2.2,** where the orientation of the fourth connection is often indicated with the letter U (up) or D (down) to complete the description in the three-dimensional terms(McCusker and Baerlocher, 2001).

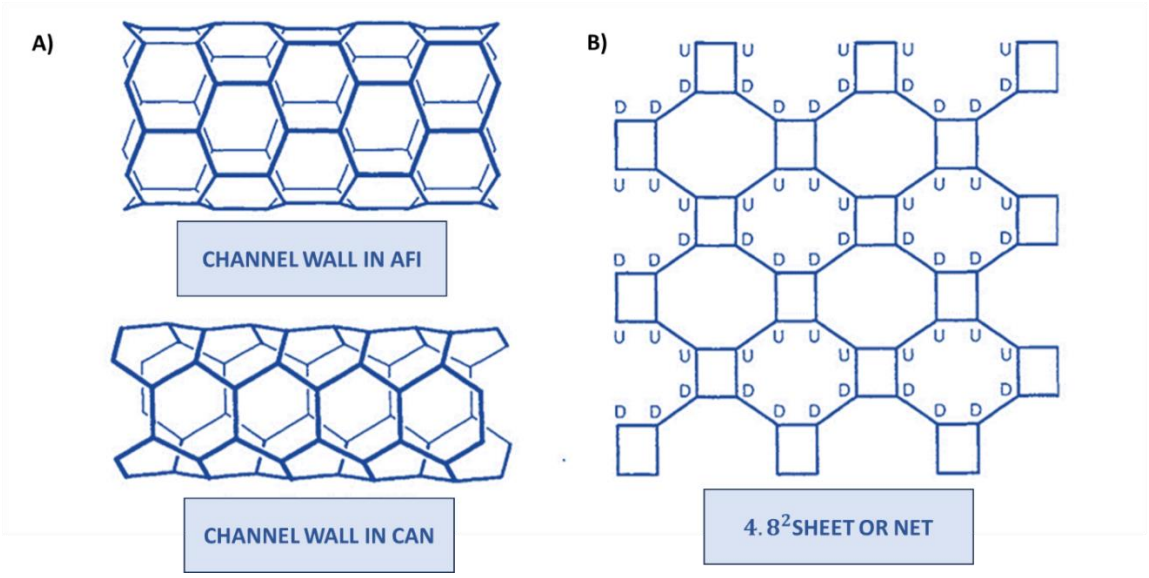

Figure 2.2: Three-letters nomenclature for framework type of 3D structures A) or 2D structures B). Illustration taken from(McCusker and Baerlocher, 2001) with modifications.

Another solution for representing the superposition of several layers within the framework is through 'ABC system'(**figure 2.3**), in which the terminology of crystal chemistry adopted to the superposition of atomic groups in metals and oxides is readapted to indicate the superposition of several zeolitic structures. This is the case of those zeolites belonging to the ABC-6 type (to which Chabazite also belongs), characterized by overlapping layers of 6-atom rings.

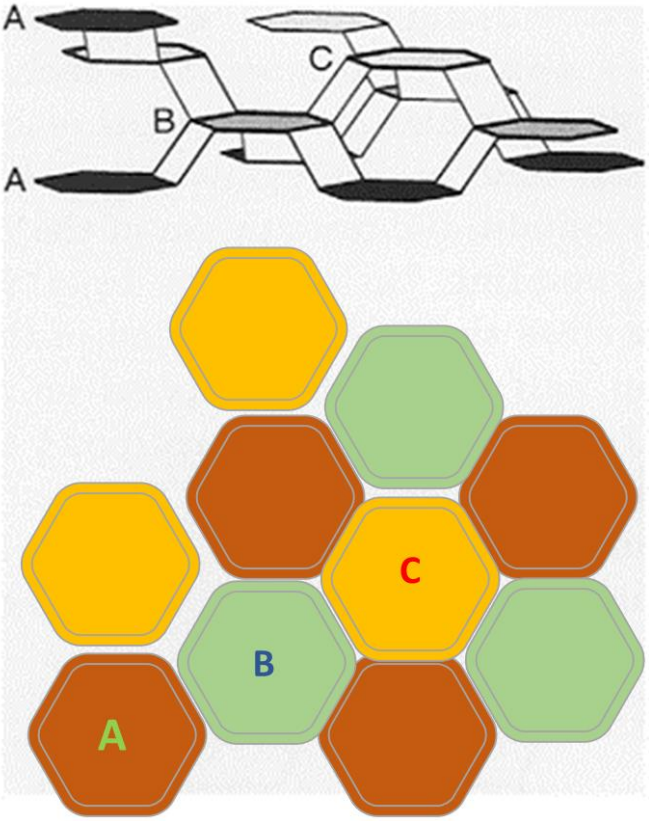

Figure 2.3: ABC nomenclature for zeolites. Illustration taken from(McCusker and Baerlocher, 2001)with modifications.

Although the framework is a useful tool to understand the type of connections, it does not describe the material as it really is, with its composition, extra framework cations, organic species, adsorbed molecules or structural defects that may be present.

As far as the composition of the framework is concerned, it should be emphasized that many properties of these aluminosilicates are based on the fact that they have an anionic framework at their base, which can bind electrostatically to a series of interchangeable cations in order to guarantee electro-neutrality conditions.In addition, it must be said that the composition of the framework significantly influences the stability of the material and that information on the chemical composition is often indirectly contained in certain salient features of the type of framework itself. Indeed, a zeolite with a high silicon content will result in a higher thermal stability than the corresponding aluminosilicate, which will tend to be more stable than other non-zeolitic materials (i.e an aluminophosphate,, less sensible to moisture than a gallophosphate).

Regarding extra-framework cations, these compensate the excess of negative charge in order to guarantee the structure's electro-neutrality. Indeed, there can be present both exchangeable

cations and water molecules as well as organic species. These elements may be residues from the synthesis process of the zeolite itself or may be inserted during post-synthesis treatments. In any case it is important to understand these elements' location. Modern crystallographic techniques usually allow the extrapolation of this information from diffraction data but with certain limitations. The first problem lies in the fact that extra-framework cations do not follow the symmetry of the framework itself and are therefore 'disordered'. This creates complications during X-ray analysis in which very weak and ill-defined peaks are generated in the electron density map, the interpretation of which requires an in-depth knowledge of all the chemistry of the material (such as chemical composition, co-ordination numbers, interatomic distances, and bond angles...) and could create ambiguities at the interpretation level in the case of the analysis of complex structures. Nevertheless, diffraction techniques are the most effective and suitable tool for this purpose.

Finally, it should be mentioned that the powder diffraction methods is regarded as a powerful instrument which provides information about the synthesis process of the material under investigation, thereby creating a kind of fingerprint of the zeolite of interest. The "Collection of Simulated XRD Powder Patterns for Zeolites"(Treacy and Higgins, no date)contains at least one powder diffraction pattern for each type of framework and can serve as a reference. Thanks to powder diffraction methods, it is possible to understand whether a post-synthesis treatment has been undergone by the material or not, simply by observing the peaks in the spectrum provided by the analysis because changes in the intensity of the peaks indicate structural modifications , whereas changes in the position of the lines in the spectrum represent a deformation of the cell unit, and finally the presence of wider or narrower lines is an index of deterioration (or improvement) in the degree of crystallinity.

2.1.1 Influence of the Si/Al ratio

Lowenstein's law plays a key role for the comprehension of the relationship between Si and Al. Indeed, according to this rule, Al-O-Al bonding is not possible because two adjacent Lowenstein negative charges would lead to the destruction of the lattice. As a result, the silicon-aluminum ratio must be equal or greater than 1 ($Si/Al \geq 1$)(Weitkamp, 2000).

Besides, if the amount of Si in Si/Al ratio influences thermal stability, Al content is inversely proportional to hydrophilic behavior. More precisely, a high silicon content positively influences the stability of the material at elevated temperatures since the breaking of the Si-O bond requires a far greater amount of energy than that required to break the Al-O bond(McCusker and Baerlocher, 2001). On the other hand, it has been demonstrated that low Al content (and consequently high Si/Al ratio) in the structure involves high hydrophilicity. In this thesis, zeolites with high affinity with water (high hydrophilicity) are the perfect candidates for water vapor adsorption in thermal energy storage applications(Olegario-Sanchez, Felizco and Mulimbayan, 2017).

In this regard, it can be added that water, a polar molecule, results quite similar in terms of polar surface area. Hence, the polar surface of the zeolite can be expanded simply by the presence of as negative charge as possible, thus making this mineral more hydrophilic.

Indeed, another way of improving the hydrophilicity of these aluminosilicates, without modifying the Al content, is acting on the valence cations because cations with a greater atomic radius (increasing from right to left and from top to bottom in the periodic table) result in a higher value of y, leading to a more pronounced hydrophilic character of the zeolite itself. (Olegario-Sanchez, Felizco and Mulimbayan, 2017).

2.1.2 Response of zeolites to heat treatment

The analysis of thermal behavior of zeolites results fundamental because most of industrial applications require the exploitation of dehydrated or calcinated zeolites where important properties like adsorption, cation exchange, molecular sieving as well as catalytic activity are expressed.

At room temperature and under normal humidity conditions, a zeolite can be found in its equilibrium condition, that is a framework characterized by channels filled with compensating cations and water molecules. However, during thermal or vacuum treatment, these aluminosilicates undergo numerous structural changes that include:

- contraction of the volume of the elementary cell caused by the loss of water molecules and/or the organic molecules used as templating agents.

- migration of extra framework cations which tend to change their coordination site to compensate the release of those water molecules they were coordinating before dehydration,

- reconstructive or dysplastic phase transitions, usually related to the formation of transient and metastable phases.

- breaking of bonds associated to the formation of new T - O - T bridges.

-Structural collapse, occurring when the structure can still be recognized by X-ray diffraction and partially retains its adsorption capacity, although the T - O - T bridges are broken.

- Structural breakdown which consists in the complete amorphization or recrystallisation, accompanied by complete loss of the material properties

Therefore, it is possible to divide zeolites into three different categories according to framework's response to heat treatment(Alberti and Vezzalini, 1984; Bısh and Carey, 2001):

- category 1 includes all those zeolites characterized by a completely reversible dehydration process, followed by the rearrangement of extra framework cations and residual water molecules that does not cause substantial changes in the framework and cell volume.

- category 2 includes zeolites which experience a reversible or almost completely reversible dehydration, but their framework undergoes major distortions with significant lowering of cell volume.

- category 3 includes all those zeolites whose dehydration occurs together with changes in the topology of the framework because of the destruction of the T - O - T bridges.

A representative example of the zeolites belonging to category 1 is **mordenite**, a pentasil zeolite which exhibits thermal stability up to high temperatures (~ 800°C) and perfectly reversible rehydration capacity.

On the other hand, in zeolites belonging to the last two categories, extreme modifications can be observed, i.e .phase transformations, as in the case of the zeolite epilstibilite.

It should be emphasized that, until now, this phase transformation has only been observed for aluminosilicate zeolites belonging to the heulandite group (HEU) and in those minerals whose topology can be described as a stacking sequence of rings of 6 tetrahedra(Bish and Carey, 2001).

As a matter of fact, zeolites of the heulandite group, such as heulandite, clinoptilolite, brewsterite, stilbite, barrerite and stellerite totally fits with the third category mentioned above. These materials usually present the cage $4^2 5^4$.Natural heulandite, if heated at temperatures

between 250-500 °C, moves to the so-called B phase, generated by the rupture of the T - O - T bridges in the 4-ring of the 4^25^4 cage. However, it should be noted that the same type of zeolite can be belong to different categories at the same time, according to specific extra-framework cations which are linked to the cell. This is the case of Clinoptilolite, whose exchanged form with K belongs to the category I whereas Na/Ca-Clinoptilolite fits category II(Bish and Carey, 2001).

In addition to this, the framework of zeolites can be non-flexible to physico-chemical changes or flexible to physico-chemical changes when frameworks can be distinguished into collapsible (i.e Natrolite) and non-collapsible (i.e zeolite A).

Unfortunately, due to the complexity of dehydration process, it is not possible to predict the thermal stability of a zeolite, even though some controlling factor related to thermal behavior of these minerals can be monitored, including:

- The amount of silicon, aluminum and thus their ratio
- Size of exchangeable cations and their ironic potential (Z/r)
- Coordination of extra framework cations after dehydration
- Topology of framework
- Other external factors.

In this regard, some researchers have demonstrated that the position of extra framework cations in dehydrated zeolites is tightly controlled by the distribution of Al in the tetrahedral sites. For instance, Armbruster (1993)(Armbruster, 1993) showed that the thermal stability of heulandite-clinoptilolite is related to the substitution of Si and Al atoms. Indeed, in all heulandite-clinoptilolites there is an enrichment of Al in the site referred to as T_2, consequently the oxygen O_1 which forms a bridge between T_2 and another tetrahedral site results not completely saturated. As a result, there is a strong interaction between Ca and O_2 ions in the dehydrated structure, strictly dependent on the ordering of Al atoms in T_2. It appears clear that this is the key to understanding the different thermal behavior within the heulandite-clinoptilolite series.

Additionally, regarding charge-compensating cations, zeolites with monovalent cations (like K^+ and Na^+) are generally more stable than bivalent ones (Ca^{2+}, $Mg^{2+}$for instance)

It should be remembered ionic radius which characterize each cation also play a role in thermal behavior since cations with a larger ionic radius, i.e K^+ in clinoptilolite, prevent the structure from collapsing as they completely fill the voids, thereby limiting the expansion of the channels, in contrast with those having a smaller ionic radius (i.e., Na^+, Ca^{2+}) that appear too small to maintain the expansion of channels. The influence of the ionic radius on the thermal stability can alternatively be expressed in terms of ionic potential, that is the ratio between the Z charge and ionic radius r (Z/r). Therefore, cations possessing a low ionic potential (which means low charge and large radius) result more thermally stable(Bish and Carey, 2001).

Moreover, the mechanisms of structural collapse and amorphization are closely associated with the type of coordination that extra framework cations assume after dehydration(Bish and Carey, 2001), when they move in search of a new low-energy configuration as well as a new coordination environment.

Besides, the geometry of the crystalline network certainly plays a key role in the stability of zeolite. In this regard, other factors to take into consideration are the framework density (FD), since zeolites with a high FD are generally more stable than those with more open channels, T-O-T angular value, strictly correlated with collapsible or non-collapsible frameworks because rings with small T-O-T angles, are more stable than elongated and distorted ones but also the

presence of specific structural units or sub-units can be associated with stable zeolites since if the structure becomes more rigid, no contraction of the channels with heating can occur. Finally, it has already preannounced that other external factors may contribute to the response of zeolites to heating, including kinetic aspects, the extent of the heating process, the distance from the equilibrium conditions, particle size distribution and, above all, water vapor pressure. In this context it must be remembered that vacuum conditions (in absence of water vapor) lower dehydration temperatures(Bish and Carey, 2001).

2.1.3 Hydration and Dehydration

In order to better understand the mechanism of thermal energy storage in zeolites, it should be remembered once again that the main structure of these aluminosilicates consists of tetrahedra of SiO_4 or AlO_4 connected by oxygen bridges, placed at the vertices of the tetrahedra (Breck, 1974; Dyer, 1988; de Gennaro et al., 2022). In this arrangement, voids are created between the tetrahedral units of SiO_4 and AlO_4 and then constitute cavities known as cages, inside which a water content of up to 30 wt% may be present (Breck, 1974; Dyer, 1988; Feng *et al.*, 2021; de Gennaro *et al.*, 2022b).

The water content inside the zeolite depends essentially on the temperature and partial pressure of the water vapor. It is known that if temperature is lower and the partial pressure is higher, the amount of water inside the cavities and channels will result greater. Conversely, a higher temperature and lower partial pressure results in less water adsorption within the zeolite (Breck, 1974; Dyer, 1988; de Gennaro *et al.*, 2022b).

Furthermore, the desorption of water vapor involves the adsorption of the heat necessary to break the physical bonds between the water and the zeolite, heat which is then returned when the water vapor is adsorbed again, thus reconstituting the physical bond broken in the previous phase. It should be emphasized that this is a bond resulting from the negative electrical charge placed on the aluminum atom (trivalent) present in the zeolite framework, which fiercely influences the hydrophilicity of the zeolite itself (Breck, 1974; Dyer, 1988; de Gennaro et al., 2022).

It is precisely the ability to adsorb and desorb water cyclically that makes zeolite a perfect material for storing thermal energy. More precisely, free water molecules perform their own motion in space, the so-called molecular Brownian motion. Since zeolite is extremely hygroscopic, it attracts water molecules. It stores the water molecules in the pores on its surface and the adsorbed water molecule, no longer able to perform its own motion, is 'slowed down'. The kinetic energy of the water molecule is converted into heat. This heat, called adsorption heat, results available to the heating system as useful heat. This is a completely reversible physical process. In other words, when the water molecule is adsorbed by the zeolite, it generates heat peaking a temperature of 80°C in a thermodynamic process, heat that can then be utilized in the heating process. Later, once high temperatures have been reached, the water can be expelled from the zeolite still as water vapor (it desorbs the water molecules) and the resulting condensation heat, called desorption heat, can be utilized as well(Banaei and Zanj, 2021).

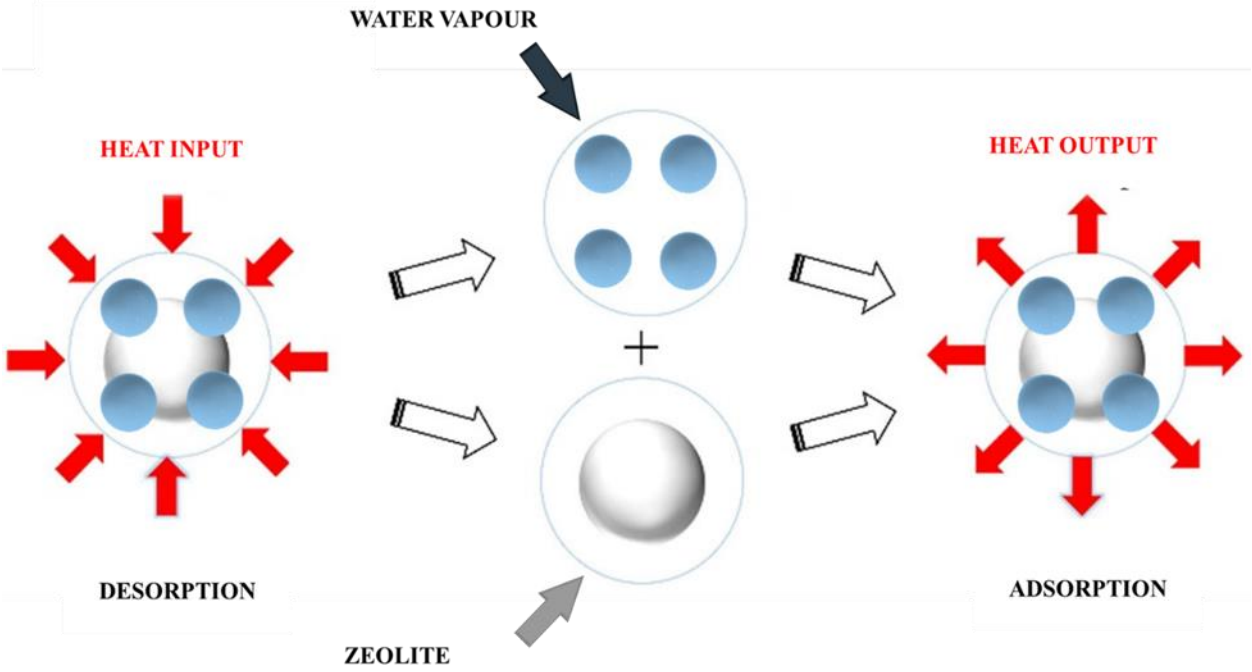

Figure 2.4: Adsorption and desorption mechanism. Illustration taken from(Banaei and Zanj, 2021) with modifications.

It is interesting to note that this system allows the storage of a certain amount of thermal energy which would be otherwise wasted, even for a long period of time , since it cannot be released from the zeolite until the water vapor comes into contact with the partially dehydrated zeolite. Numerous studies have been carried out in this regard, but at present, the technology is not yet fully mature from a technological point of view, not to mention the fact that the greatest obstacle to the use of zeolites (especially natural ones) concerns their high activation energy, which cannot be achieved using solar energy (de Gennaro *et al.*, 2022b).

Zeolites can be classified as physical adsorbents, belonging to the class of the solid thermochemical materials (TCM) used in thermal energy storage (TES). For this purpose, both natural and synthetic zeolites have been analyzed and tested in a laboratory scale. Among the synthetic ones, 13 X zeolite is the most widely used, firstly because it is relatively inexpensive compared to other synthetic zeolites and then because it shows great performance in the energy field. On the other hand, as far as natural zeolites are concerned, some researchers have identified Clinoptilolite and Chabazite as viable alternatives to the use of 13X. As a matter of fact, natural zeolites are less expensive than synthetic ones and have shorter thermal energy adsorption times. As a drawback, they are less efficient than 13X, not to mention that the adsorptive properties of natural zeolites can fluctuate depending on the origin of the mineral itself. This means that a natural zeolite from an Italian quarry could be different in terms of composition (and thus in properties) than one from Russia (VALUEVA et al., 1988; Kouchachvili et al., 2023).For this reason, if natural zeolites must be used to store thermal energy, it is essential to test and compare natural zeolites of different origins in order to be able to identify the physico-chemical properties to be taken into account for a possible application in the energy field(Kouchachvili *et al.*, 2023).

2.1.4 Ion Exchange

Ion exchange is exploited for zeolites modification, as well as for other purposes such as in the agricultural, industrial, aquacultural and environmental field. In this thesis, however, there will only be a focus on ion exchange on natural zeolites.

The applications of ion exchange in natural zeolites date back to 1950s with the studies carried out by Ames and other researchers(Roque-Malherbe, no date a).

Water is always present in the structure of any zeolite, even in minute quantities in the case of dehydrated zeolites. While its presence serves the function of completing the coordination number of certain cations in the pores, it also serves to minimize electrostatic repulsion between intra-framework oxygen atoms(Higgins, de Leeuw and Parker, 2002a).

Water also plays a key role in determining the position of interchangeable cations within the zeolite scaffold under investigation. When the latter are strongly hydrated/solvated, they have less tendency to exchange with sites where they should share one or more water molecules, as will be explained in more detail in the following paragraphs(Higgins, de Leeuw and Parker, 2002a).

When zeolites are placed in contact with electrolyte solutions, they can exchange the ions in their own lattice with those in the aqueous phase.

To sum up, this characteristic is called ion exchange, and it derives from the bond between the extra-framework cations, which ensure the electro-neutrality of the lattice, and the anionic scaffold. The above-mentioned bond is weak and can be easily broken through the dielectric action exerted by water molecules, thus enabling the substitution of these cations to modify certain properties of the zeolite itself.

In other words, the ion exchange is a process which involves both the extra framework charge balance cation in the zeolite considered and the ion dissolved in the solution.

The ion exchange reaction can be summarized with the equation **2.2** (Roque-Malherbe, no date a) :

$$z_B\, A\,\{z_{A+}\} + BZ \underset{\leftarrow}{\rightarrow} AZ + z_A B\{z_{B+}\} \qquad (2.2)$$

where:

- z_{A+} and z_{B+} = charges of cations A and B, respectively
- $A\,\{z_{A+}\}, B\{z_{B+}\}$ =cations A and B in the solution
- $AZ\ and\ BZ$ = cations A and B in the zeolite

The ion exchange process is in zeolites usually consists in three steps:

1. interdiffusion in the thin adherent liquid layer
2. an intermediate step characterized by the presence of both interdiffusion in the thin liquid layer and crystalline interdiffusion.
3. interdiffusion of cations A and B in the zeolite crystals

Every step is characterized by different kinetics.
In addition to this, in an ion exchange process the maximum amount of this substitution is called cation exchange capacity: it represents the number of milliequivalents of cations that can be exchanged per gram of zeolitic material. It is a function of the framework Si/Al ratio. It can also be stated that there is a numerical relation between the total exchange capacity in

milliequivalents and per gram and the number of Al atoms per framework unit cell (N^{Al})(Roque-Malherbe, no date a),as can be observed in eq.**2.3**:

$$C = \frac{N^{Al}/N_{av}}{\rho V_c} \quad (2.3)$$

where:

- N_{AV} = Avogadro number
- ρ= zeolite's density
- V_c= volume of the framework unit cell
- N^{Al}/N_{av}=total number of equivalents of exchangeable cations per unit cell
- ρV_c= mass of the unit cell

It is important to highlight that this parameter usually varies over a range of values, depending on the ratio between the tetrahedra occupied by silicon and those occupied by aluminum (which then translates into a different exchange capacity). Clinoptilolite, for instance, has an ion exchange capacity of between 2.19 and 3.11 meq/g.
However, it should be pointed out that the actual exchange capacity of a zeolite towards a given cation will depend on both the concentration of the competing ions in solution and the affinity of the zeolite towards each of them. The affinity of a zeolite towards a given cation with respect to another, taken as a reference (antagonist ion), is known as selectivity(Rodríguez-Iznaga, Shelyapina and Petranovskii, 2022).

On the other hand, it should be added that the exchange process can be limited by steric factors or restrictions due to space limitations. Therefore, it appears clear that the relationship between zeolites channels' size and exchangeable cation dimensions plays an important role. As a matter of fact, ions, or molecules whose dimension slightly exceeds the one of zeolite's pores can diffuse inside the framework of the zeolite itself thanks to thermal vibration. Other secondary parameters which may affect the ion exchange are temperature and pH(Rodríguez-Iznaga, Shelyapina and Petranovskii, 2022).

The evaluation of the cation exchange capacity (CEC) of natural zeolites like Clinoptilolite results more critical since these minerals can be used both in raw and purified form and usually contain other phases and/or impurities. Nevertheless, the relation between the nature of exchangeable cations and the location of exchange sites is undoubtedly a key parameter(Rodríguez-Iznaga, Shelyapina and Petranovskii, 2022).

Regarding rules for ion exchange selectivity in natural zeolites, since some experimental results pointed out that natural zeolites with high Si/Al ratio, such as Clinoptilolite, chabazite and mordenite showed a not negligible selectivity towards large cations like, for instance, Cs^+, Rb^+, Na^+, K^+, NH_4^+, some researchers struggled to find a plausible clarification. Therefore, a thermodynamic explanation, based on the cations' heats of hydration, was proposed as follows. The heat of the ion exchange can be evaluated thank to the equation **2.4**:

$$Q = \Delta H - DH \quad (2.4)$$

Where ΔH[KJ] is representative of the heat in the zeolite throughout the entire process of the exchange whereas DH[KJ] is the difference of the heats of hydration of the exchanged cations. It was observed that for zeolites with a high Si/Al ratio the heat developed in the zeolite itself is inferior respect to the one evolved in the solution, thus concluding that cations with low hydration heats are selectively exchanged by zeolites(Roque-Malherbe, no date a).

One of the main aims of this study is to find a cation that, when substituted for the natural zeolite clinoptilolite framework by ion exchange, is able to increase the water adsorption capacity of this zeolite. A greater amount of adsorbed water means a greater release of thermal energy. At the same time, however, such a cation must facilitate the desorption of water vapor in the zeolite's charging phase, enabling a lowering of the zeolite's activation energy, which is otherwise around 350°C. This could make it easier to store solar thermal energy.

2.2 Natural and synthetic zeolites

2.2.1 Natural zeolites: Clinoptilolite

Natural zeolites were discovered by a Swedish mineralogist, Freiherr Axel Friedrick Cronsted during the collection of minerals in a copper mine in Sweden. From that moment, approximately 50 natural zeolites have been detected. Before this discovery, this material was used for the construction of pyramids and temples in Mexico, as a building material for churches in Cappadocia or to produce pozzolanic cement by Romans. Later, the exploitation of natural zeolites for other purposes started in Japan and in the United States in 1950s and rapidly spread all over the world. As a matter of fact in Japan zeolites were utilized as fillers in paper, for livestock feeding, for carriers for agricultural chemicals or as additives while in the United States it was realized the first commercial application of chabazite in 1960s by the Union Carbide Corporation's Linde Division and afterward natural zeolites were adopted as material for the sewage system or for ion exchange applications, just to remember some of them(Roque-Malherbe, no date b).

As said before, among natural zeolites, Chabazite and Clinoptilolite have been most widely investigated for applications in Thermal Energy Storage (TES) systems. However, in this study only Clinoptilolite has been examined and the following paragraphs will be dedicated to this aluminosilicate.

Clinoptilolite is universally recognized as one of the most useful natural zeolites. It originates from the devitrification process, which implies the conversion of glass to crystalline material, of volcanic glass in consolidated pyroclastic rocks known as tuffs. The devitrification can be observed when there is contact between glass and saline waters. Furthermore, this natural zeolite is also present in the vesicles of volcanic rocks such as basalts, rhyolites and andesites or it can be the result of an alteration of phillipsite in deep sea sediments and with borate minerals in playa lakes. The name Clinoptilolite derives from the Greek words κλίνω, which means oblique, *φτερών,* which means feather and λίθος, that is stone, thus resulting "oblique feather stone". This name is due to the reason for which it was believed that it was the monoclinic (or obliquely inclined) phase of the mineral ptilolite. Later it was discovered that ptilolite was the earlier named mineral mordenite, thus resulting no longer in use. (Tzia and Zorpas, 2012a; Bilgin, 2017).

The chemical formula of Clinoptilolite is shown in **Eq. 2.5** (Bilgin, 2017):

$$(Na, K)_6(Al_6Si_{30}O_{72}) \cdot 20H_2O \qquad (2.5)$$

Clinoptilolite belong to the Heulandite (HEU) group. The distinction between clinoptilolite and heulandite is made on the basis of the Si/Al ratio, which for the former is always >4, while for the latter it is always <4(Boles, 1972; Rodríguez-Iznaga, Shelyapina and Petranovskii, 2022)However, there is also another distinction based on the cationic content where it has been noted that clinoptilolite is richer in alkali metals, i.e. Na^+, K^+ ,Ca^+ ,Mg^{2+}, while heulandite is richer in alkaline earth metals, i.e. Ca^{2+} Sr^+ Ba^+ Na^+ K^+ (Mason and Sand, 1960; Gottardi *et al.*, 1985; Rodríguez-Iznaga, Shelyapina and Petranovskii, 2022) . It should be highlighted that a clear distinction between these two minerals is quite challenging since the structure of clinoptilolite is so similar to that of heulandite that it cannot be distinguished on X-rays. The

substantial difference lies in the fact that clinoptilolite is richer in silicon than heulandite and more resistant to high temperatures (Bilgin, 2017). Furthermore, while heulandite already undergoes a phase change at a temperature of 230°C, turning into heulandite B and then becoming completely amorphous at 350°C, clinoptilolite withstands up to 700°C without undergoing any kind of transformation (Bilgin, 2017).
Regarding the framework, It can be said that Clinoptilolite, with its monoclinic crystal structure, possesses a two-dimensional channel system containing water molecule and cations located inside the channels aa well as in specific position inside the framework in order to compensate the superficial negative charge. The above-mentioned cations are free to move and can take part to ion exchange processes which involve other cations from other phase such as the solutions (Rodríguez-Iznaga, Shelyapina and Petranovskii, 2022).

Additionally, the two-dimensional structure consists of three types of channels (A, B.C) with dimensions of 4.4 x 7.2 A˚, 4.0 x 5.5 A˚ and 4.1 x 4.0 A˚, respectively. The A-type channels (delimited by 10-atom rings) and B-type channels (constituted by8-atom rings) are arranged parallel to each other and to the c-axis of the cell unit, while the C-type channels (also in this case delimited by 8-atom rings) lie on the a-axis and intersect the A- and B-channels. In natural zeolites, these channels are predominantly occupied by cations and water molecules.

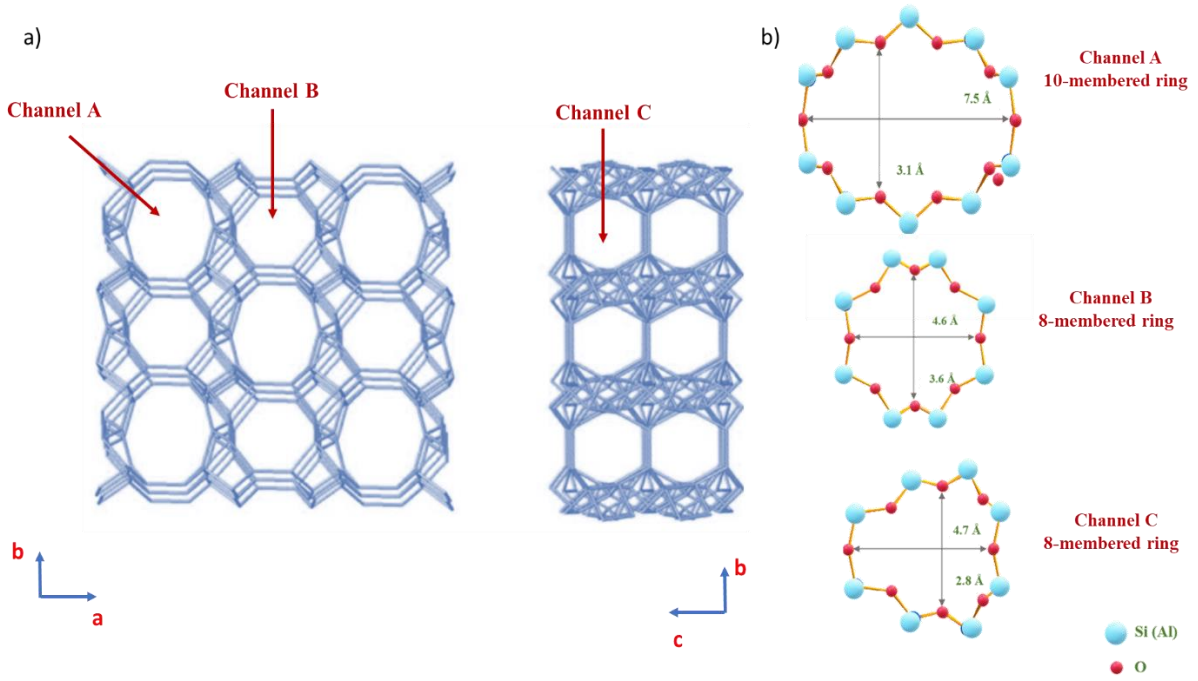

Figure 2.5: a) Schematic of Clinoptilolite's structure (illustration taken from(De Souza *et al.*, 2018) with modifictions), b) schematic of Channels A,B,C in Clinoptilolite's structure (illustration taken from (Rodríguez-Iznaga, Shelyapina and Petranovskii, 2022) with modifications)

It is possible to find in literature some models which describe the structure of the HEU type zeolites. However, Koyama and Takeuchi described the model referred to Clinoptilolite. According to it, natural cations such as Ca^{2+}, Na^{+}, K^{+} and Mg^{2+} can be present in four different cationic sites (M1, M2, M3, M4) located in A, B, C channels. More precisely two sites (M1 and M4) are located in the A channel and while M1 site usually host Ca^{2+} or Na^{+} cations (with a preference for sodium), M4 site is normally occupied by Mg^{2+}. On the other hand, M2 site is in B channel is selective for Ca^{2+}cation but it can host also sodium and finally M4 site which can be occupied by K^{+} is found in the C channel, in correspondence with the entrance of the A

channel and very close to M1. As a consequence, it is not possible to observe M1 and M3sites simultaneously occupied (Rodríguez-Iznaga, Shelyapina and Petranovskii, 2022). It appears glassy, smooth and can be transparent or semi-transparent (Bilgin, 2017)It can be colourless or can have various colours (pink, white, yellow or reddish hue), according to its different origin. Clinoptilolite is mostly known for its adsorption properties towards water, gases and oil

3.3 Synthetic zeolites

As repeated several times here, the flexibility of the bonds between tetrahedral units via oxygen bridges allows the realization of a great variety of structures, some of which already exist in nature, while others can be synthesized in the laboratory. The synthesis of zeolites is based on the hydrothermal evolution of a system characterized by the presence of an amorphous aluminosilicate gel in an alkaline environment. More precisely, since zeolites under natural conditions result from a reaction of volcanic ash with the waters of the basic lakes which lasts thousands of years, some researched attempted to simulate on a laboratory scale the hydrothermal process of formation of these aluminosilicates thanks to the help of high temperatures and pressures and starting from natural raw material or synthetic silicates. As a drawback this synthesis is expensive and energy-demanding, and this justify the higher price of synthetic zeolites respect to that of the natural ones(Król, 2020).

Nevertheless, the extraordinary commercial development of synthetic zeolites has been a consequence of the broad spectrum of applications, including, for instance, the separation of air components, the improvement of petrol quality and the separation of hydrocarbon mixtures(Król, 2020).

The characteristic structural unit of many synthetic zeolites is the sodalite unit or β-cage. This is a unit consisting of 4- or 6-sided rings interconnected in such a way as to create a closed three-dimensional structure in the shape of a polyhedron, as shown in the figure below.

2.2.2 Synthetic zeolites: 13X

As repeated several times here, the flexibility of the bonds between tetrahedral units via oxygen bridges allows the realization of a great variety of structures, some of which already exist in nature, while others can be synthesized in the laboratory. The synthesis of zeolites is based on the hydrothermal evolution of a system characterized by the presence of an amorphous aluminosilicate gel in an alkaline environment. More precisely, since zeolites under natural conditions result from a reaction of volcanic ash with the waters of the basic lakes which lasts thousands of years, some researched attempted to simulate on a laboratory scale the hydrothermal process of formation of these aluminosilicates thanks to the help of high temperatures and pressures and starting from natural raw material or synthetic silicates. As a drawback this synthesis is expensive and energy-demanding, and this justify the higher price of synthetic zeolites respect to that of the natural ones(Król, 2020).

Nevertheless, the extraordinary commercial development of synthetic zeolites has been a consequence of the broad spectrum of applications, including, for instance, the separation of air components, the improvement of petrol quality and the separation of hydrocarbon mixtures(Król, 2020).

The characteristic structural unit of many synthetic zeolites is the sodalite unit or β-cage. This is a unit consisting of 4- or 6-sided rings interconnected in such a way as to create a closed three-dimensional structure in the shape of a polyhedron, as shown in the figure below.

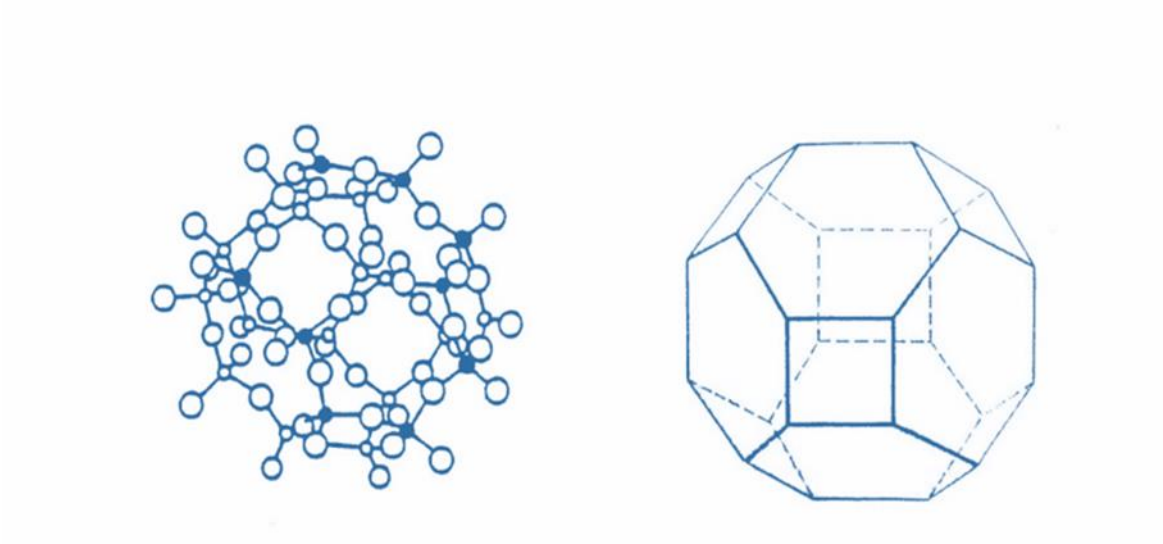

Figure2.6: sodalite unit. Illustration taken from(Bose *et al.*, 2020) with modifications.

Several sodalitic units can be interconnected to create a network with cavities and channels. When sodalitic units are interconnected, a larger cage, called an α-cage, is created.

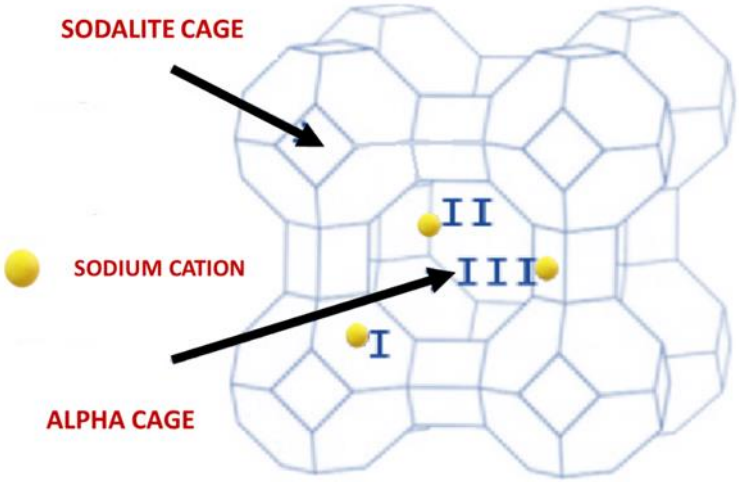

Figure 2.7: alpha cage. Illustration taken from(Tahraoui *et al.*, 2020)

Zeolite 13X (or Na-X) is a hydrothermally synthetic molecular sieve.It is characterized by fairly high adsorption capacity of water vapor compared to common adsorbent materials (Mette *et al.*, 2014; Gaeini, Zondag and Rindt, 2016; Kouchachvili *et al.*, 2023) . It is thermally stable, but at the same time has a low energy storage density above 200 kWh/m ^{3}(Dicaire and Tezel, 2011; Kouchachvili *et al.*, 2023). It should be added that it possesses a higher cost respect to inorganic salts (Kouchachvili *et al.*, 2023)(currently the cost of 13 X is around 2000-3000 €/ton) and natural zeolites but its price results to be lower than the one of other synthetic materials.
The following is a representation of the three-dimensional of the structure of 13 X, in which it can be seen that this synthetic zeolite consists of alumina tetrahedra as well as silicon-oxygen tetrahedron which form a homogeneous structure thanks to oxygen bridges. The main structural units, the sodalite cages, are interconnected by means of prisms with a hexagonal base and arranged to create a central cavity, assembled to form a 26-sided solid and connected to other cavities by means of 7.2Å channels. Because of the electronegativity of the alumina tetrahedra, there are Na^{+} cations that neutralize the negative charge. These cations can occupy three different positions in 13 X framework (SI, SII, SIII). It is importance to remember that SI

position is not able to interact with adsorbed molecules since it is not exposed whereas the other two (SII, SIII) are usually involved in adsorption process.

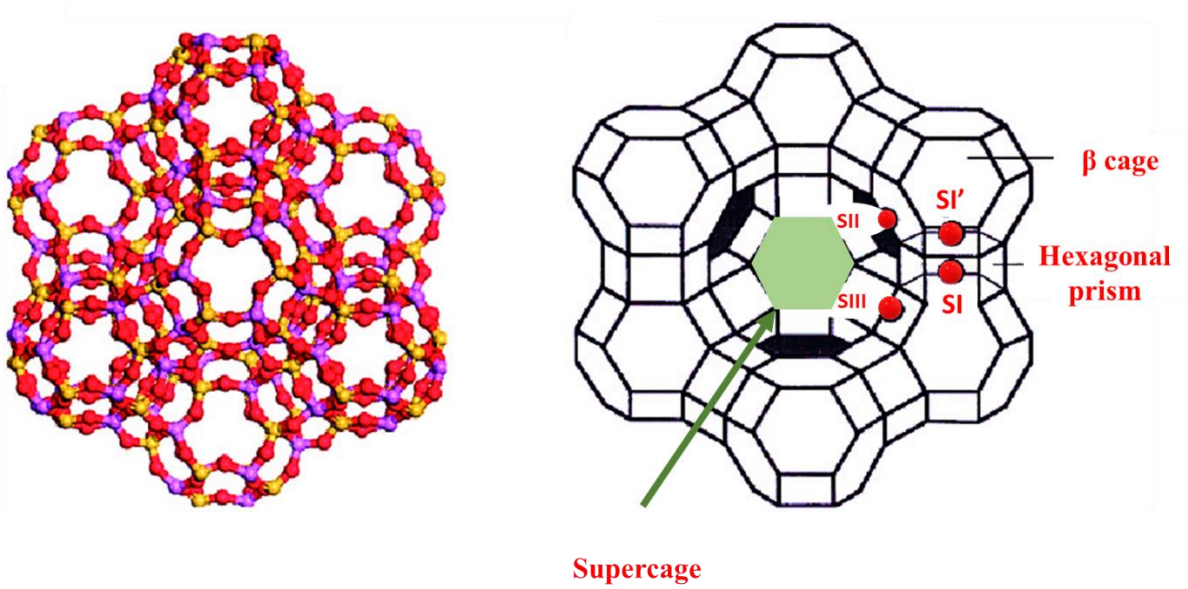

Figure 2.8: schematic of synthetic zeolite 13 X. Illustration taken from(Guo, Zhang and Liu, 2018) with modifications.

2.3 Fields of application

It is possible to divide the application fields of zeolites into four main categories(Bilgin, 2017).

2.3.1 Pollution control

The ion exchange properties of zeolites are widely known in the literature. Furthermore, it must be remembered once again that zeolites are microporous materials, and the pores are arranged in the framework to form honeycomb structures, whose size limits the access only to specific substances, thus rendering zeolites molecular sieves. The above-mentioned property makes the material attractive for selective adsorption processes. Moreover, since the regulatory effect of pollution can be addressed both to gaseous and liquid streams, zeolites can be utilized for water purification or gas removal. (Ozaydin, Kocer and Hepbasli, 2006).

More precisely, in literature some studies related to this application are reported.

Regarding purification of liquid streams, this class of aluminosilicates can contribute to the reduction of heavy metals such as Pb, Cu, Zn, Cd and Hg from industrial wastewater (Bilgin, 2017) or they can be implemented for adsorption of oil losses in remediation strategies which also involves the abatement of radioactive elements such as Cs, Sr, Rb from nuclear industry waste (Bilgin, 2017) or from nuclear accidents. For instance, the addition of clinoptilolite drastically reduced the amount of ^{90}Sr in contaminated soils, thus lowering the uptake of this radioactive compound by plants. This natural zeolite was also used for Cs absorption process in soil remediation. Moreover, it should be mentioned that in 1986, to face Chernobyl disaster huge variety of technical strategies involving zeolites were adopted(Mumpton, 1999).

Another practical application concerns their use in drinking water purification plants where they are exploited for the removal of the ammonium ion, toxic to humans (Bilgin, 2017). It can also be added that, among natural zeolites, clinoptilolite has proven to be particularly efficient due to its lamellar and needle-like structure, which gives it considerable adsorptive properties,

together with the fact that the main constituent of clinoptilolite appears to have a high affinity for ammonia, thereby showing up to 82.97% of its removal from water. Due to the same reasons, zeolites also find an application in water softening or in the regulation of conductivity and pH in drinking water (Bilgin, 2017).

On the other hand, the control of pollutants in gaseous streams involves purification of exhaust gases together with capture of gaseous pollutant such as SO_2, CO, CO_2, H_2 S, NH_3, NOx (Bilgin, 2017). In this context, zeolites result particularly attractive for the capture and conversion of carbon dioxide emitted from the combustion of fossil fuels. Among all the materials studied for the same purpose, like activated carbon, metal-organic frameworks, mesoporous silica or metal oxides, these minerals are competitive because of their strong electric fields, which preferentially tend to adsorb molecules with large dipole and quadrupole moment and CO_2 perfectly fits this description. Moreover, CO_2 selectivity depends on the zeolite's porous structure, given by specific active sites. For the same reasons, they have been implemented in industrial applications involving N_2, CH_4 or H_2 capture(Li, Li and Yu, 2017).The main natural zeolites utilized for this application are mordenite, clinoptilolite and chabazite. They are attractive materials because of their availability and low cost, although the main disadvantage regards issues of material purity, quality and strength that make them less attractive than synthetic ones for large-scale applications (Gao *et al.*, 2023).

Finally, it should be noted that zeolites play a key role in the air-pollution remediation process. Nowadays the scientific community has been recognized NO_x, NH_3 and volatile organic compounds (VOC) as the most important air pollutants, regarded as a direct consequence of excessive global industrialization. More specifically, NO_x (NO and NO_2) is the cause of acid rains a photochemical smog and their reduction is achieved by means of selective catalytic reduction with ammonia (or SCR-NH_3). In this context, metal exchanged zeolites fulfil the function of catalysts. Indeed, both synthetic and natural zeolites, such as Mordenite, ZSM5, Y and beta zeolites are exchanged (mainly with Cu) to be utilized, showing high activity, easy availability, and high thermal stability(Li, Li and Yu, 2017).

Concerning VOCs, they include compounds like benzene, toluene or formaldehyde, just to mention some of them, whose origin can be found in industrial emissions, domestic products as well as combustion engines. To avoid their concentration in the air, a total oxidation into carbon dioxide and water is performed with a process called VOCs abatement. Since zeolites are characterized by a huge surface area, high hydrothermal stability and the composition of their framework can be easily modified, they result as the perfect candidate for the role of supports of the noble metal based composite catalysts which accelerate the abatement process(Li, Li and Yu, 2017).

Despite all the advantages already described a large-scale use of synthetic zeolites in the environmental sector (for water treatment and CO_2 capture) is hampered by the high cost of the technology. This is why much work is currently focused on the production of zeolites from low-cost raw materials.

2.3.2 Agriculture and livestock breeding

As for pollution control, adsorption capacity, ion exchange properties and the function as molecular sieves play a key role in the use of zeolites for agricultural purposes. Indeed, they can be used as fertilizer, especially natural zeolites as they are easily available, non-toxic, environmentally friendly, resistant to washing out of torrential rains and finally their beneficial effects are explicated gradually and last through the decades(Rehakova *et al.*, 2004; Bilgin, 2017).

Additionally, thanks to their hydration and dehydration capacity these materials are capable of reclaiming soil by a removal of the excess water, but they have captured attention since they

can prevent washing out of plant fertilizers, stabilize pH in agricultural soils, without forgetting their function as carriers for pesticides. These aluminosilicates show great performances as moisture regulators in grain and other cereal storage warehouses or as soil nutrient carriers, as scavengers of unwanted heavy metals such as Pb, Cd, Zn, and Cu. Another application concerns the remediation process of lakes for fish farming, with the role of ensuring the right oxygen supply, thus preventing the formation of stagnant areas, undesired for life proliferation. In addition to this Some researchers have developed innovative techniques to use fine dust to produce zeolite A, an excellent carrier for the controlled release of urea (an excellent fertilizer) into the soil(Gao *et al.*, 2023)

It should be mentioned that many paper available in literature report the application of zeolites (especially natural ones) as food additive. This is the case study of natural zeolite Clinoptilolite which has been added as integrator in some cow's feed to lower the assimilation of nitrates (deriving from an excessive zootechnic and agricultural activity) as well as the level of aflatoxins in their milk, thereby explicating a detoxifying effect(Masting et al., 2019).Besides, during Chernobyl nuclear disaster in 1986 it has been observed that the zeolite's role as diet supplement for Swedish reindeer accelerated the expulsion of Cs accidentally ingested through food contaminated by the nuclear fallout(Mumpton, 1999)

This natural zeolite has also been used as a food additive in chicken's daily meals and, as a result, an antioxidant effect has been observed. Other applications of zeolites as additives are carried out to promote egg growth or as additives for bone meal (Bilgin, 2017).

2.3.3 Energy sector

From literature it is known that these minerals are not only exploited in the environmental field, but also in the energetic one for storing thermal energy deriving from photo voltaic (PV) panels or flue gases, according to zeolite's activation temperature. This is possible because, as already stated, zeolites are micro-porous crystalline materials with a unique micro-porous framework structure which enable them to be employed for several applications.

when a zeolite is firstly pre-treated and then subsequently wetted with water, releases a certain amount of energy. This application will be further discussed in the next section.

Besides, the versatility of these minerals makes them suitable for the constructions of electrodes or for composite electrolyte membranes in the building process of fuel cells, although there is the need for enhancing electrical and proton conductivity of zeolites to utilize them on a large scale. However, this aluminosilicates family plays also a key role in circular economy strategies involving waste disposal, recycling, reuse and conversion into high-valued products.

In addition to this, recent studies have focused their attention on the potential use of natural zeolites in waste to energy (WTE) technologies as additives, especially to satisfy the energy supply demand of some states that have experienced recent development, such as Saudi Arabia(Nizami *et al.*, 2016). As it is known, WTE strategy involves the conversion of different types of waste into heat, electricity or fuel through numerous processes like pyrolysis, incineration, gasification, anaerobic digestion (AD).

Moreover, regarding anaerobic digestion (AD), that consists in the conversion of organic matter into biogas (energy source) and digestate (organic fertilizer), zeolites like mordenite, clinoptilolite, zeolite 3A and zeolite 4A have a beneficial effect on the production of methane and, consequently, biogas if exploited ad inorganic additives(Nizami *et al.*, 2016).

To sum up. despite this use of zeolites is yet not mature for industrial implementation, it can already be guesses that these are just few examples among the variety of possible energy-based applications.

2.3.4 zeolites as eco-friendly catalysts for energy-related applications

Thanks to the fact that zeolites are so well renowned for their qualities of adsorption and separation of gas and moisture, they can be frequently found as ecofriendly catalysts in a wide range of processes. Their role as catalysts in the energy sector concerns, for instance, the production of Hydrogen and methanol, which are two important and competitive fuels available on market, in fuel cells where they can also be used as components and materials like electrodes and membranes.

A fuel cell is defined as an electrochemical device, frequently utilized in the automotive sector, whose main purpose relies in the conversion of chemical energy from fuel oxidation to electricity(Li, Li and Yu, 2017).Among the fuels for fuel cells, Hydrogen is the most important one, followed by methanol. In literature plenty of studies are reported, regarding unconventional methods to produce these fuels through catalytic activity of zeolites.

Indeed, to overcome the problem of electrode's poisoning due to the deposition of impurities, such as CO from steam reforming (the traditional process for hydrogen synthesis), ultrasmall Pd clusters embedded within the intersectional channels of nanosized silicalite-1, a hydrophobic, aluminum-free zeolite have been developed. Surprisingly, it has been resulted in an efficient production of hydrogen without CO generation and, thanks to this strategy a higher value of turnover frequency has been achieved(Li, Li and Yu, 2017).Besides, silicate-1 has also been employed in the synthesis of hybrid bimetallic catalysts based on Ni, Co and Pd which exhibited high thermal stability and not negligible shape selectivity as well as offered a new solution to store H_2 in fuel cells(Li, Li and Yu, 2017).

Regarding methanol, firstly it should be emphasized that its production from methane implies the overoxidation of CH_4 in syngas, thus resulting quite complex and expensive. This happens because methanol results being easier to oxidize in comparison to methane and this obstructs the direct conversion of CH_4 into CH_3OH. However, it has been demonstrated that transition metal exchanged zeolites, such as Cu-exchanged mordenite (MOR type) can provide C-H bonds of methane with active sites for their conversion into methanol. Hence, mordenite has also been used as catalyst, combined with water (source of oxygen). As alternative it has been adopted a Fe-exchanged beta catalyst, efficient even at low temperatures or Pd-exchanged ZSM5(Li, Li and Yu, 2017). Zeolites role as catalyst is also exploited in pyrolysis processes, where the catalytic conversion of waste plastic into liquid fuels occur and the product's quality is improved through catalytic reforming, for which both natural and synthetic zeolites are the perfect candidates. Respect to the synthetic ones, natural zeolites-based catalysts favor the production of a higher quantity of liquid fuels, but also with a higher viscosity, thus requiring pretreatment or hybrid configurations to decrease the heavy oil fraction (>C20) (Nizami *et al.*, 2016)

2.3.5 Innovative applications

In recent years, zeolites have been exploited also in pharmaceutical sector, for drug delivery, encapsulation and spray drying of specific active compounds for medical products. Among the parameters which control the adsorption process and the gradual release of a certain drug, Si/Al ratio, tunable hydrophilicity and pore size distribution are extremely important (Kadja, Culsum and Putri, 2023).

In medical field, instead, natural zeolites (especially Cllinoptilolite) have captured the attention of many researchers because of their detoxifying properties, as well as their anti-inflammatory and antioxidant effects. For instance, it is possible to find on the market a volcanic mineral with a honeycomb structure known as liquid zeolites, which is capable not only of removing heavy metals and toxins from the body but also of supporting a healthy immune system and regulating

the body pH levels. To support this, it has been tested on epithelial cell cancer, surprisingly showing a 100% killing rate these cells in 72h, without any collateral effect(Tzia and Zorpas, 2012b).

Still, in food packaging, zeolites find an application in active packaging, defined as a interactive type of packaging that is not merely a container for the product itself but actively contributes to prolong its shelf life. This is achieved through a constant modification of the package permeation, together with a continuous tailoring of equilibrium concentrations between O_2 and CO_2.The result is a reduction of food waste and economic loss caused by the senescence and degradation of the food itself. In this application zeolites can be added as antimicrobials, ethylene absorbers (a naturally occurring hormone in fruit and vegetables which, if in excessive quantities, leads to senescence), as filling material for food packaging (to reduce production costs), as nano food reactors. These minerals are also widely used in smart packaging, as a supplement to all the sensors that monitor the origin, quality and state of preservation of the food itself. Finally, they are suitable for immobilizing enzymes and other active components or as molecular sieves for pre-treatment of food samples. In the food industry, the property that is most appreciated is the absorption capacity that can be modulated by ion exchange with extra framework cations (i.e. Ag-zeolite incorporated into the plastic biofilm for antimicrobial purposes). The advantage of using zeolites in the packaging sector relies on the fact that these materials are not toxic or harmful to humans (no problems with migration of these substances into the food) and it must not underestimate the fact that they allow the avoidance of preservatives, thus satisfying consumer's demand of minimally processed food. Nevertheless, it is a technology that is very popular in the USA and Japan but not very well developed in Europe due to the very restrictive regulations in this area (Villa *et al.*, 2022).

Other food-related applications regard the role of zeolites in purification of carbon dioxide for use in soft drinks. Since CO_2 derives from excessive fermentation in brewery or from combustion of fossil fuels or extraction from existing gaseous sources, it requires a removal of taste and odor-causing compounds(Tzia and Zorpas, 2012b).

Additionally, it must be remembered also that ion exchange properties of zeolites are particularly advantageous for drinkable water treatments, such as softening (for the reduction of levels of calcium or magnesium), demineralization (to remove suspended solids), dealkalinization or other special processes to remove nitrate, arsenic and other impurities(Tzia and Zorpas, 2012b).

On the other hand, regarding detergent industry it can be said that zeolites represent a valid alternative to phosphates in traditional, synthetic detergents that, despite their essential role in ensuring public hygiene, are complex to dispose and tend to pollute sewers. The main advantages of zeolites in this application are their excellent ion-exchange capacity and their lack of toxicity. Used as detergents since the 17thcentury, they don't cause eutrophication, differently from phosphates formulations(Bilgin, 2017; Koohsaryan, Anbia and Maghsoodlu, 2020).

Moreover, It has been developed (on a lab scale) a new type of sustainable additive for anti-icing asphalt pavements by utilizing a surface treatment through which a zeolite containing calcium chloride ($CaCl_2$) was coated with a microporous epoxy layer. As a result, these additives provided the asphalt with a improved anti-icing capability, especially in the temperature range between -3.9°C and -9.4°C. Among the other advantages there are low-temperature anti-icing effectiveness, superior anti-icing longevity, as well as enhanced mechanical properties(Zhang and Shi, 2021).

It is possible to conclude that the multitude of characteristics of zeolites makes them very versatile and suitable for a wide range of uses in different sectors.

3 Natural and synthetic zeolites in Energy field

The scientific community considers global warming to be the major problem of the 21st century because of all the catastrophic environmental consequences it entails. In recent times, efforts have also been made to raise awareness of the possible long-term consequences that planet earth is destined to suffer if no action is taken in the coming years. Almost all over the world, pacts and agreements have been made to implement policies to combat global warming and the greenhouse effect. (*KYOTO PROTOCOL TO THE UNITED NATIONS FRAMEWORK CONVENTION ON CLIMATE CHANGE UNITED NATIONS*, 1998; de Gennaro *et al.*, 2022b).

One of the main causes of global warming is the increase in the concentration of carbon dioxide in the atmosphere, which causes the notorious greenhouse effect. Since this increase in CO_2 is mainly caused by human activities, numerous protocols have been drawn up that aim to reduce carbon dioxide emissions due to human activities (Davidson and Monteleone, 2022). However, this appears particularly complex since fossil fuels are currently the world's main source of energy, the main combustion product of which is CO $_2$(Intergovernmental Panel on Climate Change. Working Group III and Edenhofer, no date; de Gennaro *et al.*, 2022b).

Therefore, based on these considerations, the focus in recent years has been on the development of energy from renewable sources, in particular solar energy together with a reduction in energy waste. In this context, zeolites could play a key role in the storage of thermal energy. At present, thermal energy is considered a minor energy source both because it is difficult to convert into useful work (which results in a huge energy for thermal machines) and because thermal energy tends to be dispersed into the surrounding environment when it is stored for a long period of time.

Despite these non-negligible problems, thermal energy from the sun or from the gases produced by combustion (waste heat energy) could be harnessed to heat a water-saturated zeolite. The main advantage of zeolites relies on the capability to capture and store an amount of thermal energy equal to the one necessary to desorb the water vapor inside its framework.

3.1 Energy-related applications

Approximately 50 % of Europe's energy demand is currently for heating and cooling systems (Mette *et al.*, 2014) .About 35 % of this part is required in our homes, 75 % of which is for hot water and room heating (*Vision Potential Deployment Roadmap Strategic Research Agenda Solar Heating and Cooling for a Sustainable Energy Future in Europe*, no date; Mette *et al.*, 2014)]. For this reason, it is important to find an strategy to gain thermal energy from alternative sources to classical fossil fuels.

Solar energy is undoubtedly one of the most important renewable energy sources currently being researched and exploited on large scale through the use of solar panels. These are mainly used for heating and meet about 20 to 30 % of the energy demand while the remaining part is supplied by the traditional combustion of fossil fuels. In recent years, efforts have been made to further reduce dependence on the latter by trying to create more compact and robust systems for storing solar energy in the long term. Ideally, thermal energy from solar radiation should be stored during the summer and then used in the winter. Therefore, thermochemical energy storage (TCES)systems represent the first step towards a new generation of energy storage solutions thanks to their high storage energy density with almost no heat dissipation (Mette *et al.*, 2014).

3.1.1 Thermal Energy Storage (TES) systems: an overview

Thermal energy storage (TES) are innovative systems that provide the storage of a certain amount of heat even for a long period of time a with almost no dissipation.

TES can be subdivided into three main categories, according to the type of heat that must be stored (Nasruddin *et al.*, 2020; Banaei and Zanj, 2021b) :

- **Sensible heat storage** exploits the simple process of expelling excess heat within a given material without undergoing a phase change (energy density of 10-54 kwh/m^3).
- **Latent heat storage** involves phase change and utilizes the heat deriving from the passage of state of the material (energy density of 90-100 kWh/m^3) .
- **Termochemical heat storage** exploits an irreversible thermochemical reaction to store heat, unlike the previous cases (energy density of 200-500 kwh/m^3).

In any case, the working principle of this systems is based on three steps: charging, storing and discharging.

Among these classes, thermochemical (TCES)systems are particularly appealing for domestic and industrial energy applications because thanks to them, long-term energy storage can be realized together with a substantial reduction of losses, not to mention that their energy density allows for compact storage systems compared to TES systems using sensible and latent heat. As a result, there is a tenfold saving of space (Banaei and Zanj, 2021b).
TCES systems involving the use of zeolites (and in particular synthetic zeolites such as 13X) are based on adsorption which can be regarded as the movement of atoms and molecules from a bulk to the surface of an adsorbent material. Consequently, from the attractive interactions between the adsorbent surface and the adsorbed molecule, a certain amount of heat is released.

Furthermore, the attractive potential for this thermochemical reaction can be modelled wuth the Lennard-Jones potential, whose equation(eq.**3.1**) describes the interaction potential energy (V_{LJ}) between a pair of molecules:

$$V_{LJ} = 4\varepsilon\left[\left(\frac{\sigma}{r}\right)^{12} - \left(\frac{\sigma}{r}\right)^{6}\right] \tag{3.1}$$

Where, r is the distance between atoms, ε >0 is a constant (also called dispersion energy) with the size of an energy and represents the depth of the potential hole and σ >0, a constant with the size of a length, represents the distance to the null potential. The term to the sixth power is called the Van Der Waals interaction and represents the attractive interactions at long range (because this term prevails at long distance) while, on the other hand, the term with exponent 12 represents the repulsive forces, which prevail at short range. (Banaei and Zanj, 2021a).

Looking at equation 3.3, and considering what has been said before about adsorption, it becomes clear, basing on a quantum chemistry point of view, that a shorter distance between molecules leads to higher values of potential energy of interaction between the adsorbent and adsorbed molecules and thus potentially more heat can be released during the adsorption phase. Besides from the data available in the literature, it could be remembered that this potential can take values between 8 and 800 kJ /mol. Therefore, the need of increasing contact between adsorbent and adsorbate influences the design of the reactor used for TCES systems. The extent of adsorption, however, is also strongly influenced by the operating conditions as well as the nature of the adsorbent material(Banaei and Zanj, 2021a).

For TCES large scale applications, zeolites are placed on the bed of a reactor (the configuration of which varies depending on the application) and an attempt to optimize the process is made by monitoring temperature, pressure and moisture level. The most popular reactor in this configuration is the fixed-bed one:

In this setting, a steam flow at 120°C is sent to charge the zeolite, while at the same time the moisture within the zeolite itself is absorbed and expelled. This is followed by the storage phase in which, due to the tetrahedral structure of the aluminosilicates described above, thermal energy is stored for a long period without significant dissipation.

During the final discharge phase, air from the surrounding environment, with a certain amount of moisture, is drawn into the reactor. The zeolite, which is hydrophilic at room temperature, absorbs moisture from the incoming stream and releases energy in the form of heat. The duration of the process depends on both the process parameters and the reactor design adopted. It must be observed that modifications can occur to the reactor structure, the project parameters or the auxiliary equipment to produce more energy.
Despite all the advantages, their use in common houses is challenging because it requires to find a compromise between energy production, which is directly proportional to the amount of zeolite used, and the realization of a compact systems that take up little space (in other words, the ideal solution would be finding a way to use a large amount of material in a space-saving way) (Banaei and Zanj, 2021b).
The main objective in TES systems always remains maximizing performance with a minimum effort. In this regard, Andersen et al. (Anderson *et al.*, 2014)found a direct proportionality between reactor length and heat losses (the greater the length the greater the losses), while Van Essen et al. (Bales *et al.*, 2008) noted that a reduction in the thickness of the reactor walls accelerates the hydration process of the zeolite while other studies have shown that feeding the water stream from the head rather than from the bottom of the reactor resulted in better performance (Oktariani *et al.*, 2012). Process efficiency can be evaluated by several factors, including the coefficient of performance or COP, defined as the ratio between the amount of heat extracted Q_H[kW] and the work required to produce it W [kW], as it is shown in **equation 3.2** (Banaei and Zanj, 2021b):

$$COP = \frac{Q_H}{W} \tag{3.2}$$

Looking at this relationship, it is immediately clear that this is a parameter relating only to the discharge process, whereas it must be considered the (dimensionless) efficiency, as shown in **equation 3.3**, to take into account the charging phase as well (Banaei and Zanj, 2021b):

$$\eta = \frac{Q_H}{W+Q_{in}} \tag{3.3}$$

Where:

- η =efficiency [-];
- $Q_{H=}$ heat extracted [kW]
- Q_{in} =initial heat [kW]
- W= work [kW]

3.1.2 Technologies currently on the market

Despite the fact that this innovative storage system is still in a state of development, there can be found on the market some technologies which exploits zeolites, especially the synthetic zeolite 13X. The first example that can be mentioned is the **ZeoTherm integrated hybrid zeolite system** (Sistema ibrido integrato a zeolite Specifiche tecniche zeoTHERM, 2012).

As a matter of fact Valliant, a leading boiler company, has brought out a zeolite-integrated hybrid system model and renamed it Zeotherm.

With this technology, the company combines conventional condensing boiler technology, solar thermal and adsorption technology in one system

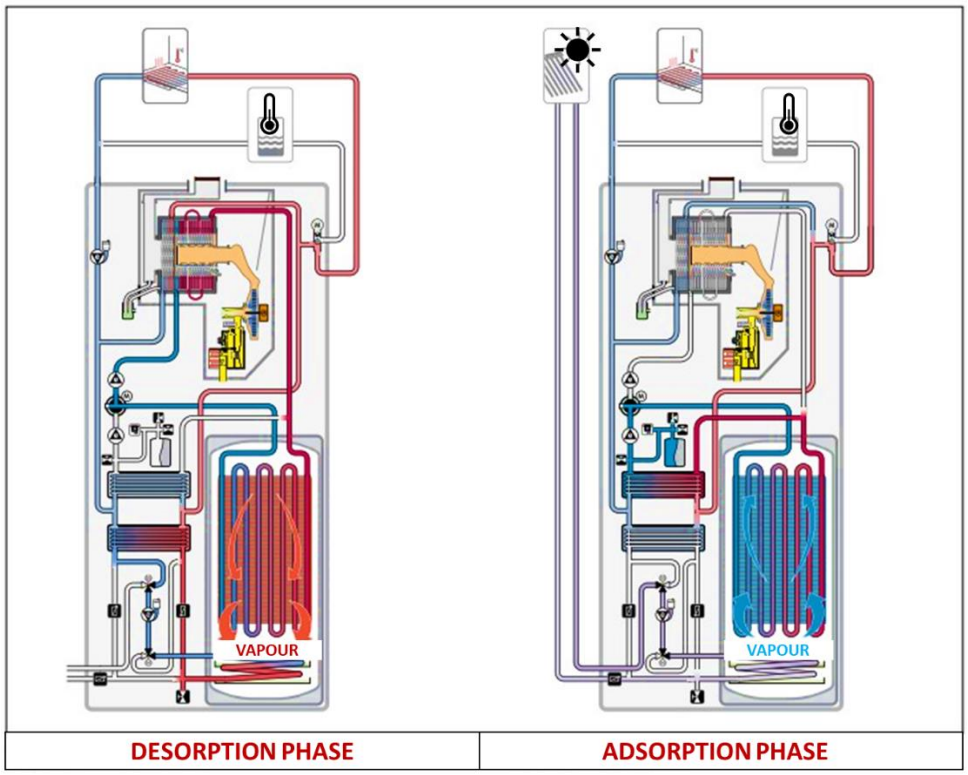

Figure 3.1: Zeotherm integrated hybrid zeolite system. Illustration taken from (*Sistema ibrido integrato a zeolite Specifiche tecniche zeoTHERM*, 2012)with modifications.

The innovative aspect lies in the arrangement of zeolite spheres in individual layers in the intermediate spaces in an adsorption heat exchanger in the form of a finned heat exchanger. This adsorption/desorption unit is located in a vacuum stainless-steel container, the so-called zeolite module. The entire adsorption process can be simply divided into two phases, one of desorption (or drying) and the other of adsorption or wetting.

When drying, the water vapour contained in the zeolite in its large inner surface is expelled. To let this happen, the heat transfer fluid, i.e., water that has been heated to approximately 120 °C by the condensing boiler module, flows through the absorber/desorber into an internal hydraulic circuit. This heats the zeolite, which then releases the water stored within it and the desorption step occurs. The resulting hot vapor flows into the lower section of the zeolite module where it cools and condenses. The energy released is used as useful heat. This phase is completed when the zeolite has reached a specific degree of drying and once water is present in the lower section of the zeolite module (the desorption phase can be monitored by means of an appropriate control system that also records the temperatures reached). In contrast, during the adsorption phase (wetting), the gas burner is switched off, the zeolite module cools down, the pressure in the module drops and the adsorption phase begins. As soon as the temperature of the evaporator falls below the temperature level of the ambient heat source, the solar pump is switched on. This means that 'cold' energy from the surroundings is sent to the evaporator. The water in the lower section of the zeolite module evaporates, the vapour flows upwards and is adsorbed by the zeolite. In the process, the zeolite generates a lot of heat, which is also supplied as useful heat. The evaporation heat for the coolant is provided by the solar collectors.

It is a perfect combination of gas condensing boiler technology and adsorption technology, consisting of an upper area with the condensing unit and a lower area with the zeolite unit (the

heart of adsorption technology). Solar heat is used as an ambient heat source to ensure the proper functioning of the evaporator. Three solar collectors are used for this purpose. In contrast, the gas condensing unit is based on wall-mounted condensing boiler technology. Regarding the advantages it should be highlighted that the zeolite unit is a maintenance-free module with no moving parts and belongs to a technology that already has an integrated solar system component. Moreover, the solar collectors associated with the system are able to guarantee proper operation even at low temperatures (3°C). The system possesses an efficiency of up to 128%, which makes it more efficient than simple condensing boilers. Finally, It should not be ignored that this solution has a minimal environmental impact and could lead to a possible reduction of up to 49% of carbon dioxide and it is Suitable for single-family dwellings, especially those with underfloor systems.(*Sistema ibrido integrato a zeolite Specifiche tecniche zeoTHERM*, 2012)

Another example regards the development of water-adsorption system based on the use of zeolite X to heat school buildings during wintertime. This eco-friendly solution has been made by the company ZAE Bayern. In the system, the adsorption process occurs during the day, when the request for thermal energy is high and involves the release of the heat stored in zeolite. More precisely, the air from the school building is firstly heated at the adsorption column and then recirculated to the heating system of the school. Besides, the regeneration process of zeolite X happens during the night, when thermal demand is not elevated, and it is done by using district heat. This technology results attractive for its energy density of about 124 kWh/m^3 which is greater than values recorded for conventional hot water storage systems(Li, Li and Yu, 2017) . It should be mentioned that the same company has designed a 2.4 MWh mobile TES system for off-sites energy uses. The idea originated from the need to recover industrial thermal waste heat from an incinerator which was 7 Km distant from the heat demand. The system was constituted by a packed bed filled with 14 tons of zeolites and was capable of saving approximately 616 kg of carbon dioxide emissions. The main advantage of this technology however relies in the possibility to reuse the same zeolite for more adsorption cycles without degrading it(Li, Li and Yu, 2017).

It is possible to note that large-scale applications of zeolites in TES systems that are currently on the market involve the use of synthetic zeolites while the use of natural zeolites ad adsorbents have only been tested on a laboratory scale. In this regard, Nasruddin et Al. investigated the adsorptive capacity of a Indonesian natural zeolite to adsorb thermal energy.

4 Natural zeolites as alternative to the synthetic ones for TES systems

Considering what has been said so far, it is possible to note that large-scale applications of zeolites in TES systems that are currently on the market involve the use of synthetic zeolites while the use of natural zeolites ad adsorbents have only been tested on a laboratory scale.

In this regard, Nasruddin et Al(Nasruddin *et al.*, 2020). investigated the adsorptive capacity of a Indonesian natural zeolite to adsorb thermal energy. They sudied a natural zeolite from Blitar (Indonesia), previously washed with demineralized water for 3hours and after dried at 300°C. The sample was then inserted in the experimental setup where there were present a adsorber (thermally insulated) and a condenser/evaporator linked together through a pipe with a valve. Moreover, the condenser, equipped with a sight glass to observe water inside, was kept under a thermal bath to regulate temperature. The heat released during the discharging process was recuperated through a heat exchanger connected to the adsorber. Before the adsorption, air was removed through a vacuum pump. Thank to this experiment, they obtained an energy density of 63.94 kWh/m^3. Despite this value is lower to the one achieved through synthetic zeolites (i.e 13X), it results to be greater than the one recorded in literature for paraffin latent heat storage (63 kWh/m^3), for silica gel as adsorbents (48 kWh/m^3) and the one measured in water heat

storage systems (52 kWh/m^3). They concluded was worth to further investigate for industrial applications.(Nasruddin *et al.*, 2020).

Additionally, numerous studies have been carried out to analyze zeolites (both synthetic and natural ones) response to heat treatment and several properties have been compared, including zeolite weight loss, water adsorption kinetics, water adsorption isotherm, zeolite thermal stability, porosity, and thermal conductivity.

For instance, De Gennaro et Al.(de Gennaro *et al.*, 2022a) compared 13 X synthetic zeolite with a clinoptilolite-based epiclastic material, and a chabazite-based volcanic rock (both materials contained 50-60% of zeolite). Regarding weight loss, an important parameter for understanding the ability of zeolite to adsorb and desorb water in the various cycles, they noted that it was double in 13 X compared to clinoptilolite or chabazite and increased linearly with activation temperature without substantial time dependence. Furthermore, it was noted that there was a significant weight loss at a temperature of 300 °C in all samples Considering instead the adsorption kinetics of the various materials after subjecting them to heat treatment with various activation temperatures, it was found that while chabazite took 170 and 220 mi nutes to reach 80% and 100 % hydration respectively, clinoptilolite-based material took 300 and 540 minutes respectively, while for 13 X this happened after 250 and 750 minutes. In the case of thermal stability, on the other hand, it was noted that both natural and synthetic zeolites retained their characteristics after numerous charge and discharge cycles. They also studied the adsorption capacity of the above-mentioned samples through the analysis of water adsorption isotherms (after an activation thermal treatment). They concluded that, even though natural zeolites showed half the adsorption capacity of 13X, they resulted thermally stable (and thermal stability is comparable with the one possessed by synthetic zeolites), less expensive, largely available and they reached equilibrium conditions in shorter time respect to 13X(de Gennaro *et al.*, 2022a).

To sum up, although natural zeolites are less efficient than the synthetic ones, they show greater performances in TES systems in comparison with other materials such as Silica gel or water. Other important advantages are:

- **Availability of raw material, including Italy.** Indeed, there are numerous clinoptilolite quarries in various regions of Italy (e.g. in Sardinia and Campania) and therefore the costs of purchasing the raw material for storage and thermal energy production could be reduced. As in the small reality of the geothermal plant in Larderello, Tuscany, the use of natural Italian zeolites for TES would make it possible to become energy self-sufficient.
- **Lower CO_2 emissions**: natural zeolites constitute a renewable source of energy and therefore enable the production of clean thermal energy. They can be integrated with heat pumps and hybrid systems that still emit a certain amount of CO_2 (as in the case of Zeotherm technology), but this is a smaller amount of carbon dioxide than is emitted with the combustion of conventional fossil fuels.
- **Reducing dependence on fossil fuels** for thermal energy storage, especially in the building sector.
- **Reduction of dependence on Critical Raw materials (CRM)**(Commission, no date)**.** These are defined as materials of strategic economic importance for Europe, which are at the same time characterized by a high supply risk. The list, drawn up by the European Commission and last updated in 2020, includes 30 of them.(Blengini *et al.*, 2020). These raw materials are crucial for numerous industrial activities and are particularly important for the ecological transition because they are used to produce energy from renewable sources. They are used, for example, in wind turbines, photovoltaic panels

and batteries. These technologies require large quantities of minerals and metals, with demand expected to continue growing in the coming years. Thermal energy production using zeolites would not require a further increase in this demand.

- **Ability to reuse thermal energy from exhaust gases.** Since it has been estimated that the activation energy for zeolites is around 300°C, they can certainly store thermal energy from exhaust gases at this temperature, thus fulfilling the directive of realizing a circular economy. This also happens at the same time as a reduction in carbon dioxide emissions.

All these aspects make them suitable for further investigations in the energy field.

5 Enhancement of natural zeolites' adsorption properties for TES systems

Although there are different strategies to improve the adsorption capacity of natural zeolites, this thesis is mainly focused on cation exchange on clinoptilolite since the cation composition of the framework directly affects the adsorption capacity in primary porosity. Thus it was studied the effect of a particular cation (mainly Na^+) in water adsorption.

5.1 Choice of the best performing cation

To understand which cation better fits ion exchange application, a literature search was carried out on the best performing cation for clinoptilolite in the energy field. At this stage, an attempt was made to understand which cation could best meet the following requirements(Langella *et al.*, 2003; Alver, Sakizci and Yörükoğullari, 2010; Aprea *et al.*, 2016; Rodríguez-Iznaga, Shelyapina and Petranovskii, 2022):

- High thermal stability (even after numerous adsorption-desorption cycles)
- High adsorption capacity of water molecules (implying a greater release of thermal energy)
- No or low hazardousness.
- Easy availability
- Low desorption temperature of water molecules.

While indeed it is important that the modified clinoptilolite adsorbs as much water as possible, it is also crucial to ensure that, by heating it up to temperatures that are not too high (around 120-150°C), a high mass loss (i.e., a high loss of water, corresponding to the desorption-recharge phase of the zeolite itself) occurs. It is quite clear that the bond with water must not be so strong as to be almost irreversible.

It is known that in clinoptilolite, most of the interchangeable cations are monovalent, which are also more numerous on the zeolitic surface than bivalent cations(Rodríguez-Iznaga, Shelyapina and Petranovskii, 2022).

Literature research shows that cations with a lower valence and greater ionic radius are more thermally stable (normally, reference is made to the ionic potential Z/r, the ratio of the charge of the cation Z to its ionic radius r). However, the greater size leaves less space available for water molecules. In addition, the higher hydration energy causes water to be retained within the zeolite scaffold up to higher temperatures, making the desorption and recharge process more complex(Alver, Sakizci and Yörükoğullari, 2010).

In the specific case of clinoptilolite It is reported in literature that at equal valence, this natural zeolite is more selective towards cations with lower hydration energy and therefore greater ionic radius.

The cations most commonly used in ion exchange are K^+, Ca^{2+}, Na^+ and Mg^{2+}, whose ionic radii are 1.33, 1.06, 0.98 and 0.78 Å (Alver, Sakizci and Yörükoğullari, 2010)respectively,

5.2 Advantages and disadvantages of Ion exchange

Ion exchange constitutes a relatively simple and effective technique for removing and replacing a whole range of cations, thus allowing certain properties of the zeolite to be modulated. In addition, most of cations which could be exploited for the ion exchange process (Ca^{2+}, Zn^{2+}, K^+ to give a few examples) are readily available and are not considered harmful to the mankind, even though some cations that are dangerous to use (Cs) or cations belonging to critical raw materials (such as lithium cations) have been found to be particularly effective. Therefore, their utilization could represent a huge obstacle to future sustainable applications(Langella *et al.*, 2003).

On the other hand, the main disadvantage of ion exchange relies on the fact that it is a time-consuming technique, as some cation exchanges can take several days to be completed.

6 Experimental

6.1 Materials and Methods

6.6.1 Materials preparation

Four different samples were studied in this thesis and all of them exhibited a particle size ranging between 212-250 µm. The natural zeolite Clinoptilolite was previously washed in demineralized water to remove all the impurities and then used in its original form, without any type of functionalization. The same material was also utilized as raw material in the ion exchange process. Finally, the synthetic zeolite 13 X was investigated for comparison purposes.

Regarding cation exchanged clinoptilolite samples, a functionalization with sodium was performed by following two different procedures.

In the first one(Cavallo *et al.*, 2023)the natural zeolite Clinoptilolite in powder form(2g) was initially washed with ultra-pure water (MilliQ) at room temperature under stirring for 10 minutes in order to remove extra-framework cations and homogenize its composition. Then the sample was centrifugated and oven-dried for 12 hours at 348 K.

After that, the zeolite was first exchanged with NH_4^+ions by immersing it for 2 h in a 0.1 M solution (60 ml) made with 0.79g of $(NH_4)_2SO_4$ under stirring at 363K. This step has the purpose of increasing Clinoptilolite's exchange capacity. Later the solution was replaced with ultra-pure water. In this way the sample was washed overnight under stirring conditions at 363K.

This procedure was repeated twice to increase the exchange ratio. It was subsequently oven dried at 348 K overnight.

The following step consisted in immersing the zeolite in the ammonic form for 18 h in a 0.5 M solution of $NaNO_3$(20 ml solution/g sample) under stirring at 333K.As in the previous step, also this one was repeated twice by replacing the solution with a fresh one. Finally, the exchanged clinoptilolite was dried in a oven at 370K overnight.

The last step of this synthesis involved calcination of half of the sample (approximately 1g) at 823 K for 4h (with a ramp of 2°C/min). The resulting sample was named as Na-Clino1.

The described procedure is schematically summarized in **figure 6.1** and **figure 6.2.**

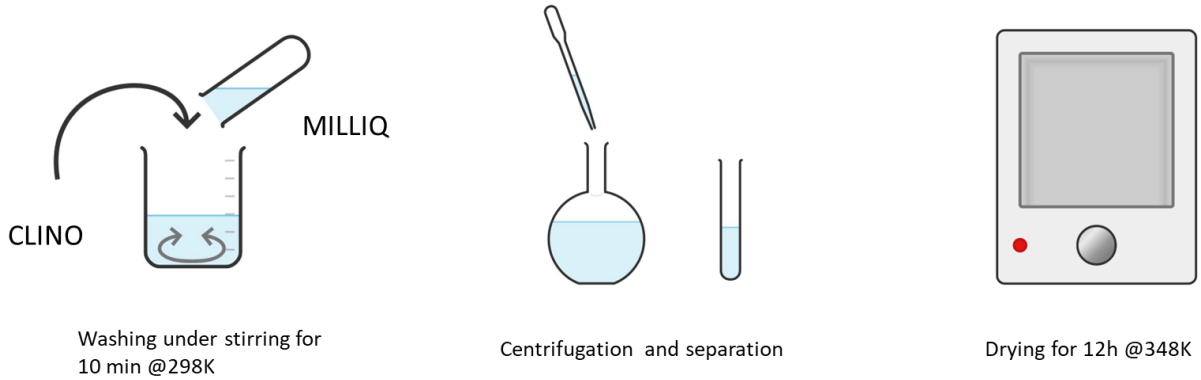

Figure 6.1: pretreatment for the synthesis of sample of Clinoptilolite exchanged with $NaNO_3$ as precursor(Cavallo *et al.*, 2023)

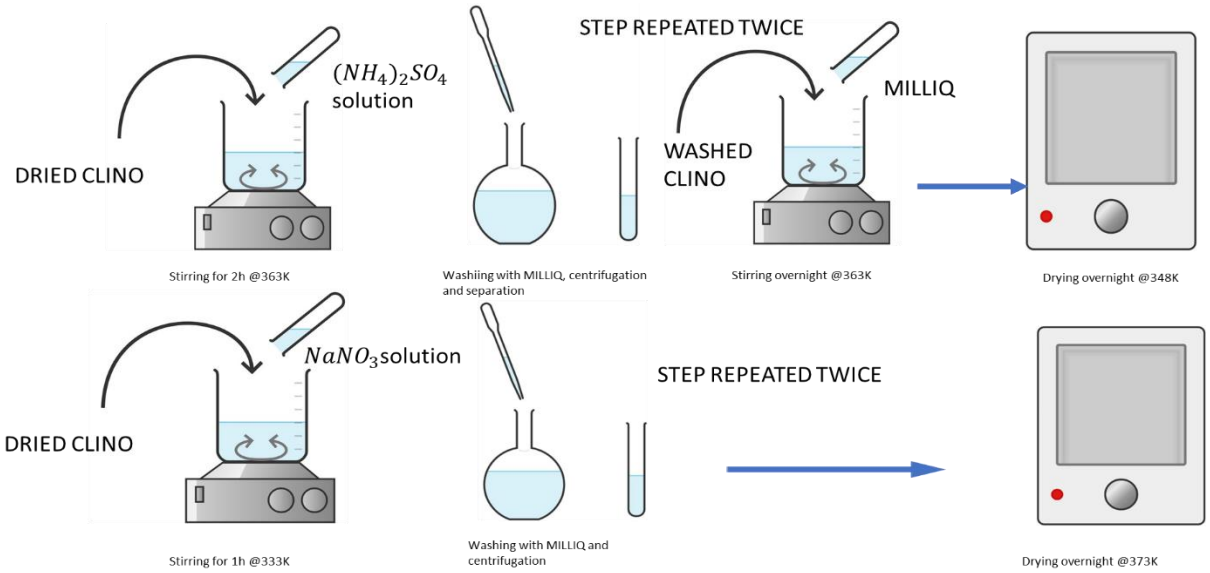

Figure 6.2: treatment for the synthesis of sample of Clinoptilolite exchanged with $NaNO_3$ as precursor(Cavallo *et al.*, 2023)

According to the second procedure (Davarpanah *et al.*, 2020), 1g of clinoptilolite sample in powder form was pre-treated by washing it with ultra-pure water (MilliQ)at room temperature, then it was centrifugated and oven-dried at 353K overnight. After this step, the ion exchange process was performed by immersing the sample in a aqueous solution of NaCl (0.6 mol l − 1, V = 250 ml) for 2 h under stirring at 323K. At the end of the procedure, the zeolite was washed and centrifugated three times. Finally, it was oven dried for 24 h at 338K and consequently calcinated at 550°C for 4h (with a ramp of 2°C/min). The resulting sample was named as Na-Clino2.
The procedure can be observed in **figure 6.3.**

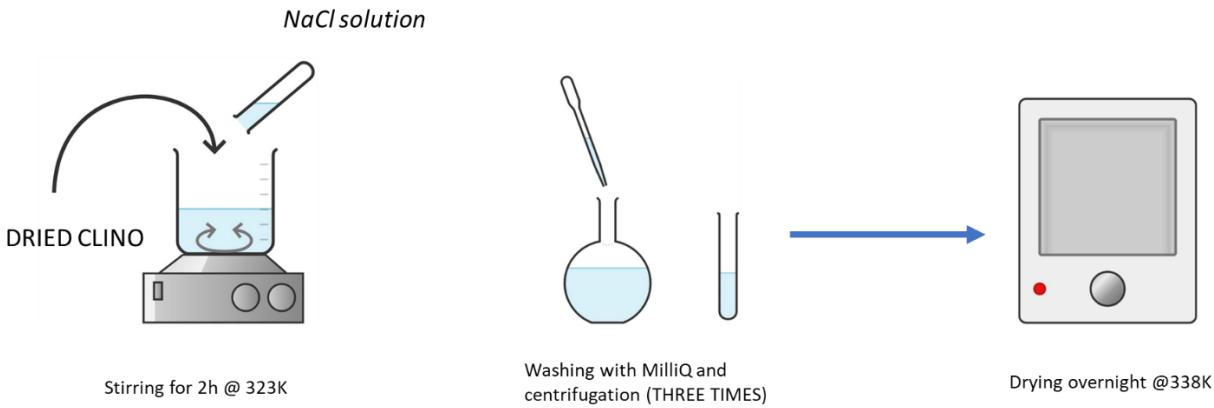

Figure 6.3: treatment for the synthesis of sample of Clinoptilolite exchanged with NaCl as precursor(Dosa *et al.*, 2021)

It is important to explain that in the following sections the samples investigated will be referred to as it follows:

- Clinoptilolite in its natural form, without ion exchange, also denominated as **Clino T.Q** (*talis et quails)*
- Clinoptilolite exchanged with NaCl, denominated as **Na-Clino1**
- Clinoptilolite exchanged with $NaNO_3$ as a precursor, denominated as **Na-Clino2**
- Synthetic zeolite **13X**

6.2 Physico-chemical characterizations

All samples used in this thesis were characterized using both the N_2 physisorption technique at -196°C and the X-ray diffraction analysis (XDR) to obtain a structural characterization. In addition to this, a Energy Dispersive X-Ray(EDX) analysis was carried out to test the effectiveness of the ion exchange procedure. On the other hand, a differential scanning calorimetry (DSC). was performed to investigate thermal properties of these zeolites whereas a thermogravimetric analysis (TG) was used to understand the type of water present inside the structures. Finally, thanks to Fourier-Transform infrared spectroscopy (FT-IR) it was possible to evaluate the affinity of each sample with water.

6.2.1 solid adsorption

Zeolites, as well as all the other solid systems, are based on adsorption which is defined as a surface phenomenon involving the interaction between the surface of the adsorbent and the adsorbate. As previously mentioned, there are two types of adsorptions:

- Physisorption or physical adsorption which is generated by week Van Der Waals forces and it is associated to low adsorption heat.This is usually explotied in TES systems.
- Chemical adsorption or chemisorption which is associated to the formation of a chemical bond between the adsorbent and the adsorbate.For this reason it usuallu does not occur below 160°C

The main difference between these two adsorption processes is that, differently from chemisorption, physisorption is generally a reversible process. However, it can become irreversible only when capillary core capable ndensation phenomenon occurs(Aghemo *et al.*, 2023).

More precisely. Zeolite is a porous adsorbent and the free space within its framework can be filled with condensed liquid which is generated by vapor phase molecules confined in the capillary which are capable of condensing below the saturation vapor pressure thanks to the enhancement of the existing Van Der Walls interactions. The direct consequence of capillary condensation is that lower pressures are required to the desorption process. Capillary condensation typically occurs in materials with mesopores whereas microporous structure are not subjected to this phenomenon(Aghemo *et al.*, 2023).Physisorption is usually the main phenomenon exploited in TES systems. Additionally, if chemisorption leads to the formation of an adsorbed monolayer, in physisorption gaseous molecules can create a multilayer adsorption. Therefore, the influence of the specific Surface area (SSA) is more important in chemisorption rather than in physisorption. The value of SAA increases from non-porous materials to microporous materials.

6.2.2 N_2 physisorption at -196°C

This is considered a non-destructive analysis, based on the physical adsorption of an inert gas (usually nitrogen), which allows to measure the total surface area of a solid, the volume of pores and their distribution (Gibson *et al.*, 2019).

The knowledge of the specific surface area (SSA) is indeed a fundamental parameter to determine how the size of a material's pores and particles can significantly influence its properties.

The procedure is based on the BET (whose name is due to its inventors Brunauer-Emmet-Teller) theory, with the following assumptions(Gibson *et al.*, 2019):

- The adsorption surface is homogeneous.
- The heat of adsorption does not depend on surface coverage.
- The multilayer adsorption is realized through Van Der Waals interactions between the individual layers. Moreover, the energy released in this context represents the heat of condensation.
- There is no interaction between two gas molecules adsorbed on the same layer.
- Adsorption of an infinite number of layer is theoretically feasible.

Before starting the analysis, the test sample must be pre-treated for 2h at 200°C to promote the desorption of all species previously adsorbed on the surface.

The sample is subsequently inserted into one of the ports of the analyzer. Then the liquid nitrogen, once brought to its boiling temperature (77.3K) will be flushed into the container with the sample(Gibson *et al.*, 2019).

Since the amount of adsorbed gas increases with increasing pressure and decreasing temperature, during N_2 physisorption test the relative gas pressure P/P_0 (where P_0 is the saturated gas vapour pressure at working temperature) is varied and the amount of adsorbed gas is recorded(Gibson *et al.*, 2019).

Finally, all the data necessary to create a adsorption curve are recorded.

Moreover, a desorption curve is collected after the adsorption one, with the aim of acquiring information about the presence of mesopores (20-50 nm)(Gibson *et al.*, 2019).

It is also known that the amount of adsorbed gas varies linearly as a function of relative pressure for P/P0 values between 0.05 and 0.3. In this range, there is a linear stretch of the adsorption curve, thanks to which the amount of gas adsorbed by the monolayer can be calculated using equation 6.1(Gibson *et al.*, 2019):

$$\frac{p}{\sigma(p-p_0)} = \frac{c-1}{\sigma_0 c} \times \left(\frac{p}{p_0}\right) + \frac{1}{\sigma_0 c} \tag{6.1}$$

Where:

- σ= Surface coverage [adsorbed molecules per unit area or per cm^2];
- σ_0=quantity of gas which has been adsorbed on monolayer [adsorbed molecules per unit area or per cm^2];
- p_0=saturation pressure of the adsorbed gas at which a infinite number of adsorbed layers on the surface is possible to be realized;
- c= It is a constant which is evaluated with equation 6.2:

$$c \approx e^{(\Delta Hads - \Delta Hcond)/RT} \tag{6.2}$$

In this equation we can distinguish the adsorption heat of the first layer [KJ/mol], the heat of condensation [KJ/mol] and temperature[K].

Therefore, by plotting $\frac{p}{\sigma[p-p_0]}$ as a function of $\frac{p}{p_0}$,it is possible to obtain a line whose slope is equal to $\frac{c-1}{c\sigma_0}$ and its intercept is given by $\frac{1}{c\sigma_0}$.
To sum up, once found σ_0, the average diameter of the single adsorbed molecule can be determined, as well as the surface area that can be measured by simply dividing the volume of the monolayer by its diameter.
The specific surface area (SSA) is thus given by the equation below(Bardestani, Patience and Kaliaguine, 2019):

$$SSA = \frac{W_{ml}}{M \cdot m} \cdot N \cdot A \quad (6.3)$$

Where:

- W_{ml}=mass of the monolayer[g].
- M=nitrogen molar mass[g].
- m=sample mass[g].
- N=Avogadro's number.
- A=nitrogen molecular cross-sectional area [nm^2].

Finally, it is important to mention The Barrett, Joyner, and Halenda method, BJH, that can estimate the pore size distribution (together with density functional theory) on the basis of the physisorption equilibrium isotherms.
BJH theory is built on these two assumptions:

- Pores have a cylindrical shape.
- The adsorbed amount depends on physical adsorption on the pore walls together with capillary condensation in mesopores.

Thanks to BJH method, the radius of pores is considered to be the summation of the multilayer thickness(t) and so the meniscus radius is obtained by Kelvin's equation 6.4 (Bardestani, Patience and Kaliaguine, 2019):

$$ln\frac{P}{P_0} = \frac{2\gamma V_M}{rRT} \quad (6.4)$$

Where:

- P/P_0= relative pressure in equilibrium with a meniscus
- γ=surface tension of the adsorbate in the liquid form [N/m]
- V_M= molar volume of the liquid [l]
- R= universal gas constant [atm*l/mol*K]
- T=temperature [K]
- R=radius of the meniscus in mesopore [m]

In this study, N_2 physisorption isotherms were obtained through the use of the instrument *Micromeritics Tristar II 3020, v1.03, Micromeritics Instrument Corp., Norcross, GA, USA, 2009*. Before the analysis, all samples were subjected to thermal pre-treatment at 400°C for 2h in vacuum conditions.

6.2.3 X-Ray diffraction (XRD)

XRD or PXRD (powder X-Ray diffraction) is a non-invasive characterization technique for analyzing the crystalline nature of materials. This is based on diffraction, a phenomenon that occurs when light is scattered by a periodic array with long-range order, producing constructive interference at specific angles. When X-rays strike the surface of a crystal they diffract in a pattern characteristic of the structure under examination, characterized by peaks whose position is closely related to wavelengt(Chauhan and Chauhan, 2014)

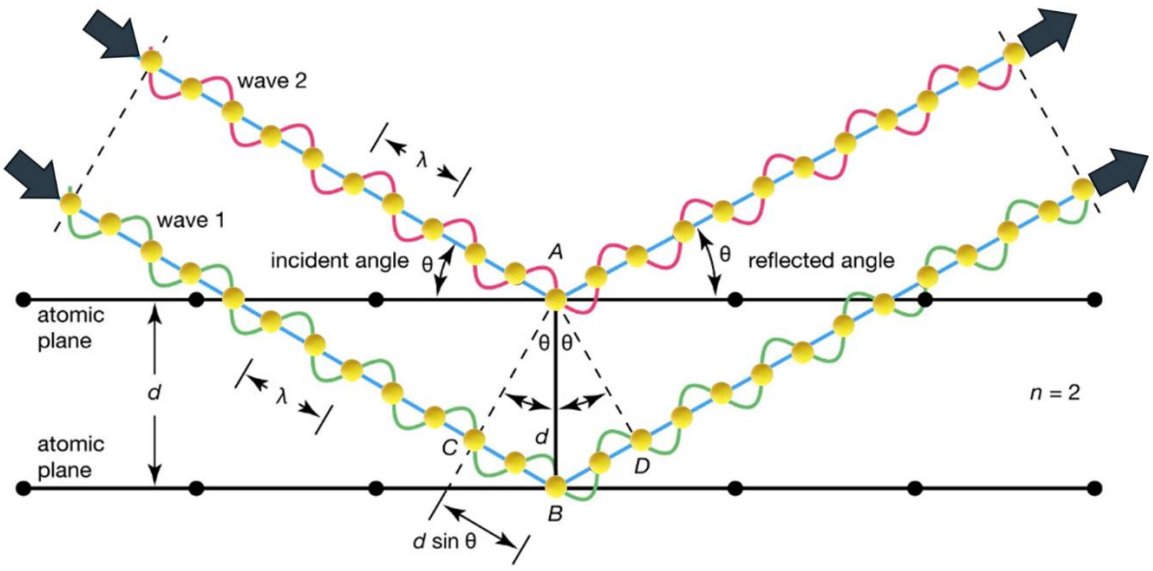

Figure 6.4:X-ray diffraction. Illustration taken from (Britannica, 2023)with modifications.

In PXRD, the diffraction pattern is obtained from the powder of the material and not from the individual crystal, so that as many crystalline planes as possible are exposed.

The result is a diffractogram, a diffraction diagram in which the intensity is represented as a function of the detector angle, 2θ (the angular range to be scanned depends on the type of material). In this thesis , the detector angle was taken in the range2θ = 5-65°.

The diffractometers used for analysis can operate either in transmission or in reflection, which is more widely employed. In reflection diffractometers, the reflected incident beam generates constructive interference if Bragg's law is respected. This law correlates the wavelength of the radiation to the distance between the planes of the crystal lattice through the measurable diffraction angle, as written in equation 6.5(Khan *et al.*, 2020):

$$2dsin\vartheta = n\lambda \qquad (6.5)$$

Where:

- d= distance between planes of the crystal lattice[nm];
- θ= angle of incidence of radiation respect to the crystalline plane [°];
- λ= wavelength of radiation[nm];

According to the Bragg's law, it is necessary to sum the waves diffracted from the various planes which constitute the crystal lattice, with differences of wave path that are equal to integer multiples of the wavelength. In commonly used diffractometers, while the X-ray source is kept fixed, the sample under examination and the detector rotate with an angular frequency of θ/min^{-1} and 2θ/min^{-1} respectively. A nickel filter is also present to monochromatize the incident radiation. A scheme of this kind of instrumentation is reported on the figure 6.2:

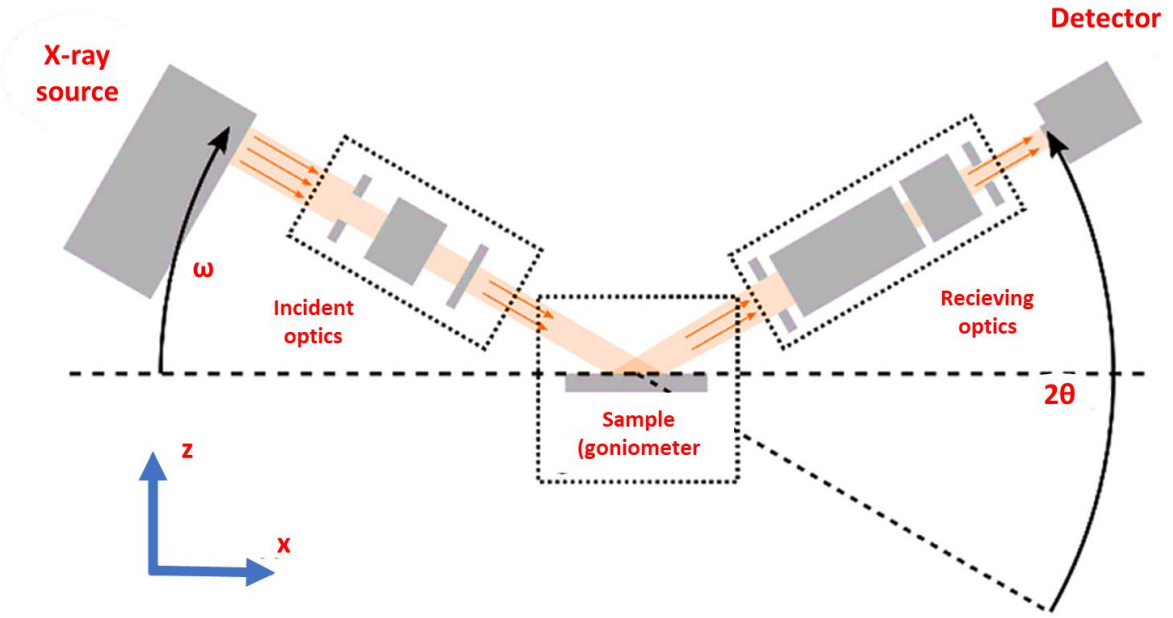

Figure 6.5: Schematic of a diffractometer. Illustration taken from(Harrington and Santiso, 2021) with modifications.

Once the diffractogram has been obtained, since the material needs to be characterized, peaks are indexed with the help of Bragg's equation. This procedure is done to find a match between experimental results and data in the database. Manual indexing is a time-consuming process based on trial-and-error approach, with the assumption of structures of increasing complexity. This is why this step is generally reduced to a simple comparison with databases.

In addition to this, there is the opportunity to determine crystallite size related to a specific peak through the diffractogram.

Speaking of crystallites or crystalline grains, they are portions of crystal that characterize the structure of the sample under investigation (rarely monocrystalline). Crystallite size is measured by means of Scherrer's equation (6.6)(Khan *et al.*, 2020):

$$\tau = \frac{\kappa\lambda}{\beta cos\theta} \tag{6.6}$$

Where:

- τ= average crystallite's dimension[nm];
- κ= It is a dimensionless shape factor whit a value equal to 0.9[-];
- λ=wavelength of the incident radiation [nm];
- β=line broadening at half of the maximum intensity[rad];
- θ=Bragg's angle[rad];

It should be added that during experimental tests, in order to better investigate Clinoptilolite's structural changes related with porosity a XRD in operando was performed. Since thermal stability is mainly influenced by Si in Si/Al ratio but EDX results, explained in the following paragraphs, showed that in natural zeolites samples Si/Al ratio remained almost unchanged, this analysis was performed only on Clino T.Q sample and results were compared with 13X ones, thereby not considering the presence of Na^+ as a controlling parameter for thermal behaviour

Hence, after a first diffractogram was taken at room temperature (T=30°C), the sample in the diffractometer was gradually heated up to 100°C, 200°C,300°C,400°C,500°C,600°C and

700°C, respectively, with a temperature ramp of 5°C/min. At each temperature an XRD measurement was recorded. The same analysis was conducted also on 13X sample for comparative purposes.

6.2.4 Energy dispersive X-Ray analysis (EDX)

This technique is usually carried out in order to identify elemental composition of a given sample.

It provides an overall mapping of the sample itself through an analysis of those elements which are close to the surface and estimates their elemental proportion at different positions.(Titus, James Jebaseelan Samuel and Roopan, 2018)

EDX is usually used together with scanning electron microscopy (SEM). It consists in an electron beam with energy of 10–20keV that impacts against the conducting sample's surface, causing X-rays to emit from the material. It is important to understand that the amount of the emitted X-rays' energy depends on the material under examination(Titus, James Jebaseelan Samuel and Roopan, 2018).This analysis was useful to understand the amount of sodium in the framework after ion exchange procedure.

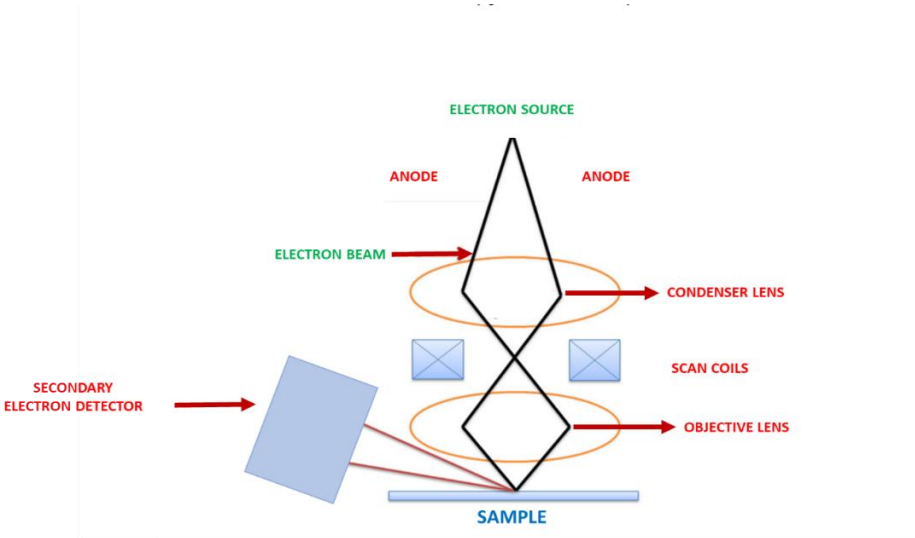

Figure 6.7: Schematic of EDX principle in the Scanning Electron Microscope. Illustration taken from(Titus, James Jebaseelan Samuel and Roopan, 2018) with modifications.

6.3 Thermal analysis

According to the International Confederation of Thermal Analysis and Calorimetry (ICTAC), Thermal analysis can be defined as "*a group of techniques that monitor changes of physical or chemical properties of a sample with time as it is subjected to a temperature program"*(Saadatkhah *et al.*, 2020).

In this thesis, two different thermoanalytical techniques were employed to investigate water desorption mechanism, activation energy of dehydration and thermal stability, as well as the effect of extra-framework cations. More precisely, Differential Scanning Calorimetry (DSC) , Thermogravimetric (TG) and Differential Thermogravimetric (DTG) analyses were performed.

6.3.1 Differential Scanning Calorimetry (DSC)

This is a non-destructive technique which allows some information about physical properties of a material to be obtained. This thermal analysis consists in sending a heating or cooling signal to the investigated sample and then evaluating temperature and energies that are associated with a specific interval of thermal events, among which there are melting, glass transitions or decomposition reactions. This technique can be considered as an improvement of the earlier method of differential thermal analysis (DTA), which has been now largely (but not entirely) substituted by DSC.

Unlike DTA, which measures a temperature difference, DSC enable the quantification of an energy flux (in the form of heat), adsorbed or released by a sample relative to a reference under controlled temperature program.

It should be added that this calorimetric analysis was initially developed for the characterization of polymers and, consequently, much of theory behind DSC is though for this application. Nevertheless, basic principles can also be applied to pharmaceuticals, biological systems, ceramics and inorganic materials(Craig and Reading, 2006).

More specifically, the sample undergoes to a heating signal and the response is measured by evaluating energy and temperature relative to those thermal events which occur in temperature range investigated.(Craig and Reading, 2006)

To perform the analysis, it could be adopted a heating or cooling temperature profile, as well as an isothermal program, even though the heating temperature profile is the most used.

As previously anticipated, DSC provides the measure of a heat flux which is not an absolute value and therefore it requires to be compared to a reference sample that experiences the same thermal treatment as the sample under exam but responses in a different way, thereby allowing a differential signal to be achieved. This signal allows to understand thermal behavior of the specific material(Stagnaro, Luciano and Utzeri, no date; Craig and Reading, 2006).

Among the advantages of this technique, it can be remembered(Stagnaro, Luciano and Utzeri, no date):

- Small sample size is required.
- It is possible to investigate thermal behavior of a sample in a wide temperature interval, ranging from -120°C to 600°C with most commercial instrument.
- Simplicity and velocity of the measurement.

It should be noted that there are two different types of DSC instruments, heat flux and power compensation. It is called power compensation DSC because the electrical power supplied to the furnace is constantly tailored in order to keep temperature difference between sample and reference near to zero. In this instrument the reference pan is subjected to s strictly linear temperature program and the sample is forced to experience program. As a result, the power difference between reference and the sample put in its pan indicates the sample's heat capacity as well as enthalpies associated with phase transitions(Craig and Reading, 2006).

On the other hand, in heat flux DSC two crucibles, one of which is empty whereas the other one contains the sample, are located symmetrically inside a furnace and two thermocouples, one for each crucible, are place in contact with them. A back-to-back arrangement is used to connect the thermocouples and in this way the direct voltage from the pair represents the temperature difference between the sample and the reference. In this configuration, the heat

paths between from the furnace to the sample and the reference are identical and the resulted heat flow can be calculated through the following equation(Craig and Reading, 2006):

$$\frac{dQ}{dt} = \frac{\Delta T}{R} \tag{6.7}$$

Where:

- Q= heat [J]
- t= time [s]
- T= temperature difference between the furnace and the crucible[°C]
- R= thermal resistance of the heat path between the furnace and the crucible [J/°C*s]

It appears clear from equation (5.6) that the difference in the heat flow due to the presence of the sample in one of the two crucibles, indicates the temperature difference between the sample and the reference. Therefore, from this heat flow it is possible to evaluate all the properties of the sample investigated, without considering heat losses through convection or the heat adsorbed by the crucible, just to mention some examples, because these have already been eliminated by the comparison with the reference (Craig and Reading, 2006).

It is also possible to enhance the power signal through a multiple thermocouple configuration. In heat flux instruments the temperature program is set on the furnace.

A schematic of the heat flux DSC is given in figure **6. 8**:

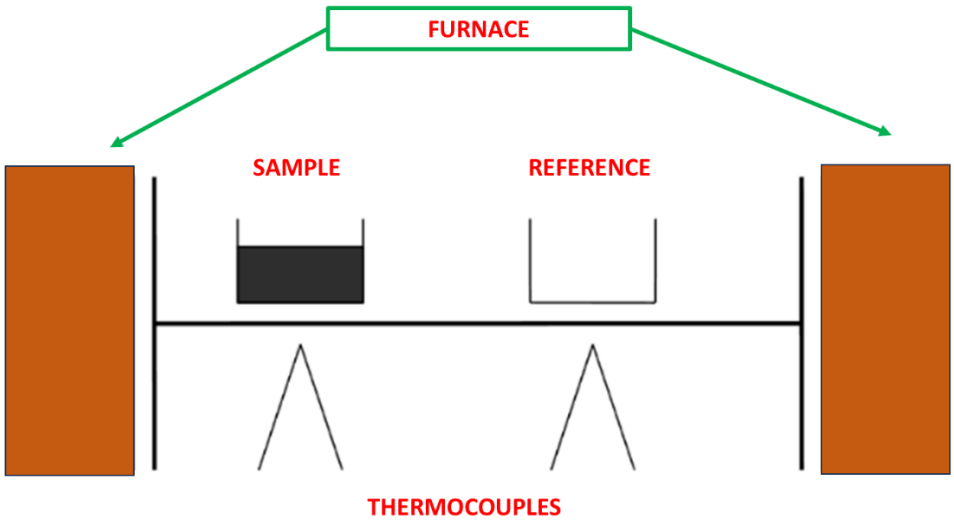

Figure 6.8: heat flux DSC instrument configuration, Illustration taken from (Craig and Reading, 2006)with modifications.

The primary outcome of this analysis is the heat flow rate as a function of time. However, if temperature of the sample position is not unknown, it is possible to represent the heat flow rate as a function of temperature(Schick, 2009).

DSC is usually performed to evaluate specific heat capacity, which is strictly correlated to the sample properties, as well as stability and order(Schick, 2009). Cp is defined as the energy required to raise the temperature of a given sample by 1K, In DSC this parameter is expressed through the following equation:

$$\frac{dQ}{dt} = cp\ \frac{dT}{dt} \quad (6.8)$$

Where $\frac{dQ}{dt}$ is the heat flow [J/s] while $\frac{dT}{dt}$ is the heating rate [°C/s]. Considering (5.7) the heat capacity of the sample could theoretically be calculated from the heat flow value which corresponds to the baseline(Craig and Reading, 2006). However, since an instrument calibration under the operative conditions is required, and since the baseline may be influenced by several factors, a practical way to evaluate specific heat is illustrated through equation 6.9(Craig and Reading, 2006):

$$cp = K\Delta Yb \quad (6.9)$$

Where K represents the calorimetric sensitivity, ΔY is the difference between the baseline values obtained with and without the sample and finally b stands for the heating rate. It should be added that it is possible to evaluate the calorimetric sensitivity through a calibration with a substance with a known heat capacity. It is necessary to perform three scans to obtain the correct value of specific heat for a given sample. From the first scan, achieved by running the two empty crucibles at the desired operative conditions, an empty-pan baseline is obtained while from the second scan, repeated in the same way but with the calibrant, K factor is recorded and finally the last scan is recorded by running the sample under exam and the reference and provides ΔY(Schick, 2009).

The apparatus employed in this study is a Perkin-Elmer Pyris 1 Heat flux differential scanning calorimeter, working in a Ar atmosphere. Specific heat (cp) measurements were held with the dried samples whereas the evaluation of zeolites enthalpy required full hydration. Therefore, each sample was fully hydrated by putting it in a 100% relative humidity (RH=100%) environment. Later each sample was introduced in the DSC chamber and a temperature range between 50°C and 350°C was investigated (with a temperature ramp of 10°C/min). The output of this analysis was a thermogram from which the enthalpy of dehydration (enthalpy of transition) was calculated thanks to the following equation:

$$\Delta H = \int_{t1}^{t2} Q dt \quad (6.10)$$

Where Q is the differential power[mW] necessary to complete a certain transition. It should be pointed out that it is possible to obtain the specific enthalpy of transition [J/g] (in this case, the specific enthalpy of dehydration) simply by dividing this quantity by the mass of the sample taken into consideration while the energy density [J/m^3] is measured through the sample's density.

6.3.2 Thermogravimetric analysis (TGA)

Minerals and hydrates can be involved in a wide range of thermal reactions, such as dehydration, dehydroxylation, oxidation, decarbonation, phase transition, decomposition or melting. All these reactions have as a consequence a change of mass in the sample or the release of heat and temperatures at which these reactions occur depend on the nature of the material(Scrivener, Snellings and Lothenbach, 2018).

Thermogravimetric analysis (TGA) is a quantitative analytical technique capable of measuring changes in mass of a given sample put into a furnace by varying temperature ramp up to 1600°C under a stable or variable gas flow. In this analysis, the sample is heated, and the mass loss is recorded. TGA allows to understand all the mechanisms for any process in which a change of mass occurs by isothermal, non-isothermal or quasi- isothermal methods. Thanks to this technique it is also possible to evaluate kinetics and conversions. As a drawback, TGA is unable to detect phase transitions, polymorphic transformations and in general reactions where the mass does not change(Saadatkhah *et al.*, 2020).

Furthermore, from the differentiation of TGA curve differential thermogravimetry or DTG is obtained. It is indeed an effective method to gain a precise identification of consecutive weight losses. Besides, DTG is usually couple with DSC (or DTA) analysis in order to better analyze DSC plot, by separating physical changes from chemical ones(Saadatkhah *et al.*, 2020) . As a matter of fact, TGA and DSC resulting curves often show similar peaks because several reactions that involve a change in weight like, for instance, water loss, are also associated to endothermic changes in enthalpy(Scrivener, Snellings and Lothenbach, 2018).

Regarding the instrument, the thermogravimetric analyzer records and monitors time, temperature and mass of the sample. Among the main items it is possible to observe a furnace where the pan connected to a precise microbalance is located. In this configuration, temperature is regulated through the programmer and controller in the furnace whereas mass variation is recorded by the balance. Additionally, the sample can be loaded either from the top or the bottom or the side and, once place in the pan, it is protected from the heating system of the furnace by a protective tube. Finally, it should be mentioned that a dynamic purge gas (20-200 ml/min) passes over the sample (Saadatkhah *et al.*, 2020)

The output of a TGA is a thermogram or thermal curve where mass change is plotted versus temperature or time. Hence, thermal stability, multi-component composition, product time, kinetics, decomposition, moisture, and the presence of volatile components are just some of the information provided by the curve (Saadatkhah *et al.*, 2020) Although the shape of a thermogram can vary according to the sample investigated, some sections are usually always detected. More specifically, below 150 °C there is the section where physisorbed water, solvents, trapped gas or light volatile components undergo changes. Besides, between 150°C and 250 °C it is possible to observe a mass loss due to chemisorbed water or relative to components with a low molecular weight like additives or volatile decomposition compounds. On the other hand,the section above 250 °C is the one where decomposition between onset and endset temperature occurs, In case of multi-component systems or multi-step reactions multi onset and endset temperatures can be studied. Finally,above the endset temperature there is a region where non-volatile ashes and metals are located(Saadatkhah et al., 2020).It must be remembered that, in a oxidizing environment,metallic compounds gain mass as their oxidation state rises.

As previously mentioned, it is possible to differentiate TG curve and in particular, it must be said that the first derivative of the mass loss profile (DTG)identifies inflection points whereas the second derivative (DDTG) is a useful tool to distinguish overlapping phenomena caused by reactions between multicomponent mixtures(Saadatkhah *et al.*, 2020)

6.4 Infra-red (IR) spectroscopy

Infrared (IR) spectroscopy is considered one of the most effective spectroscopic methods that can be adopted for characterization of surface chemistry of matter, since it allows the identification of chemical compounds, functional groups, bond length as well as the prevailing structure in all kinds of phases and the purity of a compound. This technique is built on the vibration of molecule's atoms(*INFRARED SPECTROSCOPY*, no date). Vibrational spectroscopy dates to 1905, when Coblentz obtained the first IR spectrum. However, it was only in 1960s that the era of Fourier transform IR (FT-IR) began because of the introduction of a new optic element, the Michelson interferometer, as well as the development and miniaturization of lasers, introduction of the algorithm for fast Fourier transform (FFT), development of microcomputers, and the triglycine sulphate (TGS) pyroelectric bolometer.

IR spectroscopy is based on the adsorption spectroscopy where a beam electromagnetic radiation crosses a sample and, at selected wavelengths its intensity diminishes, leading to the adsorption phenomenon.

Before focusing on IR-spectroscopy, it must be specified that all the spectroscopic methods, except mass spectrometry, can be categorized according to the energy involved during measurement. Besides, infra-red radiation (IR) can be defined as part of a electromagnetic spectrum between the visible and the microwave region.

Electromagnetic radiation exists as waves that are propagated from a source and follow a straight line during their motion unless they are not reflected or refracted. The undulatory phenomenon can be described as a magnetic field associated with an electric one. The speed of the electromagnetic wave is a universal constant c= $3*10^{-8}$ m/s. There are two ways of representing this wave:

- Wave as a sinusoidal function of time (Sun, 2009):

$$y = A \cdot sin(\omega t) \tag{6.11}$$

Where:

- A= signal amplitude
- ω= pulsation [rad/s]
- $t = time\ [s]$

The shape of this wave is repeated $\frac{\omega}{2\pi}$times and this value is called frequency ν [Hz]

- Wave as a function of the covered distance(Sun, 2009)

$$x = c \cdot t \tag{6.12}$$

Where:

- x=covered distance [m]
- t=time[s]
- c= speed of electromagnetic wave[m/s]

It should emphasize that wave is also expressed with another value known as the wavelength which can be defined as the distance covered by light during a full cycle and is expressed by the equation 6.13(Sun, 2009):

$$\lambda = \frac{c}{\nu} \tag{6.13}$$

Where:

- λ= wavelength [m]
- c=speed of electromagnetic wave [m/s]
- ν= frequency [cycles/s]

The inverse of wavelength is defined as wavenumber and it is usually expressed in cm^{-1}-^{1}(Sun, 2009):

$$\bar{\nu} = \frac{1}{\lambda} \tag{6.14}$$

Where λ is the wavelength in cm

In spectroscopy it is common to use different units of measure for the wavelength in order to avoid counting with huge numbers, even though the most preferred unit is nanometer [nm].

The definition of the wavelength is fundamental to define spectral regions:

- X-ray region (λ=0.5-10 nm)
- Far-ultraviolet region (λ=10-200 nm)
- Near UV region (λ=200-350 nm)
- Visible region (λ=350-800 nm)
- Near- infrared region, also known as NIR (λ=800-2500 nm or 12500-4000 cm^{-1})
- Mid-infrared region, also known as MIR (λ=2500-25000 nm or 4000-400 cm^{-1})
- Microwave region (λ=100μ -1cm)

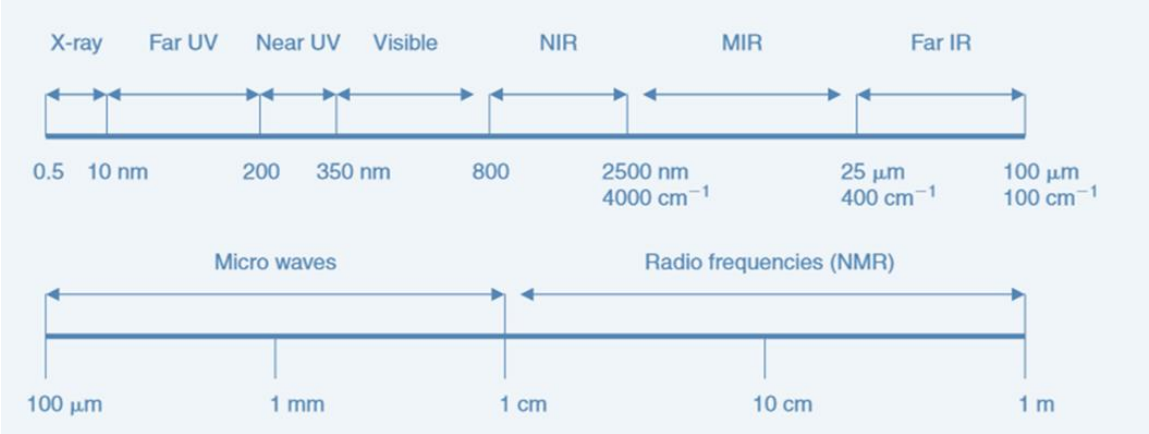

Figure 6.9: spectral regions. Illustration taken from (Sun, 2009)with modifications.

As it can be deduced, IR-spectroscopy investigates only the infrared region (including NIR MIR and far IR spectral regions).
NIR is the first region where it is possible to observe the absorption bands (mainly harmonic and combination bands) of molecule's vibrations although MIR is the main region of vibrational spectroscopy. In general, the adsorption of an infrared radiation leads to an energy change between 2 and 10 Kcal/mol.
It can be added that in the mid-infrared region (MIR) two main types of vibrations are observed(Berthomieu and Hienerwadel, 2009a):

- stretching vibrations **ν,** that are vibrations along chemical bonds which cause bond-length changes.
- bending vibrations (**δ** if in plane, **π** if out of plane) which involve changes in the bond angles.

As already stated, vibrational movements of molecules induce adsorption in the infrared region thus generating adsorption bands that are later exploited not only for quantitative and qualitative analyses of the sample investigated, but also to identify cations. In this way it is possible to

attribute every single band to a particular chemical group so that information on the sample itself are provided.
Infrared radiation can also give rotational bands, later superimposed on the vibrational ones, which are born from the stimulation of rotational movement of molecules and can be detected only by high-resolution spectrometers.
Therefore, there is the necessity of modelling the vibrations of a given molecule, starting from a diatomic one. The simplest model is the harmonic oscillator which can be introduced through classical mechanics and then improved with the help of quantum mechanics, thereby allowing a rough calculation of the position of the adsorption bands.
Harmonic oscillator corresponds to a mass m bound to a spring with no mass, which responds to the Hooke's law (6.15)(Sun, 2009):

$$F = -k(r - r_0) = -kq \tag{6.15}$$

- Where:
- F= strength applied to the particle [N]
- K=strength constant which measure spring's tightness [N/m]
- q= molecule's displacement [m]
- r= final position of the molecule[m]
- r_0=equilibrium position of the molecule[m]

From this equation potential energy is easily calculated whereas Newton's law constitutes the basis for the evaluation of the vibration frequency ν, strictly dependent on mass and spring constant as it is showed in the following equation (6.16)(Sun, 2009):

$$k = 4 \cdot \pi^2 \cdot \nu^2 \cdot m \tag{6.16}$$

Where:
- k=spring constant [N/m]
- m=mass [kg]
- ν=frequency [Hz]

As preannounced, this model is improved through the introduction of quantum mechanics where vibrational energy is calculated with Schrödinger's equation.
In addition to this, the simplest model of the harmonic oscillator also represents the starting point for the calculation of the stretching vibration observed in a spectrum since it is simply required a modification of the Hooke's law (6.17)(Sun, 2009):

$$\bar{\nu} = \frac{1}{2\pi \cdot c}\sqrt{\frac{k}{\mu}} \tag{6.17}$$

Where:

- $\bar{\nu}$ = stretching vibration [cm^{-1}]
- c= speed of electromagnetic wave [m/s]

- k=spring constant[N/m]
- μ = reduced mass [kg]

However, the harmonic oscillator is a good model only for small molecules while the complex model of the anharmonic oscillator provides a more accurate idea of the location as well as the fundamental bands of real molecules.

Considering a molecule constituted by N atoms, each of which can be located by three coordinates (x,y,z), it has 3N degrees of freedom or 3N vibration modes whose values are not constant because a real molecule is able to move and deform in space at room temperature. Moreover, the degrees of freedom are split in groups corresponding to translation, rotation, and vibration. A translation movement three degrees of freedom among the 3N ones are necessary (3N-3 degrees). In non-linear molecules, three additional degrees of freedom are required in order to properly describe rotation movements, thus resulting in 3N-6 degrees or fundamental vibrations or normal modes. It is known that a fundamental vibration is infrared active, which means that it adsorbs the incident infrared light, if there is a change in dipole moment of the molecule itself during its vibration(Berthomieu and Hienerwadel, 2009a).

It should be emphasized at this point that a polyatomic molecule is usually characterized by a state of vibration where each atom possesses a harmonic movement around its equilibrium position with a constant frequency (their oscillations are in phase). Additionally, a molecule can present one (or more) plane of symmetry and, consequently, symmetric or antisymmetric vibrations. It should be noted that symmetric vibrations are infrared inactive because in presence of a center of symmetry, all those vibrations that result symmetric to that center are usually not detected in the infrared whereas the antisymmetric ones do not present this problem.

According to a specific convention, vibrations are classified on the basis of the wavenumber as a function of their degrees of symmetry. A general rule is that the vibration of bonds between light atoms is observed at higher frequencies respect to the one related to the bonds between heavy atoms.

6.4.1 Fourier Trasform (FT)-IR spectrometer

Fourier-Transform infra-red spectroscopy (FT-IR) is a useful tool which provides an infrared spectrum of adsorption or emission of a solid, a liquid or a gas. It is called “Fourier-Transform” because the output recorded by the detector does not resemble a spectrum and there is the need of a mathematical process, known as “Fourier-transform”, to convert the raw data into the actual spectrum(Kafle, 2019).
A spectrophotometer is the instrument utilized to obtain the spectrum of the sample analyzed. A fundamental part of most of FT-spectrophotometers is the Michelson interferometer, where a collimated beam of radiation is conveyed in a splitter and separated in two beams of equal intensity. Later these two beams are recombined by means of mirrors (one fixed while the other is mobile), thus generating an interference that can be destructive or constructive, depending on the optical path difference created by mirrors’ movement(Spragg, 2016). Finally, the interference arrives to the detector, as it is shown in the next illustration.

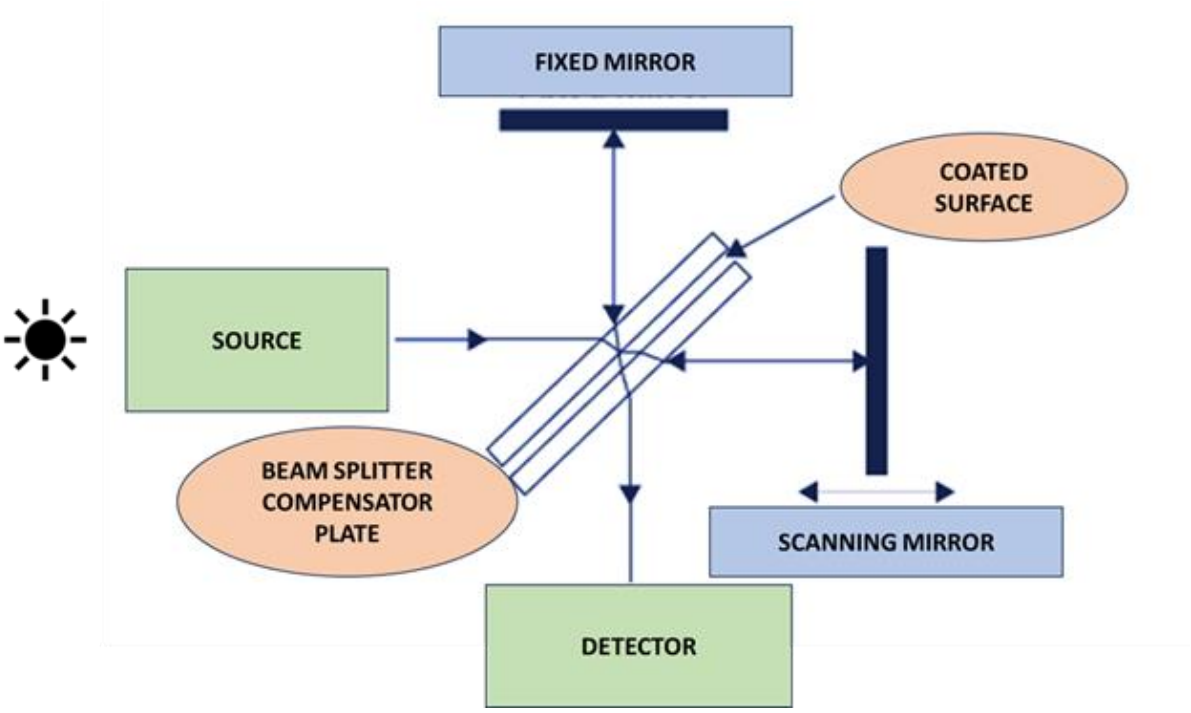

Figure 6.10: Scheme of a Michelson interferometer, illustration taken from(Spragg, 2016) with modifications.

On the other hand, the working principle of the spectrophotometer is quite simple. After the beam of IR radiation is emitted by a source, it arrives at the interferometer, thereby allowing the beginning of the spectral encoding and the creation of an a interferogram, constituted by constructive and destructive interference. Therefore, the beam passes through the sample which adsorbs specific frequencies of energy, strictly reliant on the relationship between the interferogram and the sample, thus arriving to the detector. The signal of the interferogram is then measured by a detector which evaluates the energy as a function of time for all frequencies simultaneously.This technique results particularly efficient since it generates a spectrum in few seconds, thus allowing the short-time acquisition of a huge number of spectra which are also exploited to remove fluctuations in the signal. In other words, the main advantage relies upon the fact that a small concentration of analyte is sufficient to achieve a good spectrum and that it is possible to record a lower limit of detection of measurement. As a drawback, the atmospheric CO_2 and H_2O vapor in the air are also capable of adsorbing IR radiation, thus provoking an obscuration of the analyzed sample. Differently from the other IR spectrometers (double-beam devices), in a FTIR there is a single optical path. Therefore, the absorbance of atmospheric CO_2 and water vapor is compensated through the collection of a separate spectrum, called the background spectrum, which is subtracted from the sample's spectrum by a ratio of the two signals(Kafle, 2019).

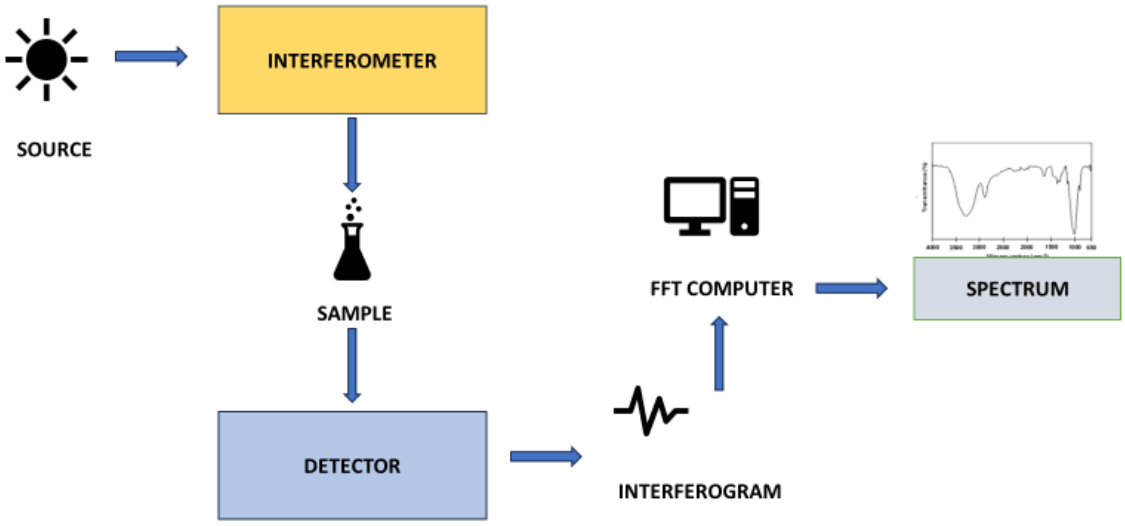

Figure 6.11: Basic components in a FT-IR spectrometer. Illustration taken from (Mohamed *et al.*, 2017)with modifications.

6.4.2 FT-IR spectroscopy using water as probe molecule.

In this thesis, Fourier Trasform Infrared (FT-IR) spectroscopy was adopted to evaluate surface properties of the four samples. More precisely, the aim of this analysis was to investigate the affinity of zeolites (both natural and synthetic ones) with water and to observe which type og changes occur in the spectra because of the introduction of sodium after the ionic exchange.

The FT-IR spectra were recorded at 2 cm^{-1} resolution on a BRUKEREQUINOX-66 spectrometer, equipped with a mercury cadmium telluride (MCT) cryodetector.

The above-mentioned samples were activated at high temperatures in order to remove possible impurities (i.e water and carbonates) and hence gaining a clear surface before starting the analysis.

Firstly, tablets preparation from the samples occurred. A thin layer of zeolite powder was deposited on the top of a stainless-steel disc which was then covered by another identical disc. Thanks to hydraulic pressure applied to the system, the tablet to perform IR analysis was obtained. This procedure was repeated for each sample. Additionally mass and surface of each tablet was measured and superficial density, crucial for further normalization, was calculated. Later four different FT-IR studies were conducted, one at time for sample. In each analysis, the tablet was placed inside a golden protective envelope and then a pretreatment at 400 °C for 2h took place in a homemade quartz cell equipped with Kbr windows.

It should be added that two spectra were recorded before sending water, one before and the other after pretreatment.

Therefore, IR study of water adsorption was performed at room temperature, by gradually increasing pressure of the line from 9.4e -4 mbar to 1 mbar, until reaching saturation. At this point it followed a gradual expansion.

6.5 Adsorption tests with humid stream

The aim of this test was to simulate the dehydration and hydration processes, corresponding to charging and discharging steps respectively, which occur to zeolites in TES systems.

The experimental setting is illustrated in **figure 6.12.**

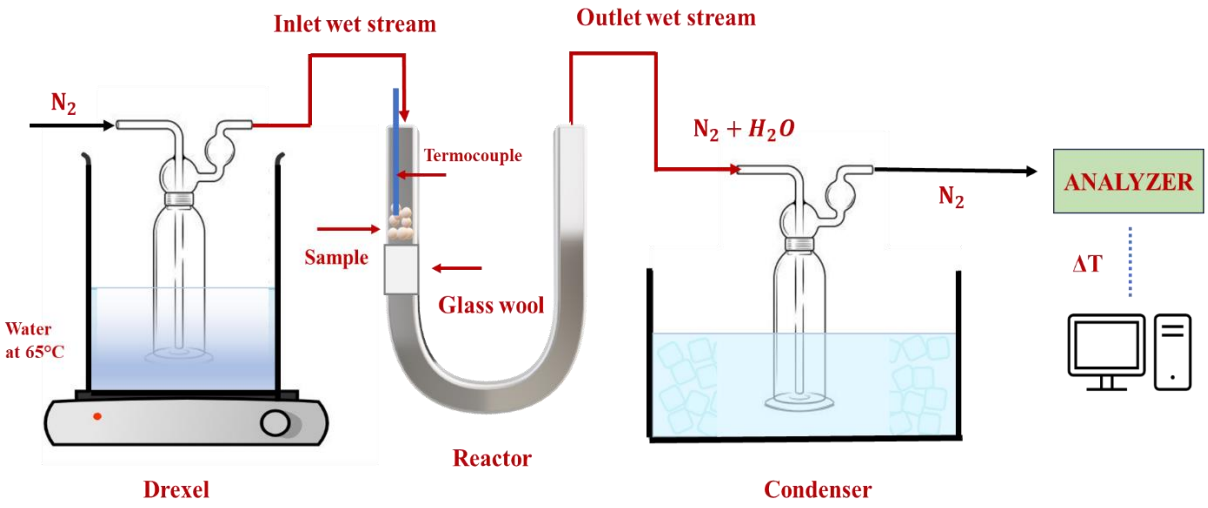

Figure 6.12: Adsorption test with humid stream, experimental setting.

For each sample, test was executed on 500 mg of pellets (size range between 212µm and 250µm) placed inside a fixed bed-quartz U shaped reactor (ID= 4mm) where quart wool was used as support. The reactor is then liked at the extremes to the inlet and outlet line of the gaseous mixture that will be send during the test execution. Moreover, a thermocouple is located in the inner channel in proximity of zeolite's pellets in order to accurately record temperature. This structured system is placed within a furnace whose temperature can be easily regulated. The test was subdivided in two steps, a pretreatment the treatment at well-defined temperature.

As a matter of fact, before performing the adsorption test, the sample was pretreated at 400 °C for 1h and during this phase a flow rate of 100 ml/min N_2 was sent to the reactor. It should be highlighted that the pretreatment phase simulated the discharging step in TES system, and it allowed to desorb all water and CO_2 bounded to the zeolite's framework. The choice of the temperature was driven not only by data available in literature (Castaldi *et al.*, 2005) , but also from TGA and XRD in operando analysis, which confirmed thermal stability up to 500-700°C..Additionally, it is known that Clinoptilolite (and natural zeolites in general) has a high activation temperature of about 350°C(de Gennaro *et al.*, 2022a) . Additionally, it should be remembered the CO_2adsorption on zeolite framework is competitive to water. Consequently, it is fundamental to eliminate residual traces of carbon dioxide, and this is obtained at high temperatures.

After pretreatment, the adsorption phase took place. Temperature furnace was set at 50°C and a stream of humid air at 10% RH (50 ml/min N_2) was sent to the reactor. To reach the proper amount of relative humidity a Drexel was connected to the inlet line, before entering the reactor. Therefore, the flow rate of humid air entered the reactor, passed over the zeolite pellet bed and then was conveyed to a condenser before arriving to the analyzer. The aim of this adsorption test at 50°C was to simulate the discharging phase of zeolites in TES systems. Finally, during

the adsorption test, temperature increase inside the reactor was recorded and then investigated. The operative conditions of the adsorption tests for each sample are summarized in **table 6.1.**

Table 6.1. Adsorption test operative conditions.

Sample	**Heigh Of bed [cm]**	**Pretreatment Temperature [°C]**	**Treatment Temperature [°C]**
Clino	4,5	400	50
Na-Clino1	4,5	400	50
Na-Clino2	7,5	400	50
13X	6,5	400	50

After adsorption with humid stream, a series of optimization tests performed to gain a better temperature increase with ClinoT.Q sample. During the first adsorption tests the mass of the sorbent together with the size of the sorbent (pellets of 212-250 μm) and pre-treatment were kept constant. The height of the bed depended on the sample taken into consideration and a treatment temperature of 50°C was chosen.

Since XRD operando measurements demonstrated an excellent thermal stability of all samples up to 600-700°C and since from literature data it is possible to understand that a dehydration temperature of at least 350°C is required for natural zeolites the pretreatment remained the same. Besides, also the inlet flowrate of 50 ml /min N_2 (RH=10%) remained unchanged because to many variables would be modified otherwise and consequently the controlling mechanisms would result difficult to individuate and understand.

7 Results and discussion

7.1 N_2 physisorption at -196°C

It is well known from literature that adsorption of a gas by a porous material can be quantitatively represented by adsorption isotherms where the amount of gas adsorbed by the material is plotted at a fixed temperature as a function of pressure. It is also possible to plot the desorption curve in a hysteresis loop and when the latter does not coincide to the first one because of the presence of cavities in porous materials, as in the case of zeolites(Alothman, 2012).

Nitrogen adsorption isotherms of the investigated samples can be observed in figure **7.1.**

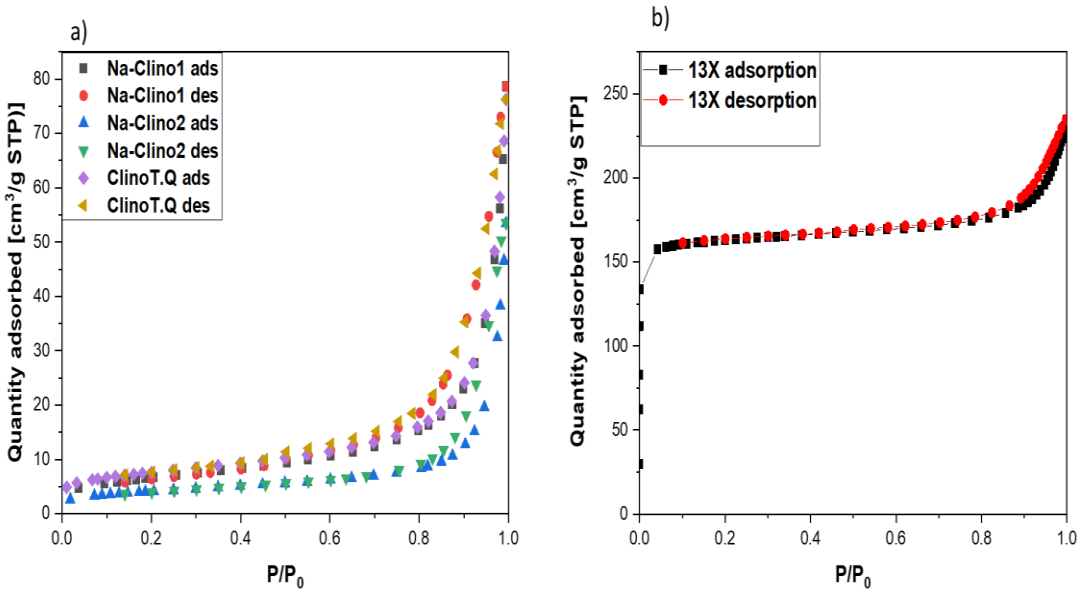

Figure 7.1: N_2 physisorption isotherms for all samples investigated.

According to IUPAC empirical classification of Hysteresis loops, based on the previous classification made by de Boer(Alothman, 2012), the shape of the loops of Clino T.Q, Na-Clino1 and Na-Clino2 perfectly suited H3 hysteresis lop which can be ascribed to materials having slit shaped pores(Alothman, 2012). As for H3 isotherm type, these ones did not present any limiting adsorption at high P/P_0 and in the desorption curve of the hysteresis cycle it was possible to observe a slope associated to the tensile strength effect occurring to nitrogen at 77 K in the relative pressure range between 0.40 and 0.45. The isotherms gave data on the surface area, pore volume and size, as it is shown in table 7.1.

Table 7.1 N_2 adsorption at -196°C data of investigated samples

Adsorbent material	Specific surface area SSA [m^2/g]	Total Volume [cm^3/g]
Clino T. Q	32	0.12
Na-Clino1	32	0.14
Na-Clino2	43	0.14
13X	528	0.44

Table 7.2: dimension of channels in Clino T.Q sample(Dosa *et al.*, 2022)

Channel type	Dp [Å]
Channel A	3 X 7.6
Channel B	3.3 X 4.6
Channel C	2.6 X 7.4

It is known that zeolites are considered microporous materials (pore diameters up to 2nm), according to IUPAC classification(Scrivener, Snellings and Lothenbach, 2018), Besides, the surface area decreased passing from Clino T.Q to Na-Clino1 and Na-Clino2. Channel's dimension for Clino T.Q sample resulted in agreement with literature data(Davarpanah *et al.*, 2020) as well as SSA values. It should be emphasized that the greater surface area recorded for 13X coul results in higher water adsorption capacity, as it will be shown in the following paragraphs.

7.2 X-Ray diffraction (XRD)

The XRD analysis was executed to determine the crystal structure and chemical composition of the investigated samples. In addition, there was the necessity to prove that ion exchange process did not affect the structure of the exchanged zeolites (Na-Clino1 and Na-Clino2).

Experimental results are shown in the graphs below:

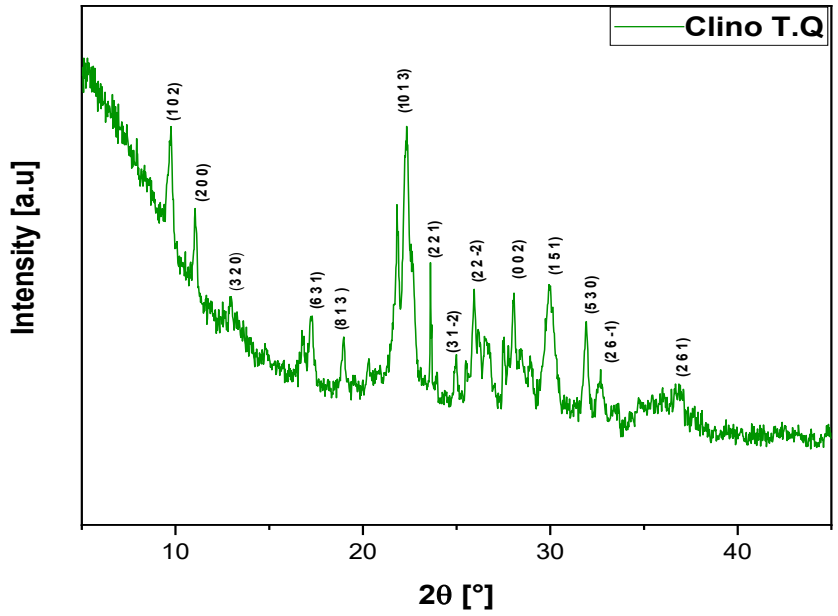

Figure 7.2: XRD pattern of Clino T. Q sample (ref.code: 00-039-1383)

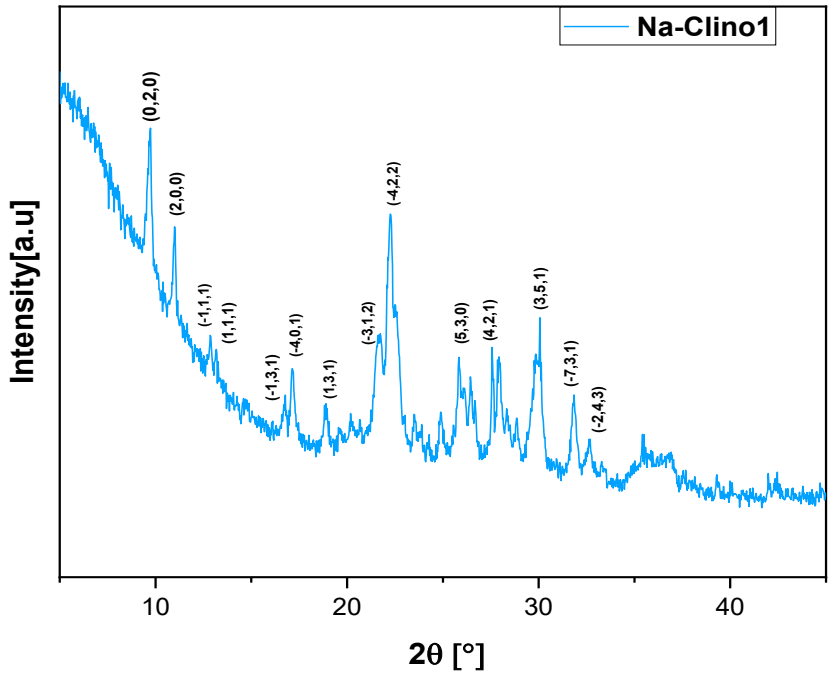

Figure 7.3: XRD pattern for Na-Clino1 sample (ref.code=96-900-1393)

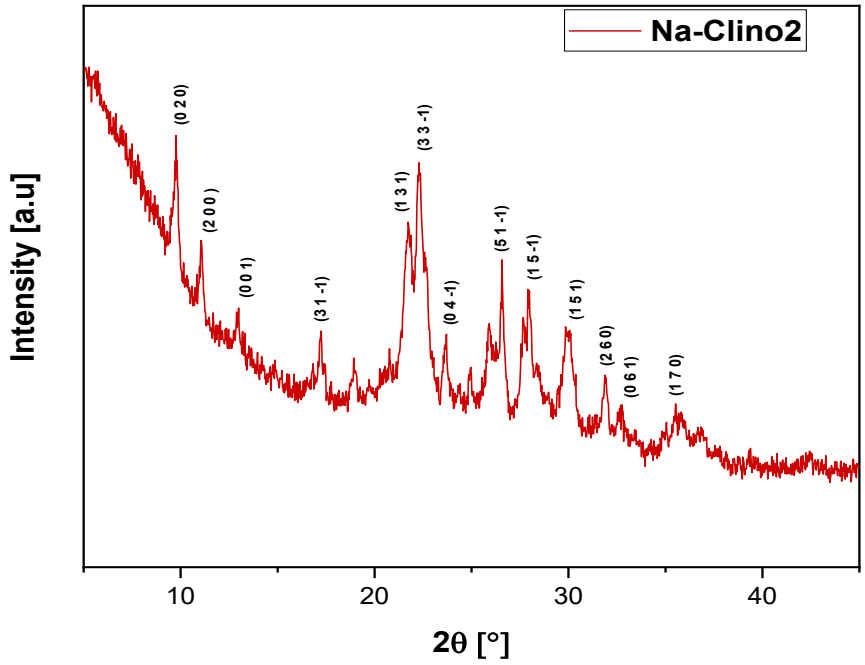

Figure 7.4: XRD pattern for Na-Clino2 sample (ref.code= 96-900-1393)

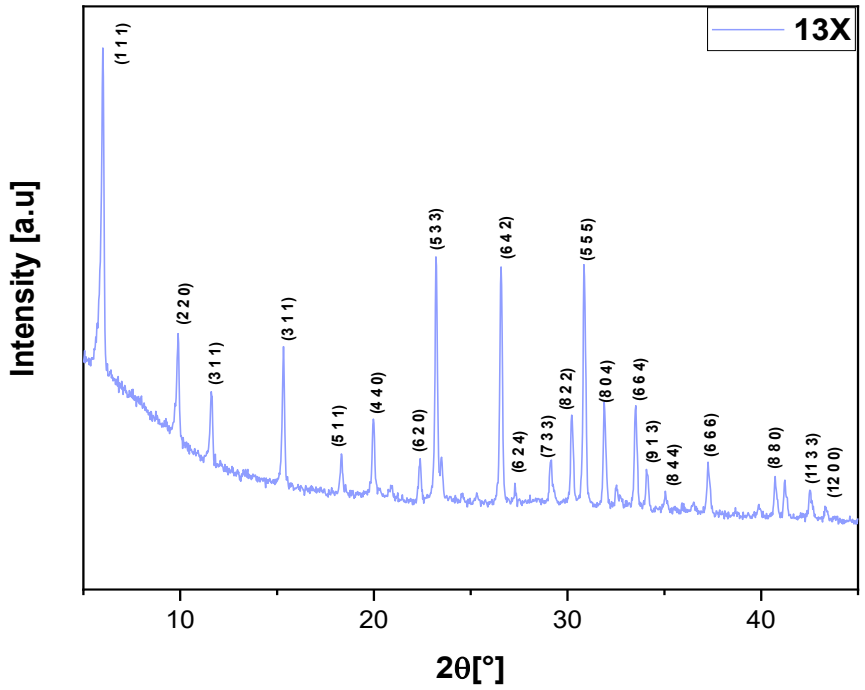

Figure 7.5: XRD pattern for 13 sample (ref.code= 00-100-8756)

It should be emphasized that XRD patterns have been indexed thanks to the software High Score plus and confronted with reference data files from ICD-PDF database. XRD diffraction peaks of all samples taken into consideration matched with the ones from the database.

More precisely, the most intensive characteristic peaks of Clinoptilolite are located at 9.67°, 22,3°, 27.9° and 28.5°. Moreover, the broader peaks which can be distinguished in the XRD patterns of natural zeolites can be attributed to smaller crystals respect to 13X zeolite, as reported in literature(Cavallo *et al.*, 2023).Finally the proof that the structure in functionalized samples was not altered by ion exchange was found in the position of the main peaks of the pattern, which remained the same in all samples.

7.2.1 XRD operando measurements

XRD in operando results are shown in the graphs below.

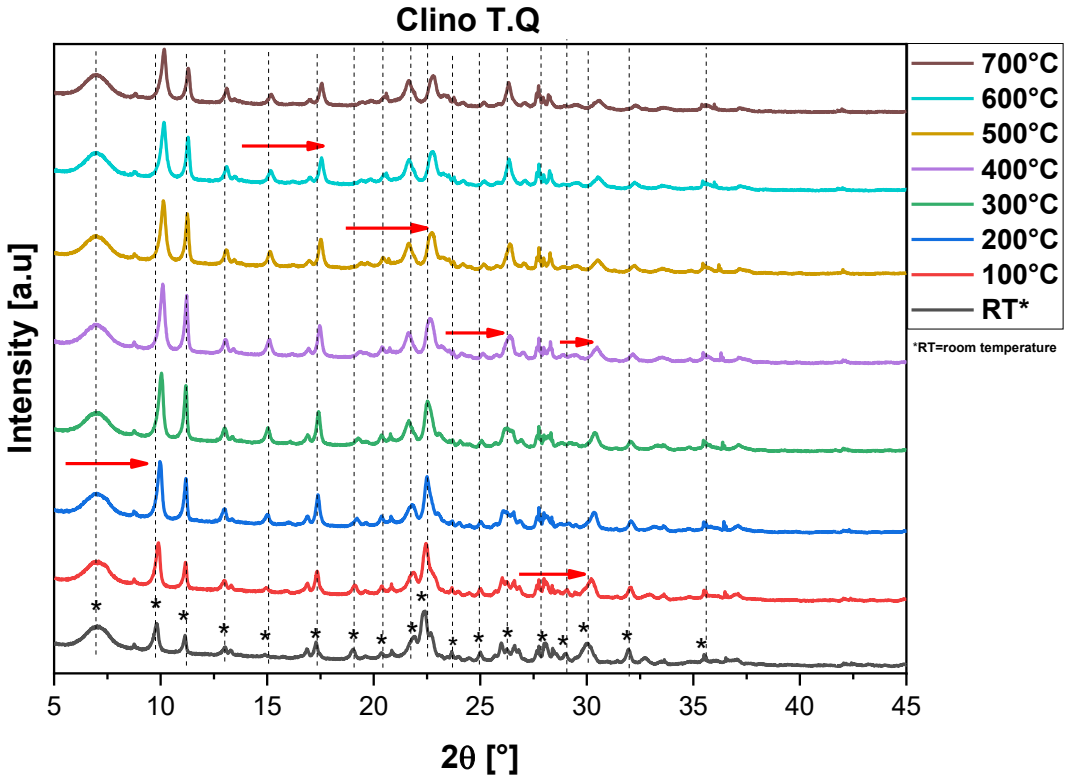

Figure7.6.: XRD operando measurements at RT (room temperature), 100°C,200°C,300°C,400°C,500°C,600°C and 700°C for Clino T.Q sample.

Red arrows in the graph indicate shifts of the diffraction peaks in higher angle regions. As reported in literature(Kukobat *et al.*, 2022), these shifts may indicate changes in the crystalline lattice of the monoclinic structure of the sample. More precisely, it was possible to observe that the diffractogram did not undergo great variation with temperature increase. As a matter of fact, the diffraction peak at 2θ=10° slightly shifted at 200°C and after it did not shift anymore. Another shift was observed at 600°C for the peak between 15° and 20°as well as for the one in the range 2θ=20-25°C at 500°C and for the one in the range 2θ=25-27° at 400°. In all these cases after the shift, the location of the peak remained stable. Finally, the diffraction peak at 30°C firstly shifted from 30°C tom100°c and then changed slightly its location when T=400°C was reached- In addition to this, it should be emphasized that the total disappearance of diffraction peaks did not occur, even at high temperatures, although is possible to note ,in certain cases, a decrease of the diffraction peaks intensity as temperature increase that is an index of the loss of crystallinity by the decomposition of the framework. In conclusion, the structural stability of natural clinoptilolite at high temperatures (up to 700°C) was proven.

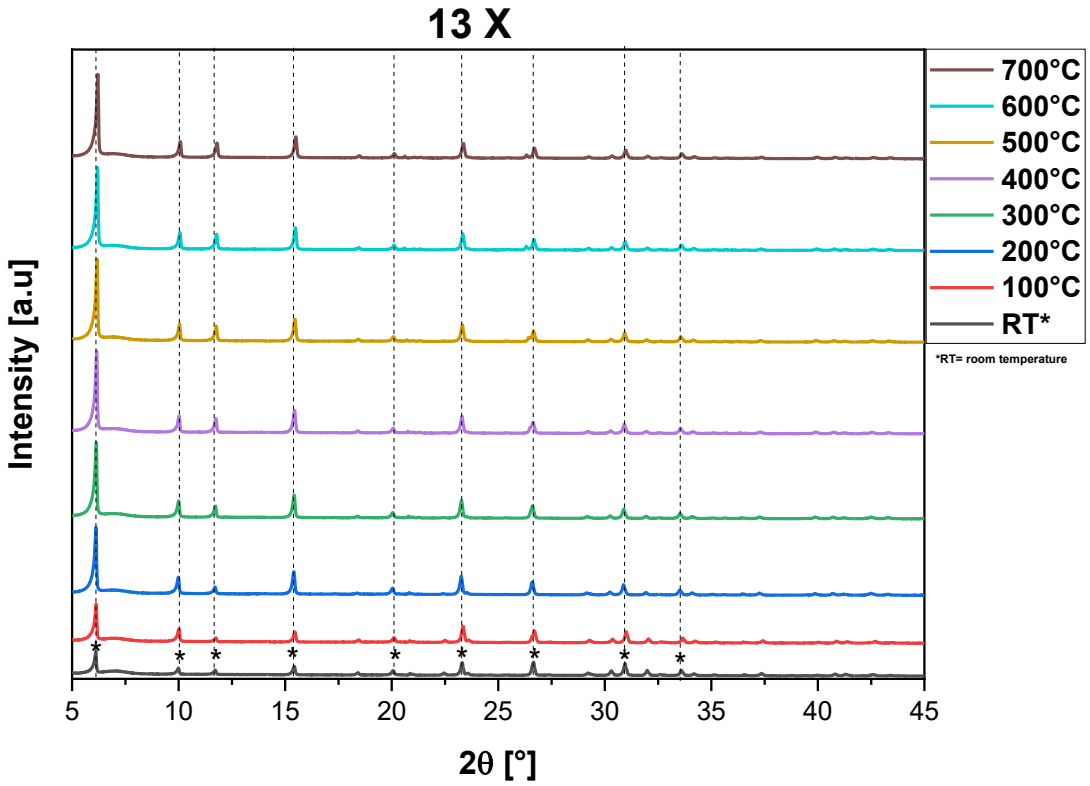

Figure7.7: XRD operando measurements at RT (room temperature), 100°C,200°C,300°C,400°C,500°C,600°C and 700°C for 13 X sample.

13 X diffractograms are reported in figure7.21. As can be observed, no significant shifts were appreciable. Finally, it can be mentioned the fact that, ranging from room temperature to 700°C some diffraction peaks, like the one located at 6.41°, seemed to change intensity. Even in this case thermal stability was demonstrated.

To sum up, thanks to XRD operando measurements it was possible to choose a pretreatment at 400°C with a temperature ramp of 5°C/ min because it was found in literature that activation temperature (i.e dehydration temperature) of clinoptilolite is T=350°C. Hence and these conditions did not affect the structure of all samples (higher temperatures are uneconomically advantageous and difficult to achieve, not to mention that diffractograms did not change significantly from T=400°C).

7.3 Energy-dispersive X-Ray analysis (EDX)

EDX results provided an analysis of the elemental composition of all natural zeolites sample whereas 13X analysis was taken from literature(Davarpanah *et al.*, 2020).

Results are summarized in the following graphs:

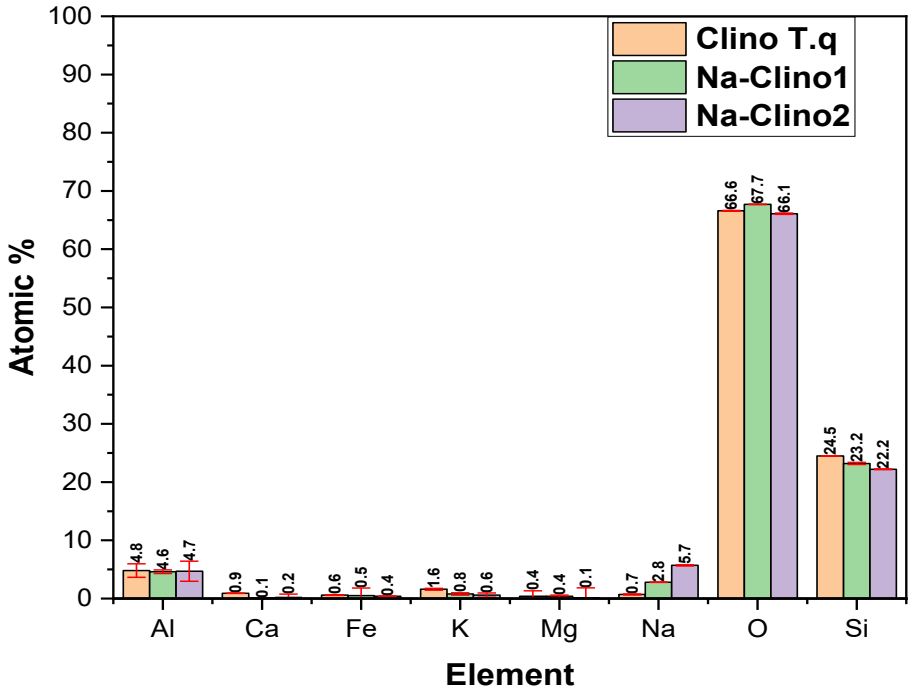

Figure 7.8: Elemental composition of the samples investigated as evaluated from EDX analysis.

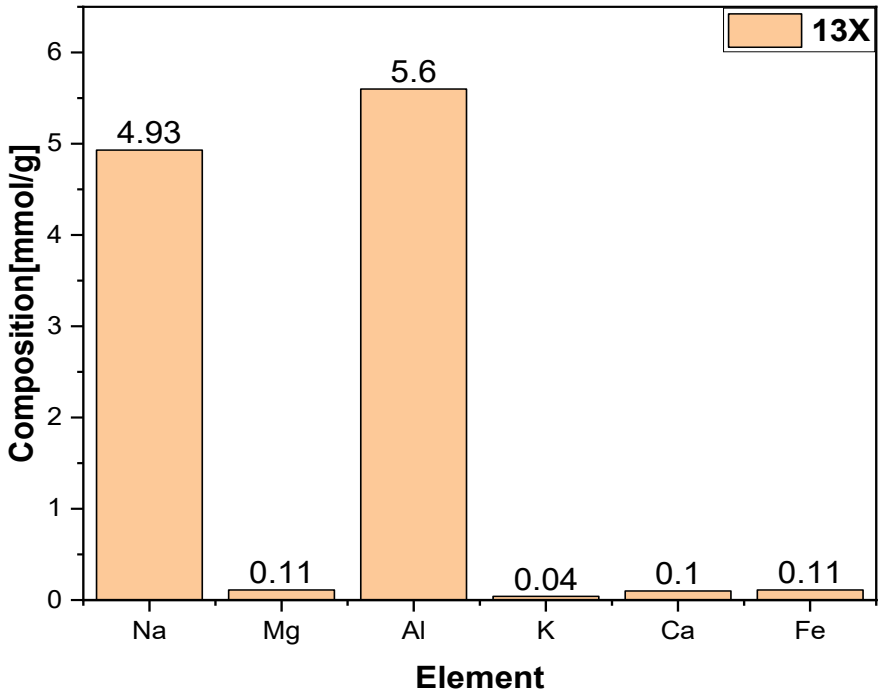

Figure 7.9: Elemental composition of synthetic 13X zeolites as reported in EDX results from(Davarpanah *et al.*, 2020)

Table 7.3: EDX elemental composition (atomic % and wt%)

Sample	Clino T Q	Na-Clino 1	Na-Clino2	Clino T. Q	Na-Clino1	Na-Clino2
Element	**Atomic %**	**Atomic %**	**Atomic %**	**Wt%**	**wt%**	**wt%**
O	66.6	67.7	66.1	52.3	54.4	53.01
Na	0.7	2.8	5.7	0.7	3.3	6.6
Mg	0.4	0.4	0.1	0.5	0.3	0.1
Al	4.8	4.6	4.7	6.3	6.2	6.3
Si	24.5	23.2	22.2	33.8	32.7	31.1
K	1.6	0.8	0.6	3.1	1.2	1.2
Ca	0.9	0.1	0.2	1.7	0.4	0.5
Fe	0.6	0.5	0.4	1.6	1.3	1.2
Total	100	100	100	100	100	100

From the values reported in **table 7.3,** both NaClino1 and Na-Clino2 presented an increased amount of sodium respect to Clino T.Q., thus confirming the successful occurrence of the ion exchange processes. Additionally, the quantity of Na^+ cations in Na-Clino2 sample doubled the one relative to Na-Clino1 sample and was sixfold the one of ClinoT.Q. On the other hand, the amount of Si and Al, and therefore Si/Al; remained almost unaltered.

By a comparison between natural and modified clinoptilolite it was possible to observe the in functionalized samples the increase of Na^+ cations led to a parallel reduction of potassium and calcium content. As a matter of fact, the atomic percentage of K^+ from 1.6% (3.1wt%) in Clino TQ climbed to 0.8% (1.2 wt%) and 0.6% (1.2 wt%) in Na-Clino1 and Na-Clino2, respectively while the amount of Ca^{2+} ions changed from 0.9 atomic %(1.7 wt%) in Clino T.Q

To 0.1 atomic % (0.4 wt%) in Na-Clino1 and to 0.2 atomic % (0.5 wt %) in Na-Clino2.

Finally, it should be noted that the quantity of Mg^{2+}ions was reduced only in Na-Clino2 sample.

It should be emphasized that these results were in agreement with the Scanning electron microscope (SEM)-EDX mapping images shown in figures 7.7, 7.8, 7.9 where it can be seen that sodium was homogeneously dispersed on samples surface of all natural zeolites samples.

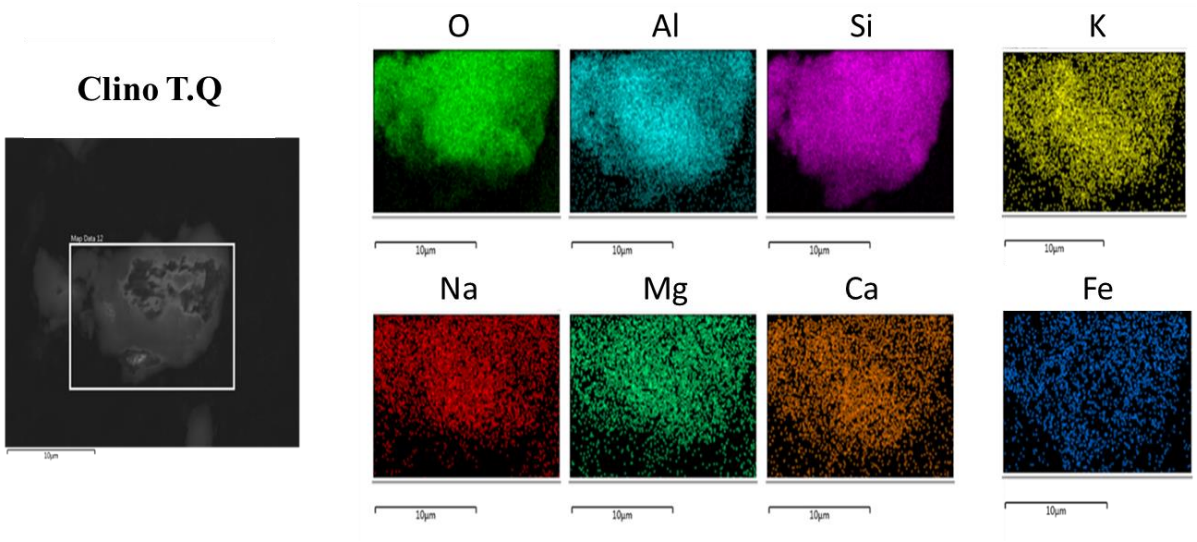

Figure 7.10: EDX mapping analysis of Clino T.Q sample

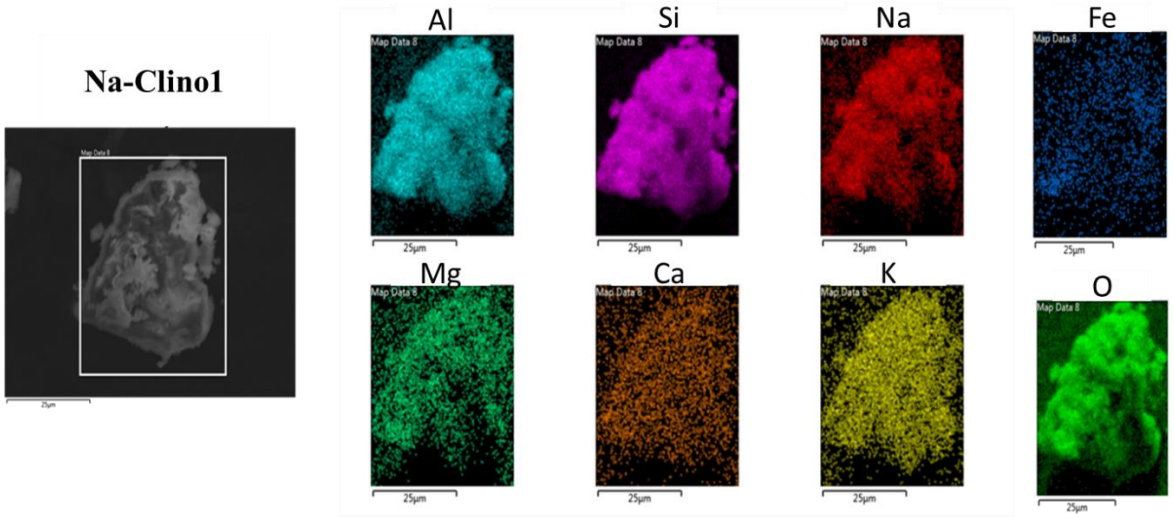

Figure 7.11: EDX mapping analysis of Na-Clino1 sample

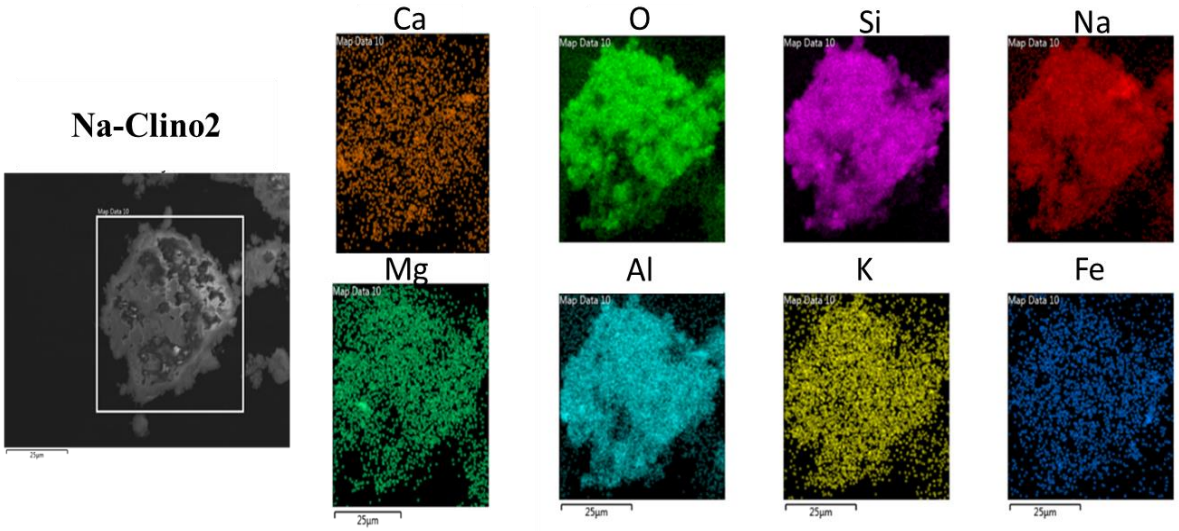

Figure 7.12: EDX mapping analysis of Na-Clino2 sample

7.4 Thermogravimetric analysis (TGA)

TG thermograms reported in literature usually show a water loss which can vary according to the sample investigated and the size of the non-framework cations. In order to understand the type of water loss, the first derivative of the TG curve is calculated to obtain DTG curve. More precisely, DTG curves usually shows three different peaks, corresponding to three different water loss phenomena. The first one is usually recorded between 60°C and 150°C and it is referred to the loss of the weekly bound water, then at higher temperatures (150-250°C) the desorption of water bound to non-framework cations and usually deposited within zeolites cavities occur while the desorption of structural water (and consequently the destruction of zeolites structure) is characterized by a DTG peak after 500°C(Castaldi *et al.*, 2005).

In this thesis, experimental results resulted perfectly in agreement with literature data, as can be observed in the following graphs.

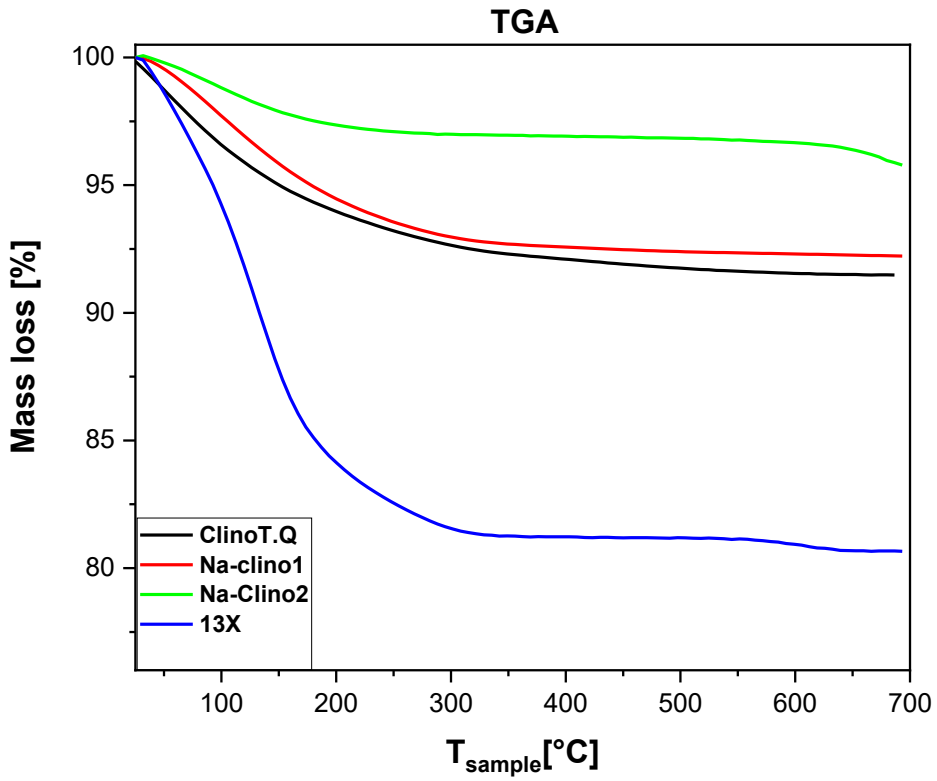

Figure 7.13.:TGA curves of the investigated samples

From TGA graphs it was possible to observe the highest mass loss for synthetic 13X zeolite, followed by Clino T.Q, Na-Clino1 and Na-Clino2. More precisely, while for 13X it was recorded 20% of mass loss from initial conditions (saturation at 25°C), Clino T.Q showed 9% of mass loss, which was slightly higher than the one related to Na-Clino1 sample (8%).Finally, Na-Clino2 showed the worst performance since only 4% of mass loss was recorded.

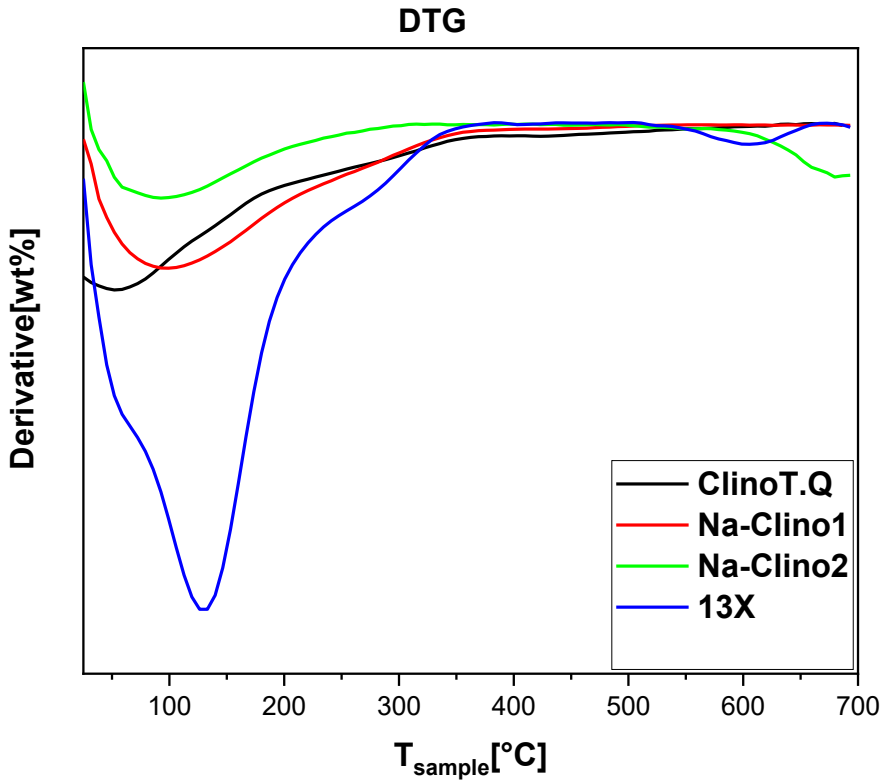

Figure 7.14: DTG curves of the investigated samples

DTG curves, on the other hand, allowed to better understand at what temperature range mass loss occurred. Therefore, it was possible to understand which type of water is lost during the analysis. As showed in the following paragraphs, the trend of DTG curves resulted quite similar to DSC's one. Firstly, it should be emphasized that all curves revealed the loss of physisorbed water, thereby not including structural water.

Additionally, it came out that for Clino T.Q sample mass loss occurred between 25°C and 150°C, thus revealing the removal of weekly bound water whereas 13X zeolite showed a broader peak between 25°C and 300°C which indicated the loss of weekly bound water, together with the removal of physiosorbed water deposited within zeolite's cavities. On the other hand, Na-Clino1 DTG showed a different slope from Clino T. Q's one, probably because of kinetic effects of mass loss, which occurred between 25°C and 225°C while it should be mentioned that Na-Clino2 sample peak was visible between 25°C and 175°C.To conclude it was observed that Clino T.Q peak seemed truncated at T=25°C,probably because dehydration process started at lower temperatures for this sample.

7.5 DSC

DSC results performed with dried samples in the temperature range between 50°C and 350°C led to the evaluation of specific heat. These values were calculated using Alumina as reference, thus obtaining specific results with an error of less than 6%. Thanks to the evaluation of the accuracy of measurements it was possible to elaborate a corrective factor which was multiplied by the cp values to obtain the final results, summarized in the table below.

Table 7.4: specific heat (cp) of the samples investigated at T=50-350°C

T	Cp Clino T. Q	Cp Na-Clino 1	Cp Na-Clino 2	Cp 13X
[°C]	**[J/K/kg]**	**[J/K/kg]**	**[J/K/kg]**	**[J/K/kg]**
50	1147.612	1394.471	1313.88	1339.82
75	1116.519	1356.782	1278.37	1177.76
100	1103.328	1338.88	1261.51	1152.32
125	1089.195	1320.036	1243.75	1056.22
150	1113.692	1344.534	1266.83	926.192
175	1119.345	1352.071	1273.94	950.69
200	1145.727	1381.28	1301.46	1033.6
225	1160.803	1400.124	1319.21	1062.81
250	1170.225	1413.315	1331.64	1175.88
275	1157.976	1402.008	1320.99	1158.92
300	1182.474	1438.755	1355.61	1179.65
325	1189.069	1448.177	1364.49	1318.15
350	1286.117	1566.895	1476.34	1451

It is also possible to visualize graphically the specific heat trend of all natural zeolites in figure 7. As can be noted, Na-Clino1 resulted in the highest cp value whereas the lowest one was possessed by synthetic 13X. Additionally, for all natural zeolites samples a downward trend was visible between 50 °C and 125°C(except for 13X, which showed a first downward trend between 50°C and 150°C, followed by one more decreasing slope of the curve between 100°C and 150°C), probably due to mass loss recorded by TG analysis, after which cp increased with temperature, recording two changes of slope at 275°C and 325°C, respectively.

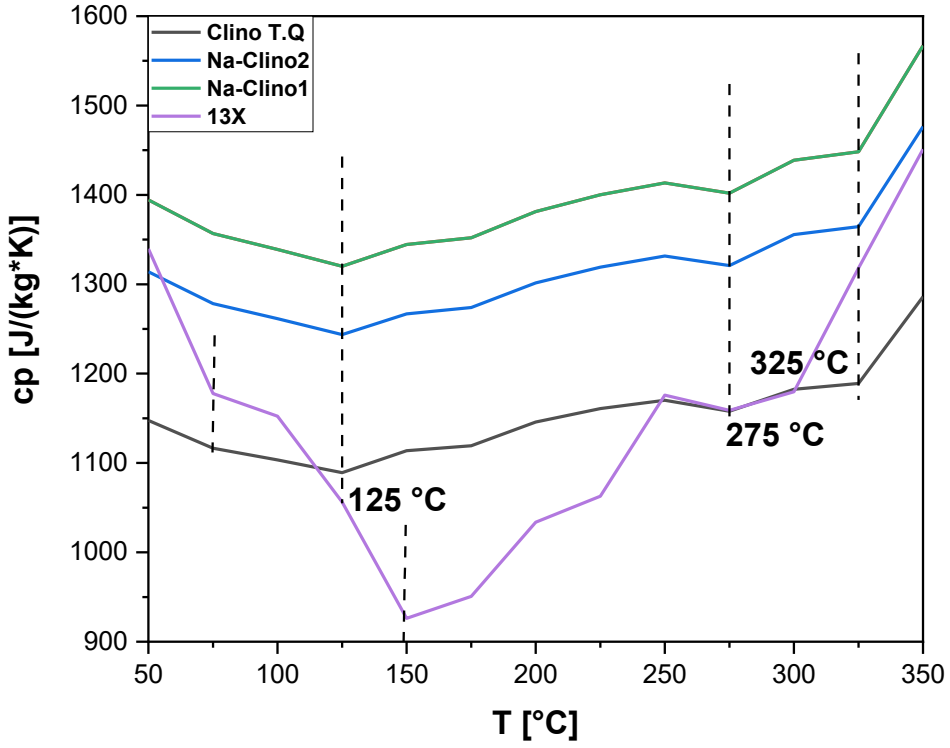

Figure 7.15: specific heat of natural zeolites samples in temperature range between 50°C and 350°C

On the other hand, DSC outcomes, related to the evaluation of specific enthalpy (ΔH [J/g]) in the temperature range between 25°C and 350°C resulted in agreement with TGA results. DSC curves for all saturated samples are reported in the graph below:

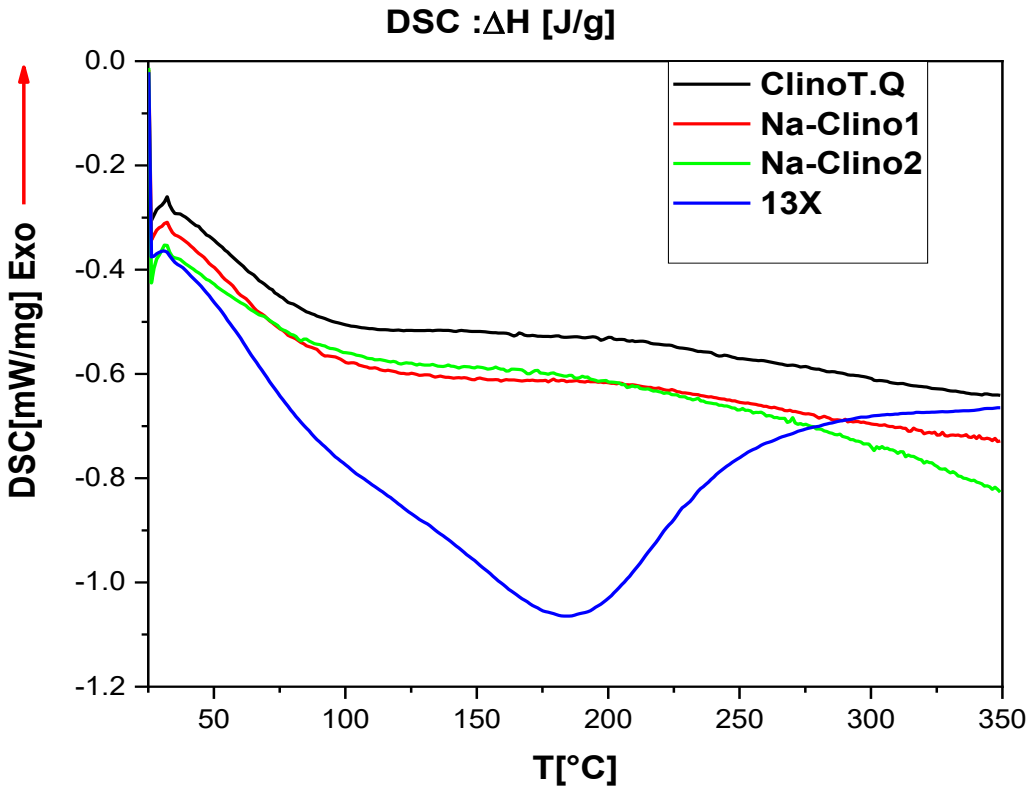

Figure 7.16.: specific enthalpy of dehydration (ΔH [J/g]) evaluated for all saturated samples in T range between 25°C-350°C.

All samples showed a broad endothermic peak approximately between 35°C and 232°C, with the exception of 13X sample, which showed a more pronounced peak in a wider range (between 39°C and 329°C), corresponding to the desorption of the physiosorbed water, that is weekly bond water (50°C-150°C) and mass loss of water placed in zeolites cavities and bound to the non-framework cations (150-250°C)(Castaldi *et al.*, 2005)

Enthalpy of dehydration values (calculated in correspondence with the endothermic peak) increased in the following order: Na-Clino2<Na-Clino1<ClinoT.Q<13X, as summarized in the following table.

Table 7.5: Enthalpy of dehydration of the investigated samples

Sample	T range[°C]	ΔH [J/g]	Endothermic peak [°C]	Energy density [kJ/m^3]
Clino T. Q	38-232	65.9	95	131840
Na-Clino1	36-222	62.9	92	125900
Na-Clino2	41-215	39.8	83	79600
13X	39-329	402	182	804000

Therefore, it was possible to draw back to the conclusion that, among the natural zeolites' samples, ClinoT.Q showed the highest specific enthalpy of hydration. In the last column of the table energy density values are reported. Energy density was calculated by diving the enthalpy

for sample's density, which was estimated from literature data [2000 kg/m^3] and values increased according to the following order: Na-Clino2<Na-Clino1<ClinoT.Q<13X.

7.6 FT-IR results

7.6.1 Identification of FT-IR spectra

As already mentioned, the final IR spectrum lies in the mid IR (MIR) region (λ=2500-25000 nm). Since transition energies caused by modifications in vibrational energy state are in this region it is possible to analyze the bands in the mid IR region to understand what type of functional groups are present in the molecule. For a proper analysis, the spectrum is typically divided in three regions(Kafle, 2019):

- Functional group region (wavenumber from 4000 cm^{-1} to 1300 cm^{-1}), where the characteristic stretching frequencies for important functional groups such as OH, NH and C=O take place.
- Skeletal bands (strong bands located in the region between 1600 cm^{-1} and 1300 cm^{-1}) are typical of the presence of aromatic and hetero aromatic molecules which show a strong out of plane C-H bending and ring bending adsorption bands in the low frequency region (wavenumber = 900-650 cm^{-1}).It can also be added that the presence of strong and broad adsorption band in the low frequency region indicates the presence of carboxylic acid dimers, amine or amides whereas its absence suggests a non-aromatic structure.
- Fingerprint region (wavenumber= 1300-900 cm ^{1}), whose portion of the band is fundamental because all those small differences in the structure and constitution of the molecule cause not negligible modifications in the appearance and distribution of adsorption bands in this region.

However, it is possible to find in literature another division of the spectrum, based on the type of bonds(Berthomieu and Hienerwadel, 2009a):

- Single bond region, detectable at higher frequencies (wavenumber=4000-2500 cm^{-1})
- Triple bond region, detectable in the middle wavenumber between 2500 and 2000 cm ^{1}
- Double bond region, located in a range between 2000 and 1500 cm $^{1.}$
- Fingerprint region (wavenumber =1500-600 cm^{-1}) where a complex pattern of vibrations, specific for a determined molecule as a whole, occurs and provides useful information for identifying the molecule itself.

7.6.2 FT-IR spectra: effect of pre-treatment and water adsorption

During the FT-IR analysis, a spectrum of each sample was taken either before or after the pretreatment. It appeared clear that, after pretreatment at 400°C, in all cases profile and intensity of bands appeared lower, as it is possible to observe in figures below:

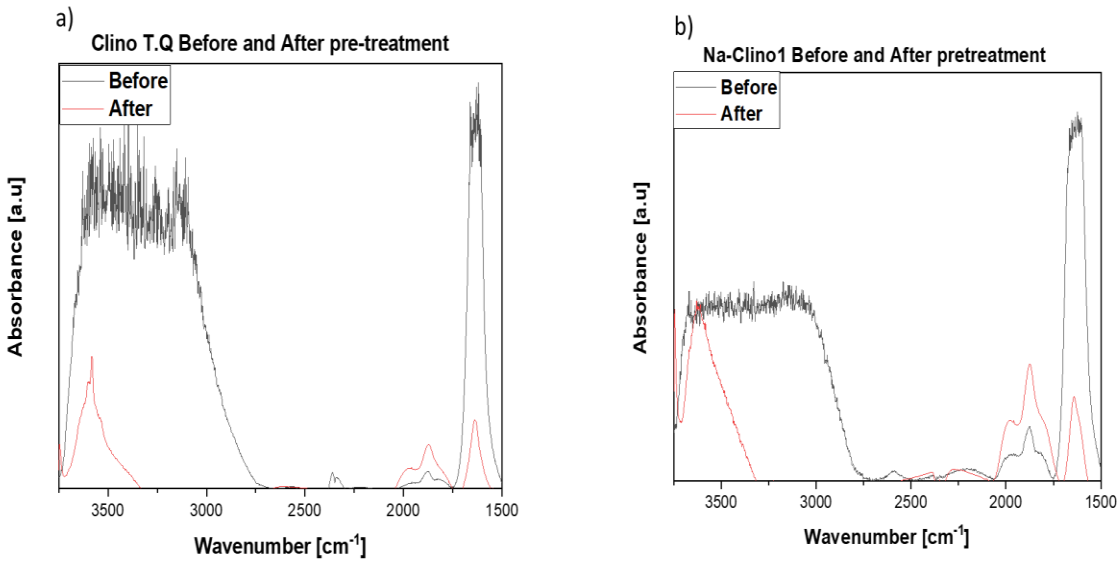

Figure 7.17: a) ClinoTQ and b) Na-Clino1 comparison between spectra before and after pretreatment at 400°C for 1h

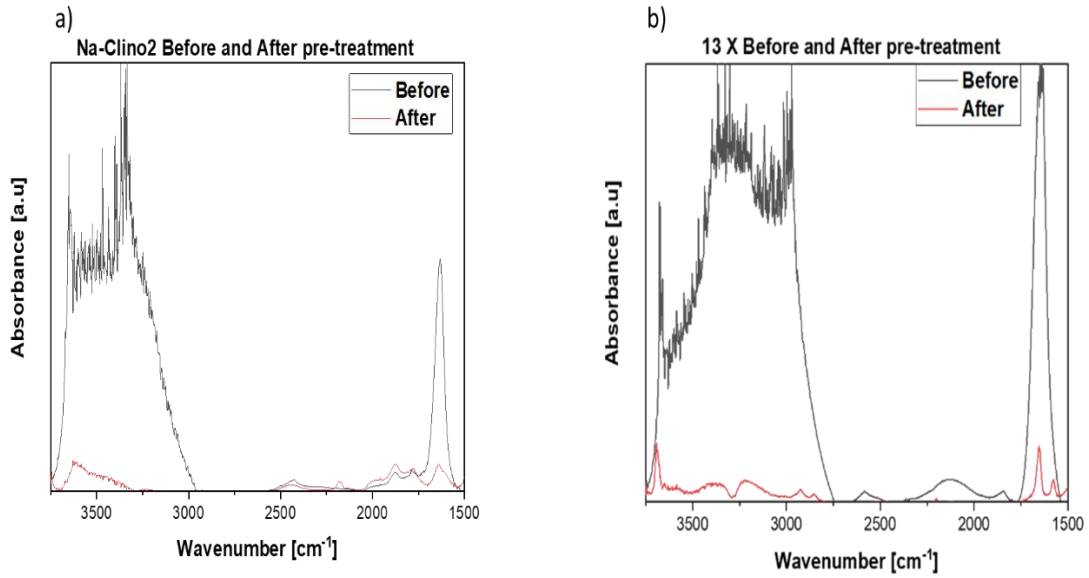

Figure7.18: a) Na-Clino2 and b) 13X comparison between spectra before and after pretreatment at 400°C for 1h.

As already mentioned, FT-IR spectroscopy was exploited to quantitatively evaluate zeolites' affinity with water. It is known from literature(Higgins, de Leeuw and Parker, 2002b; Berthomieu and Hienerwadel, 2009b; Ruiz-Serrano *et al.*, 2010; G Carotenuto and Camerlingo, 2020; Cocuzza *et al.*, 2022) that water molecules are responsible for two types of adsorptions in a FT-IR spectrum. The first type of adsorption is related to the stretching vibration of hydroxyl groups (-OH) and corresponds to the band located in the spectrum region between 3750 and 3100 cm^{-1} whereas the other type of adsorption consists in the bending vibration of these -OH groups and it is visible in the spectrum region between 1700 and 1500 cm^{-1}, creating a tight adsorption peak centered between 1650-1639 cm^{-1}, according to the sample investigated. This peak can be attributed to water associated with Na^{+} and Ca^{2+}cations located in zeolites

'channels. In figure 7.9 there is a comparison among all the bands, and it is possible to observe changes in the position of all peaks in the above-mentioned bands.

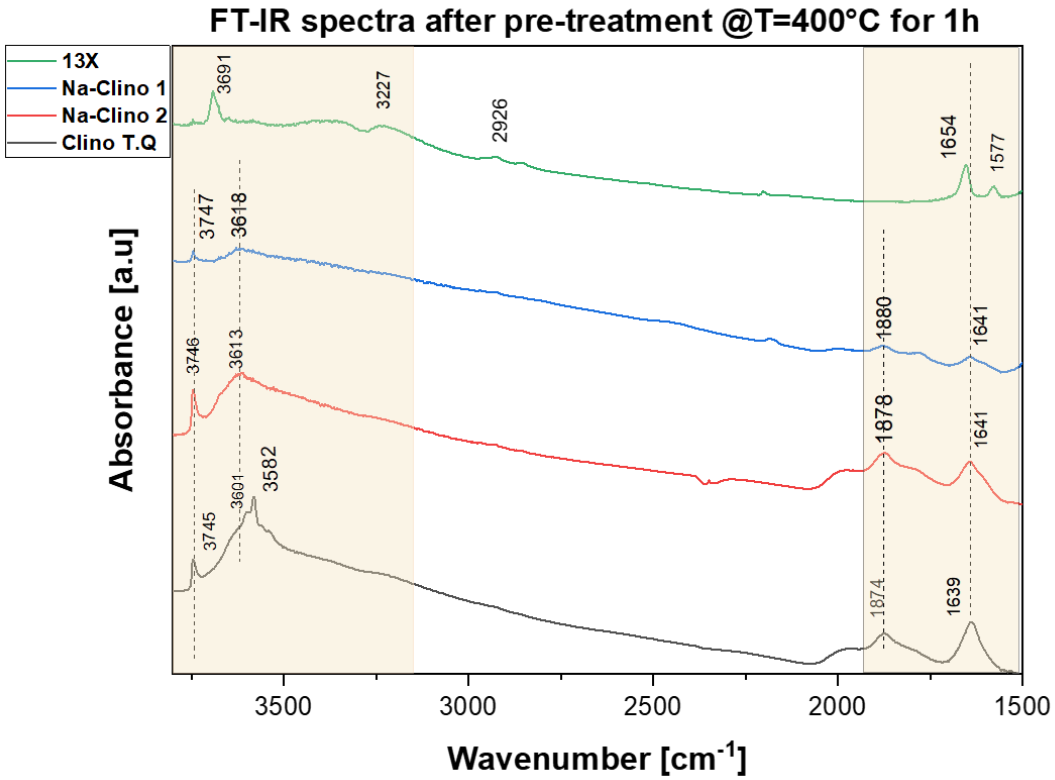

Figure 7.19: Overview of all the spectra after pretreatment with indexed peaks.

It must be added that the -OH stretching region (3750-3100) cm^{-1} in natural clinoptilolite is characterized by the presence of one broader peak. More precisely, the peak located at 3582cm^{-1} or the adjacent one at 3601 cm^{-1} could correspond to the one which, according to literature data, is usually located at 3610cm^{-1}(G Carotenuto and Camerlingo, 2020) or 3621cm^{-1} (Cocuzza *et al.*, 2022) and can be attributed to -OH in isolated external silanol groups (Si-OH). This peak is shifted to 3613 cm^{-1} and 3618 cm^{-1}in Na-Clino1 and Na-Clino2, respectively whereas it is not visible in 13X spectrum. Moreover, in the broad bands of the three clinoptilolite samples is not clearly noticeable the peak that according to other studies should be placed at 3354cm^{-1} (G Carotenuto and Camerlingo, 2020)or at 3420 cm^{-1}(Ruiz-Serrano *et al.*, 2010) , attributed to the -OH groups which belong to H_2O molecules and are involved in the hydrogen bonds with the superficial oxygen atoms or the external silanol groups. This latter peak could correspond to the one at 3582 cm^{-1} in ClinoT.Q sample, shifted in space. Regarding the -OH bending region, the tight peak is centered at 1639 cm^{-1} in Clino T. Q, while Na-Clino1 and Na-Clino2 present a peak slightly shifted at 1641cm^{-1} and finally. These peaks correspond to the one located at 1654cm^{-1} in zeolite 13X. Therefore, it was possible to conclude that there were no significant changes in peaks location in the investigated samples after pretreatment. As a matter of fact, according to literature the effect of heating in natural and modified zeolites could be observed in the bands between 710-600 cm^{-1} due to pseudo-lattice vibration(Higgins, de Leeuw and Parker, 2002b).As a matter of fact, peaks located in this region can be attributed to vibrations of SiO_4 or AlO_4 tetrahedra due to the stretching of intertetrahedral bonds that are typical of crystalline structures(Higgins, de Leeuw and Parker, 2002b; Ruiz-Serrano *et al.*, 2010). However, this region of the spectra was not investigated in this thesis.

Once identified the most important regions, a focus of all the spectra was done in two different wavenumber ranges:

- One in the range between 3750-3100 cm^{-1} related to -OH stretching vibrations.
- One in the range between 1800-1500 cm^{-1} related to -OH bending vibrations.

After pretreatment water was used as a kind of probe molecule to investigate its affinity with each zeolite.Hencet, water at different line pressures (ranging from 9e-04mbar to 1 mbar) was gradually sent and adsorbed to each sample, until reaching saturation. As already stated, this analysis was performed in order to understand the hydrophilic behavior of each sample, usually strictly correlated with the Si/Al ratio. However EDX results have shown that the content of Si and Al remained quite unchanged in all natural zeolites and therefore, the hydrophilic behavior was investigated in relation with the content and influence of extra-framework cation (i.e Na^+).It should be noted that stronger hydrophilic behavior does not always correspond to higher adsorption performance(Aghemo et al., 2023).

Studies reported in literature stated that the presence of small cations such as Na^+ whitin zeolites structure causes an increase in the adsorption heat. Hence FT-IR spectroscopy helped to understand the surface chemistry of a water adsorbed zeolite as well as the influence of alkali metal cations. From these spectroscopic analyses it came out that natural unexchanged zeolites tend to exhibit preferential water clustering, which means that the interaction between two water molecules tend to be stronger than the one between a water molecule and the adsorption site, especially at low pressures. On the other hand, in exchanged zeolites at lower pressure water clustering is prevented by the stronger interaction between the sorbate molecule (i.e water) and the cation itself and then all water molecules result bound to the adsorbent surface through the help of cations(Aghemo et al., 2023).In this scenario, since the interaction between other water molecules and cations is favored respect to the one between only water molecules, chemisorption in exchanged zeolites tend to replace the traditional physisorption, thus theoretically enhancing the adsorption ability.At higher pressures a second adsorbed layer starts to form(Jentys et al., 1989; Lavagna et al., 2020).It should be noted that the main consequence of a stronger interaction is the higher amount of energy for desorption (i.e regeneration) phase.

A scheme of the mechanisms of adsorption on zeolites is reported in figures below:

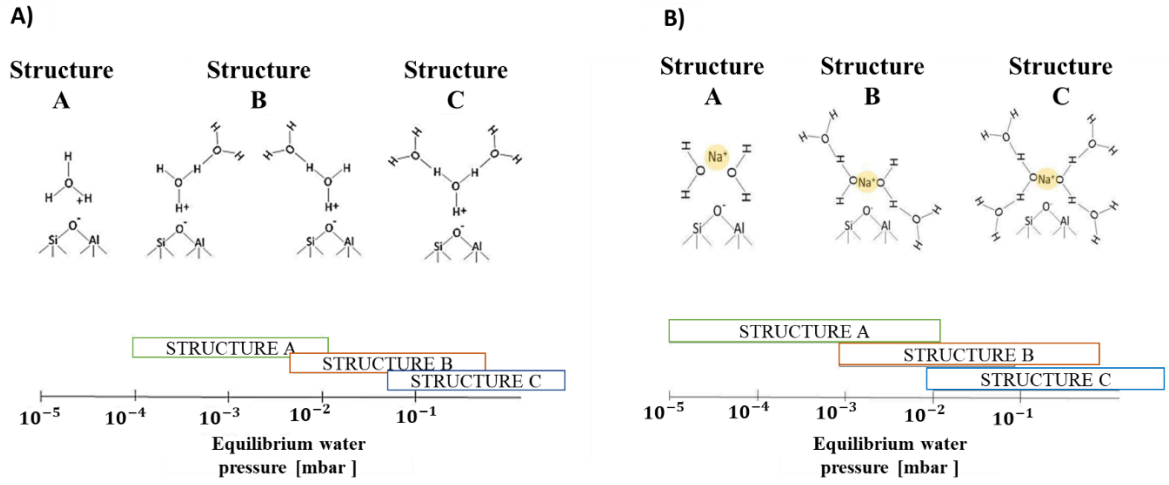

Figure7.20: schematic of water adsorption mechanism on unexchanged zeolites A) and zeolites exchanged with sodium B). Illustration taken from(Jentys *et al.*, 1989) with modifications.

Spectra were collected, normalized respect to the superficial density of the given sample and respect of maxim intensity of peaks spectra and therefore were plotted in order to verify, if the adsorption process was effective. A gradual expansion followed the adsorption phase. This last

step was executed in order to investigate if it was possible to desorbed water simply by reducing pressure, without thermal treatment. Experimental results are described below for each sample.

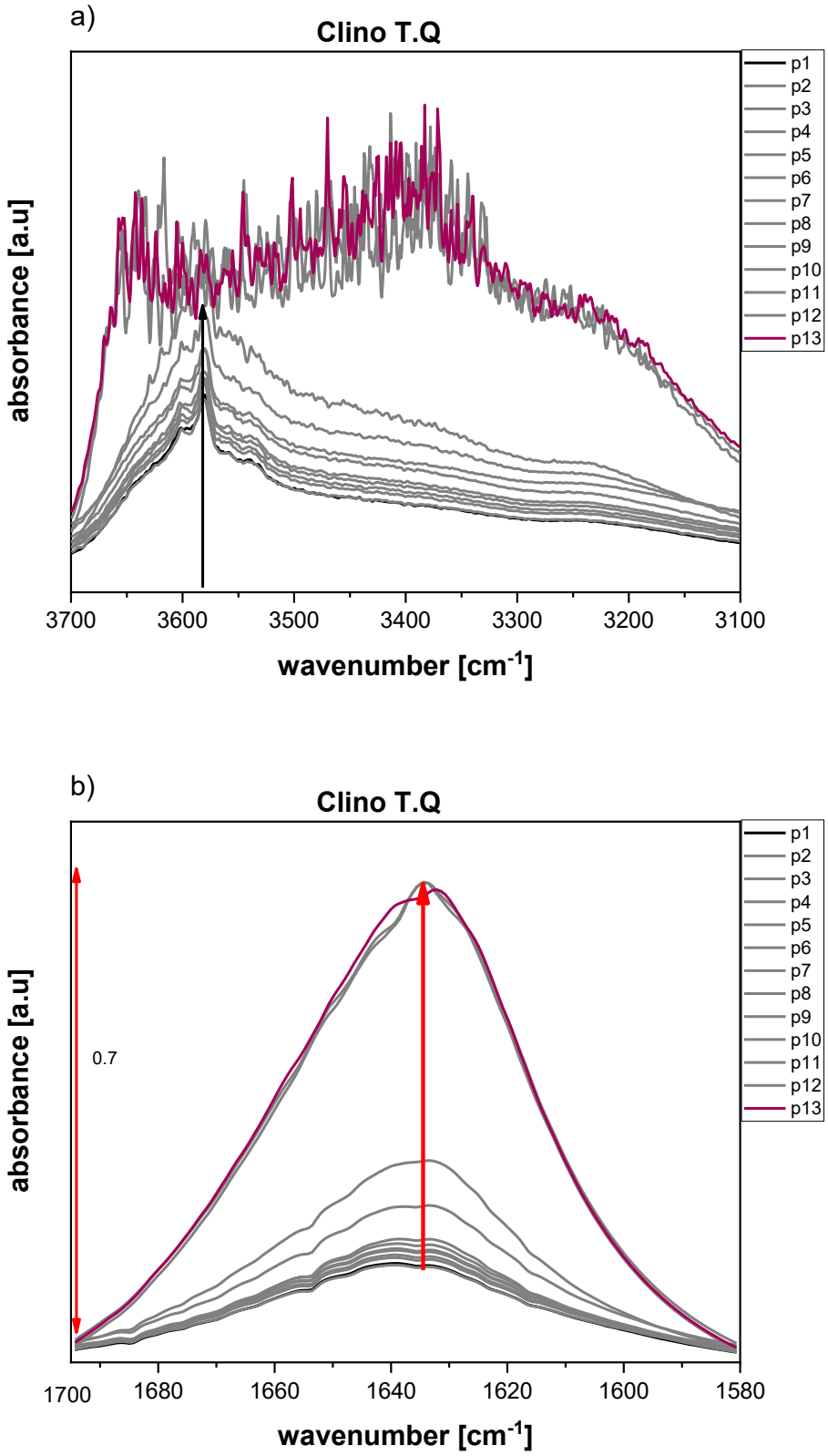

Figure 7.21: FT-IR spectra related to the adsorption of water at different pressures, magnification of the regions of interest related to a) -OH stretching and b)-OH bending for Clino T.Q.

Table 7.6: Pressures of the line related to water adsorption process.

Sample identification	P Spectrum[mbar]
P1	6e-3
P2	5.1e-3
P3	7.6e-2
P4	6.6e-3
P5	6.8e-3
P6	6.1e-3
P7	1.1e-2
P8	1.63e-2
P9	2.4e-2
P10	4e-2
P11	1,3e-1
P12	2.2e-1
P13	

Looking at figure 7.21, in both investigated regions the amplitude of the bands followed an upward trend with the increase of pressure, thus confirming that water adsorption took place. This is evident especially at higher values where there is no overlapping between spectra. As a drawback, spectra related to the gradual expansions resulted to be quite overlapped, especially between 3750-3100 cm ^{1}, as can be seen in figure 7.22. Only in the region related to -OH bending there was a slight decrease of the peaks at t=60min, before the last expansion it was not possible to perceive the curve's lowering. To sum up, expansions' spectra proved that the water desorption process could occur properly only with a thermal treatment.

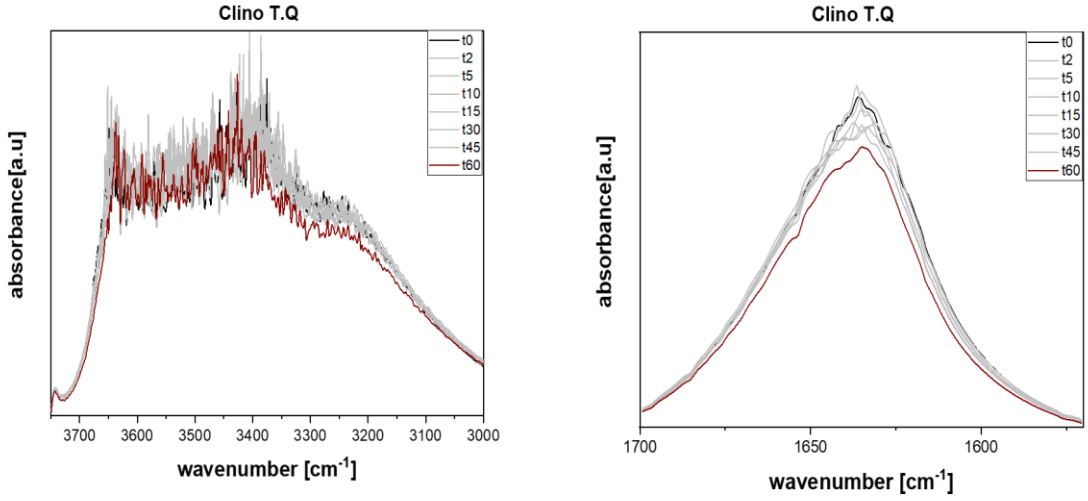

Figure 7.22: FT-IR spectra related to gradual expansion.

A similar trend is noticeable for Na-Clino1 sample, as shown in the following section. It should be emphasized however that there was the need of collecting more spectra to reach saturation.

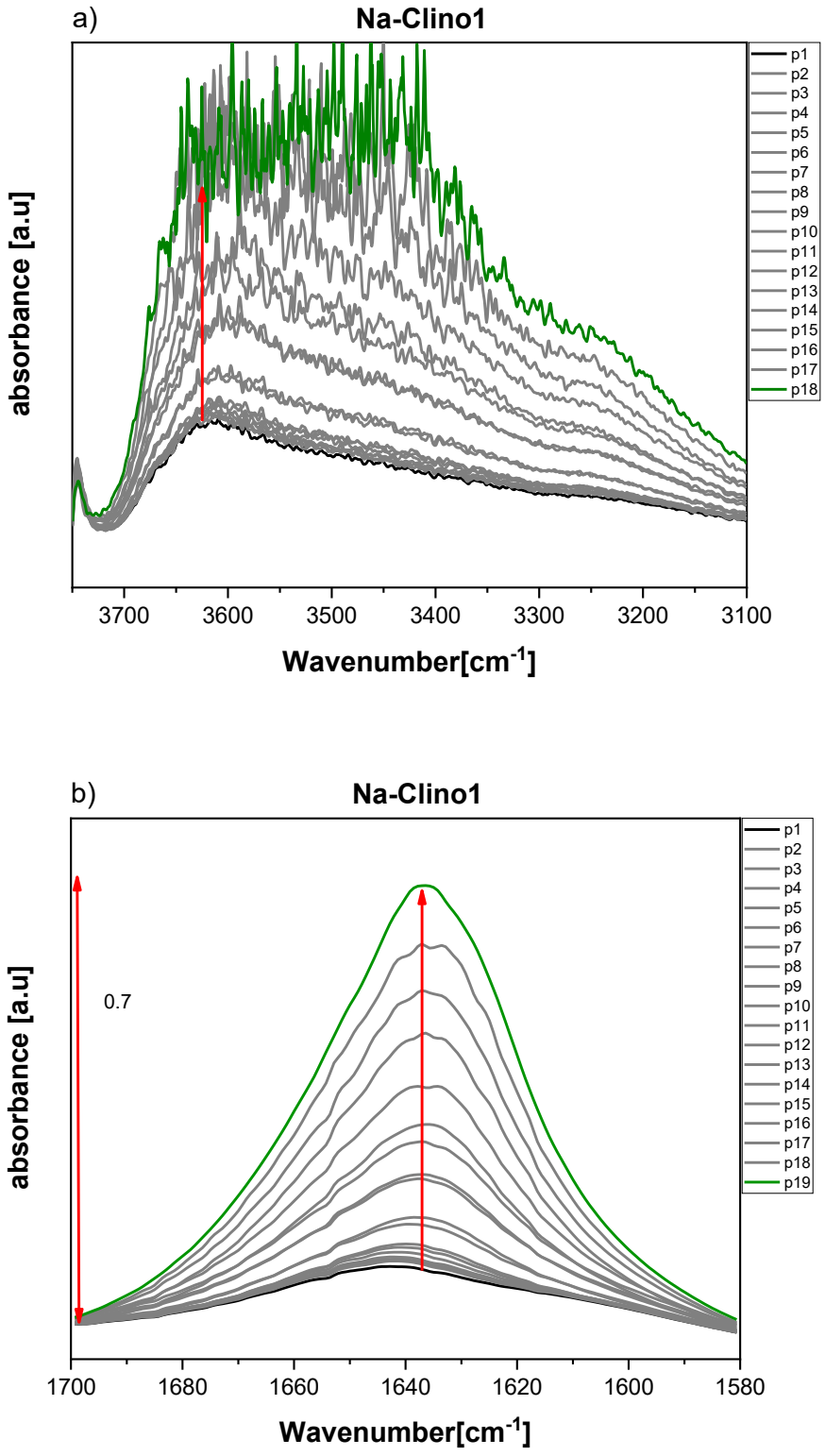

Figure 7.23: FT-IR spectra related to the adsorption of water at different pressures, magnification of the regions of interest related to a) -OH stretching and b) -OH bending for Na-Clino1.

Table 7.7: Pressures of the line related to water adsorption process.

Sample identification	P Spectrum[mbar]
P1	5e-03
P2	4.30e-03
P3	3.70e-03
P4	3.90e-03
P5	6.00e-03
P6	6.30e-03
P7	5.40e-03
P8	7.40e-03
P9	1.40e-02
P10	2.30e-02
P11	2.50e-02
P12	3.00e-02
P13	3.70e-02
P14	4.70e-02
P15	5.40e-02
P16	5.7e-02
P17	6.3e-02
P18	8e-02
P19	1.2e-01

As shown in figure7.23 case the vertical expansion of the band due to pressure's rise was as evident as the previous case Finally even in this case thermal treatment resulted necessary to achieve desorption since the signal resulted disturbed and it was not possible to notice the gradual drop of intensity peaks, as can be seen in figure 7.24.

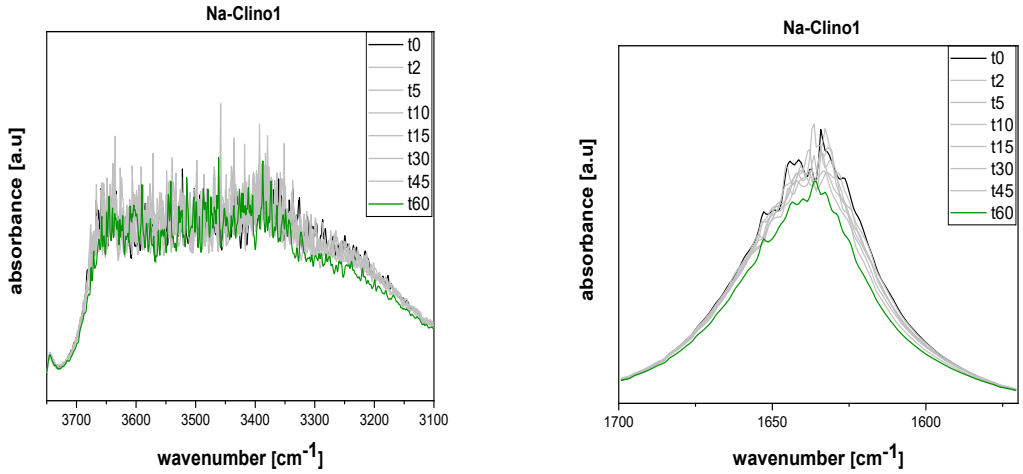

Figure 7.24.: FT-IR spectra related to gradual expansion for Na-Clino1.

On the other hand, Na-Clino2 sample was the only one that seemed to show minor affinity with water, this appeared to be clear during the expansions especially in the region relate to -OH bending, where the gradual decrease of the height of peak centered at 1641cm^{-1}demonstrated

that water in this zeolite could be desorbed simply by increasing pressure. This could also justify the results obtained during the adsorption tests, as will be shown in the following sections. Experimental results are given below.

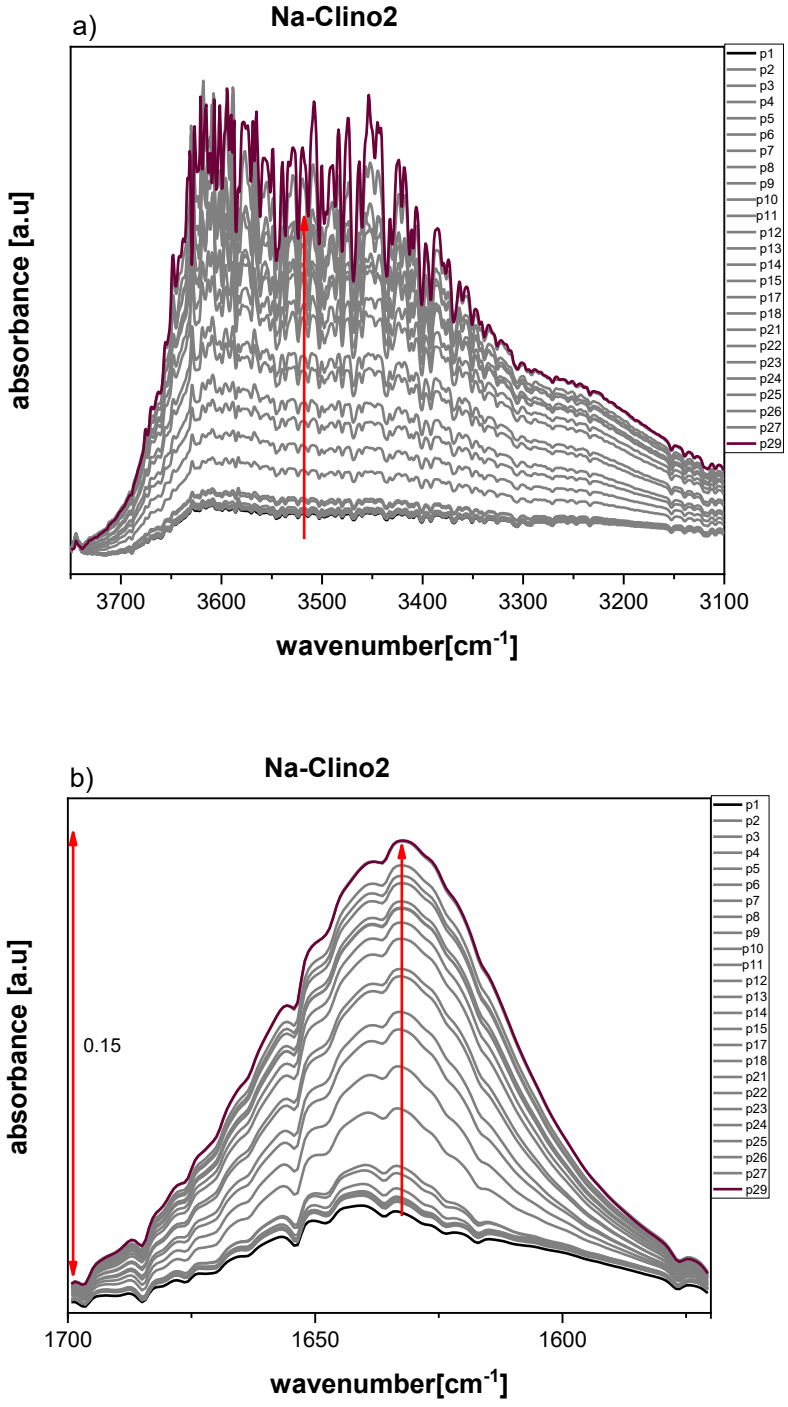

Figure 7.25: FT-IR spectra related to the adsorption of water at different pressures, magnification of the regions of interest related to a) -OH stretching and b) -OH bending for Na-Clino2

Table 7.8: Pressures of the line related to water adsorption process.

Sample identification	P Spectrum[mbar]

P1	
P2	4.00e-03
P3	3.20e-03
P4	4.10e-03
P5	8.10e-03
P6	9.10e-03
P7	1.26e-02
P8	1.90e-02
P9	2.30e-02
P10	4.10e-02
P11	5.50e-02
P12	8.30e-02
P13	1.16e-01
P14	1.52e-01
P15	2.10e-01
P16	2.50e-01
P17	3.13e-01
P18	4.1e-0.2
P19	5.5e-02
P20	8.3e-01
P21	1.16e-01
P22	1.52e-01
P23	2.5e-01
P24	3.13e-01
P25	4.45e-01-
P26	5.88e-01
P27	6.83e-01
P28	7.7e-01
P29	8.76e-01

Finally, in **figure 7.26** the downward trend of FT-IR spectra is undoubtedly distinguishable.

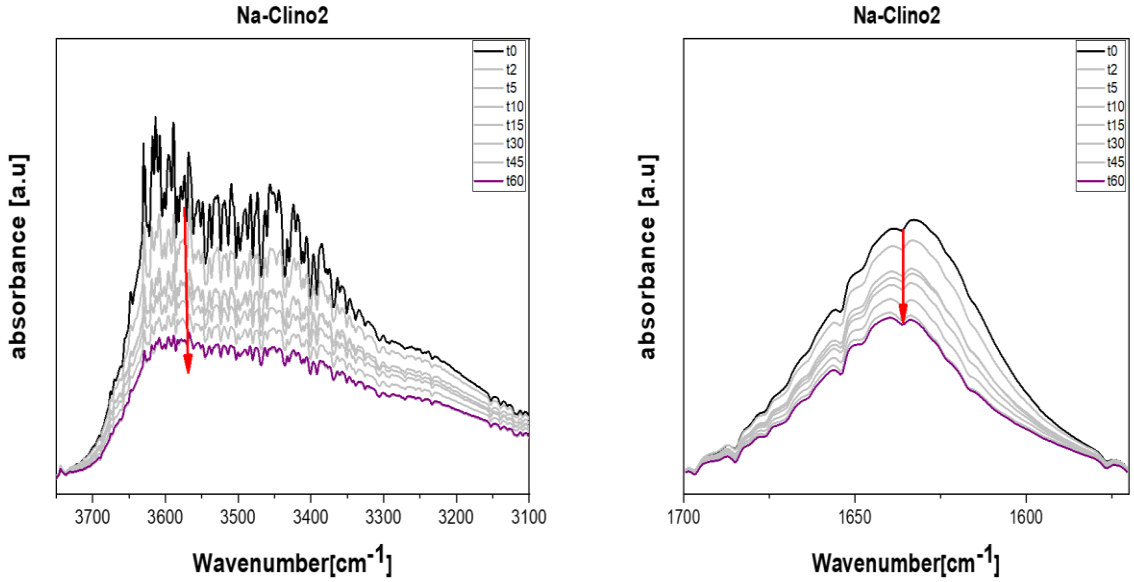

Figure 7.26: FT-IR spectra related to gradual expansion for Na-Clino2.

The last spectra collected were the ones related to 13 X, reported in figure 7.16. The synthetic zeolites demonstrated great adsorption capacity towards water molecules. This was supported by a net increase in peak's intensity, especially in the bending zone. Moreover, in this case, looking at the stretching region the presence of three peaks was noted, one centered at 3691cm $^{-1}$, the other one between between 3500 cm^{-1} and 3200 cm^{-1}(the shoulder of the band) and the last one around 3200 cm^{-1}. As previously mentioned, these peaks could be identified with the ones reported in literature:

- A peak at 3354 cm^{-1} has usually been identified with the one related too -OH groups involved to hydrogen bonds or linked to external sylanol groups (G Carotenuto and Camerlingo, 2020) .The same peak was detected by Ruiz-Serrano et al. at 3420 cm^{-1}(Ruiz-Serrano *et al.*, 2010)
- A peak centered at 3256 cm^{-1}has been attributed to -OH stretching surface silanol involved in hydrogen bonds (Carotenuto and Camerlingo, 2020).

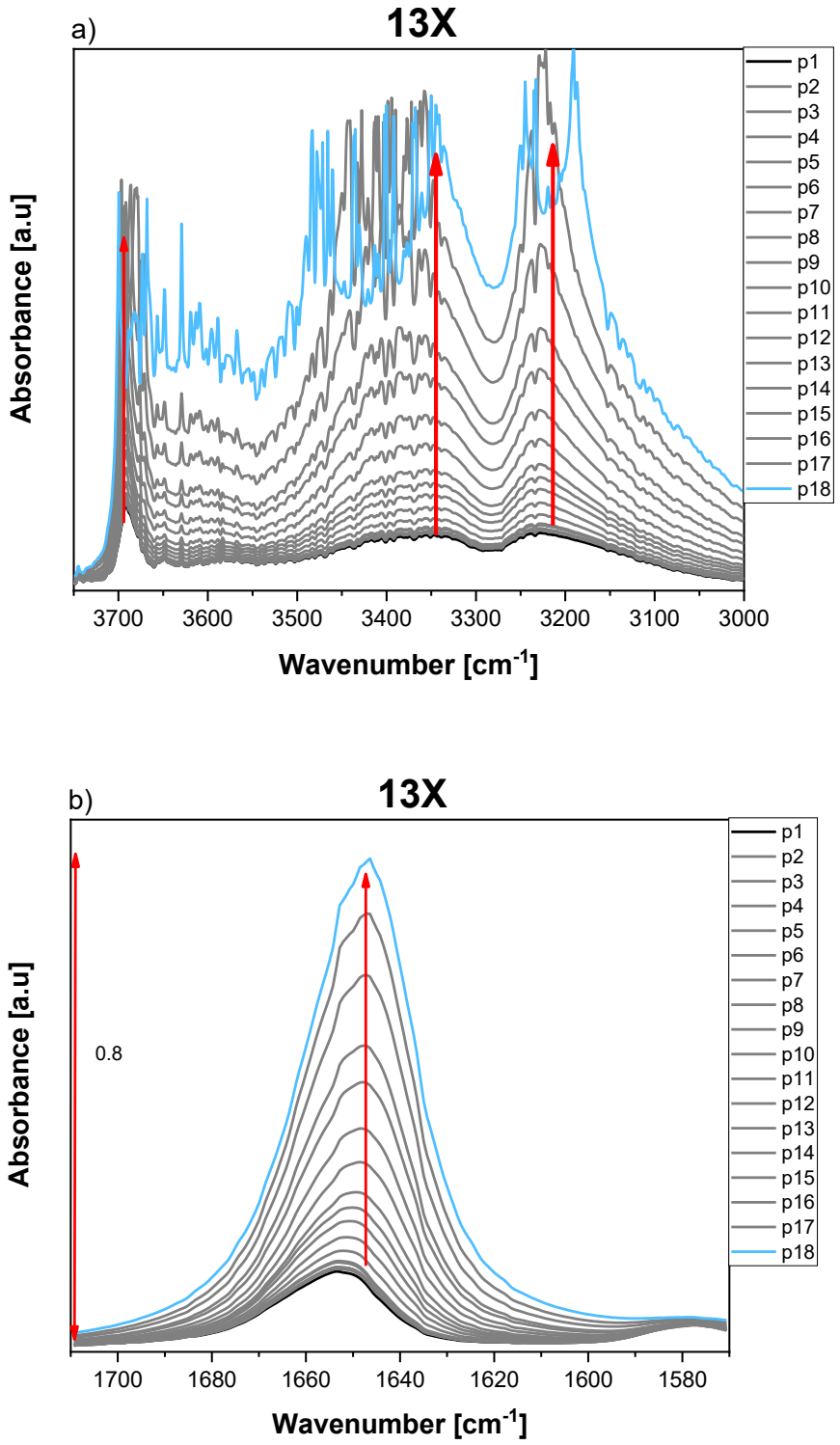

Figure 7.26: FT-IR spectra related to the adsorption of water at different pressures, magnification of the regions of interest related to -OH stretching and -OH bending for 13 X.

Table 7.9: Pressures of the line related to water adsorption process.

Sample identification	P Spectrum[mbar]
P1	6e-03
P2	5.30e-03
P3	4.00e-03
P4	4.90e-03
P5	5.80e-03
P6	4.00e-03
P7	3.80e-03
P8	5.55e-03
P9	7.30e-03
P10	1.16e-02
P11	1.60e-02
P12	2.18e-02
P13	2.95e-02
P14	3.5e-02
P15	4.5e-02
P16	6.05e-02
P17	8.08e-02

Finally, it could be added that the greater affinity of 13 X with water was also testified by the spectra relative to gradual expansion where there was an almost complete overlapping, thereby demonstrating that the desorption process didn't occur. Only a slight decrease of the spectra occurred between 3300 and 3200 cm^{1}, as shown in the figure below.

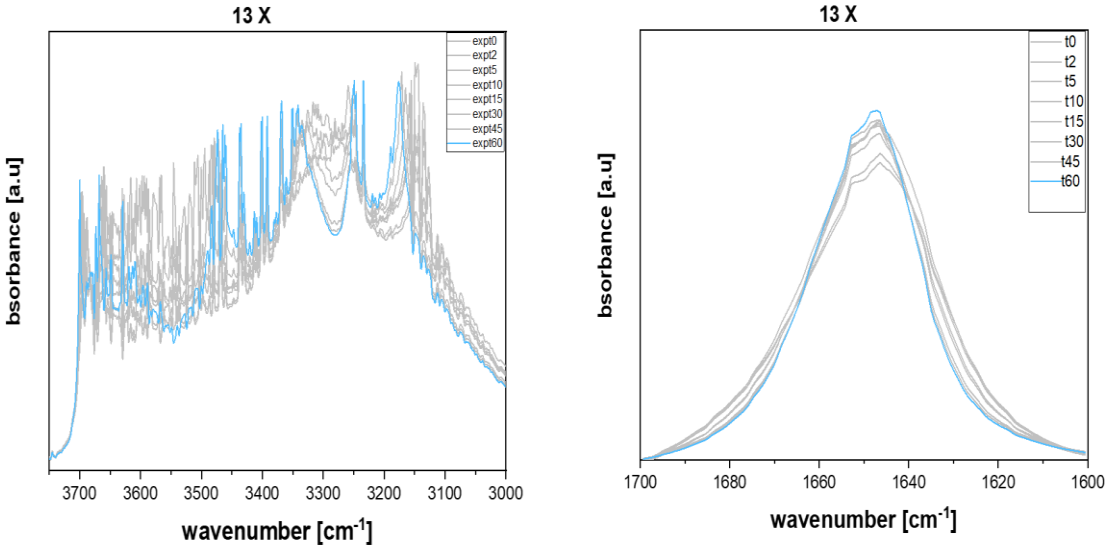

Figure 7.27: FT-IR spectra related to gradual expansion for 13 X.

To conclude this section, it should be highlighted that FT-IR adsorption tests with water were utilized to evaluate natural zeolites' affinity toward water. Firstly, a comparison between spectra in -OH bending region (representative of zeolitic water) at low, medium and high pressures was observed through the following images.

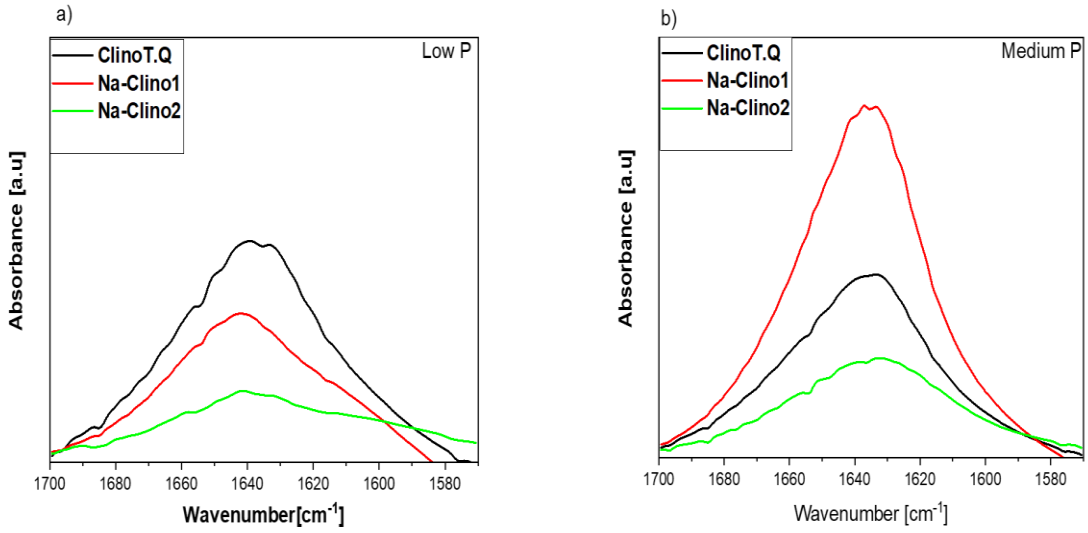

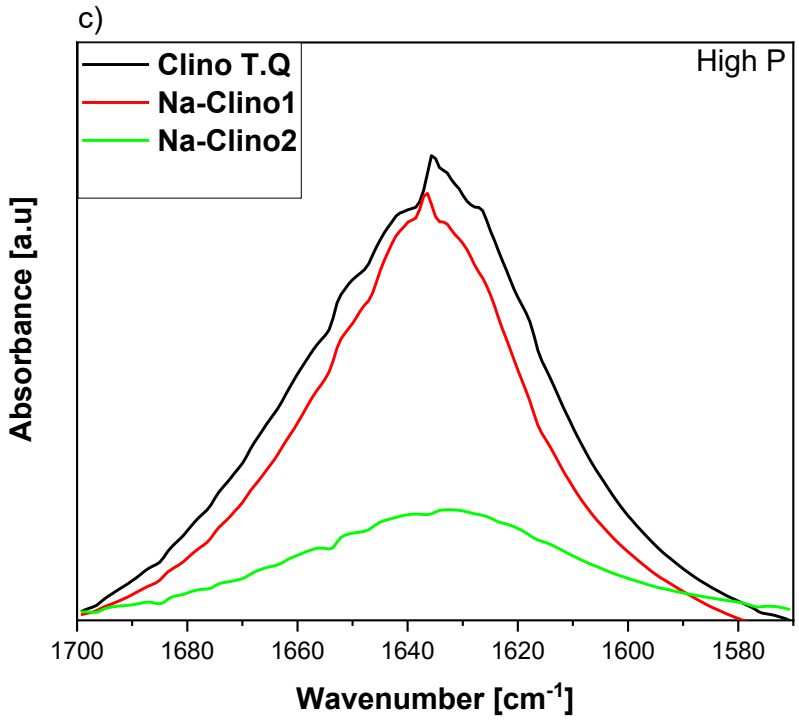

Figure 7.28: FT-IR peak of zeolitic water in -OH bending region at a) low pressures, b) medium pressures, c) high pressures.

As it can be seen, at low pressures (10^{-3} mbar), Clino T.Q showed a higher peak in -OH region (and consequently greater affinity with water respect to Na-Clino1 and Na-Clino2 samples). However, as pressure increased (10^{-2} mbar) Na-Clino1 showed a higher intensity of the peak than natural Clinoptilolite. This could be explained by hypothesizing that the interaction between water molecules and cationic sites on Na-Clino's surface is a two-step process involving a first slow step (at lower pressures) which consists in the capture of water molecules by the electric field generated by Na^{+}cations , together with the formation of water-cation adduct and a second faster step (at higher pressures) which includes the rearrangement of water molecules that move to the cation-framework interface in order to maximize physical interactions , as well as the formation of hydrogen bond, as suggested by Carotenuto and Camerlingo(G. Carotenuto and Camerlingo, 2020).However, at higher pressures (0.9-1 mbar) water adsorption resulted inhibited by the presence of sodium in Na-Clino 1 sample and Clino T.Q adsorption capacity prevailed once again. In all cases it was find out that Na-Clino 2 sample had the worst affinity with water.

Finally, by plotting the intensity of -OH bending peak located between 1630-1650 cm^{-1} as a function of equilibrium pressure of the line (which varied from $9 \cdot 10^{-3}$ mbar to 1mbar) it was possible to globally compare the affinity with water for all samples , which increased in the following order :Na-Clino2<Na-Clino1<ClinoT.Q<13X, as showed in the figure below.

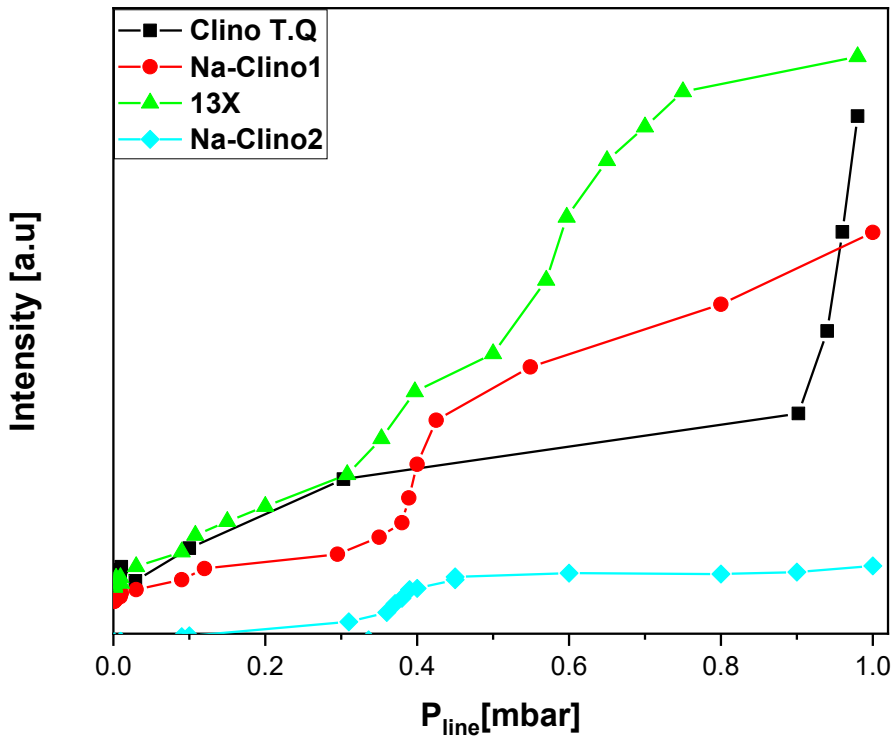

Figure7.29: Affinity with water for all investigated samples

7.7 Adsorption tests with humid stream

As already explained in the experimental procedure, the same quantity of all samples (500 mg) was tested in the same conditions (pellets in size range between 212µm-250µm) in order to investigate the variation of one parameter (the height of the bed) by keeping constant all the others (temperature, mass and the inlet flowrate of 50ml /min of N_2, RH=10%). Results are given in the following graphs .

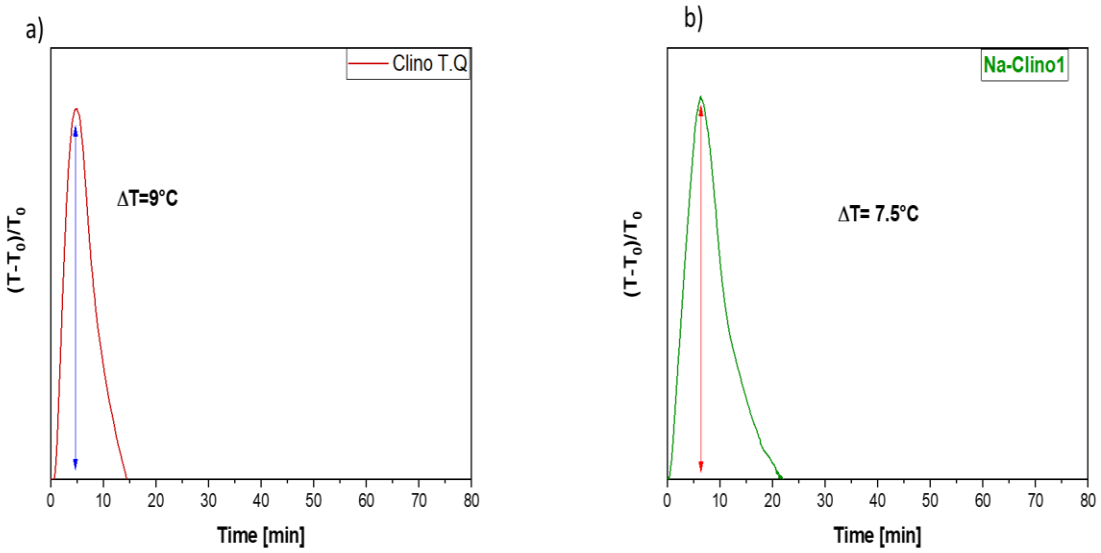

Figure 7.30: Energy tests at 50°C with inlet flow rate of 50 ml/min N_2 (RH=10%) for a) Clino T.Q on and b) Na-Clino1.

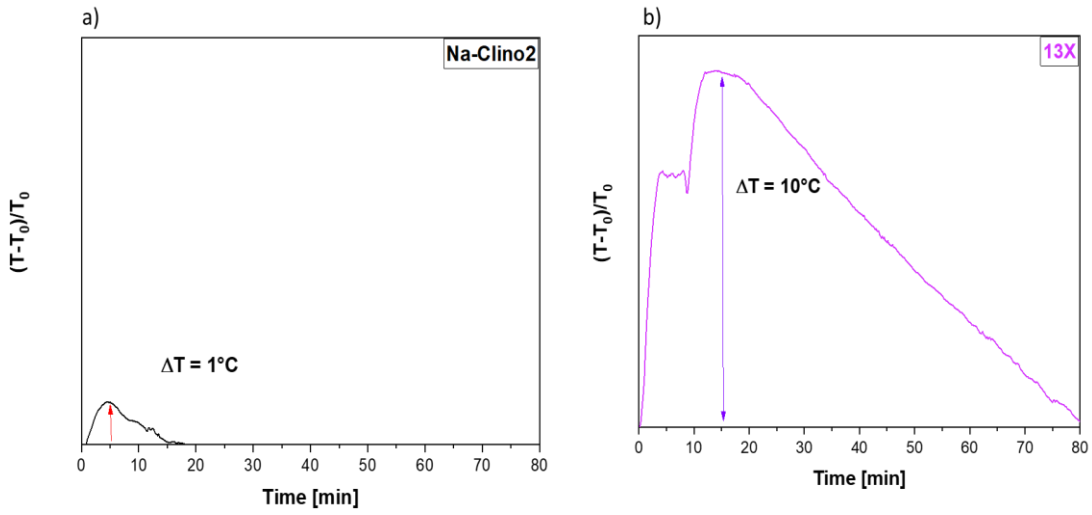

Figure 7.31: Energy tests at 50°C with inlet flow rate of 50 ml/min N_2 (RH=10%) for a)Na-Clino2 and b) 13X.

Regarding natural zeolites, the best performance was obtained through natural clinoptilolite which accounted for 9°C output temperature enhancement whereas the worst outcome was obtained through Na-Clino2 sample where only 1°C temperature increase was observed. This could be explained by the hypothesis of Na^+ inhibition in the functionalized samples. As a matter of fact, it was already noticed from EDX results that the atomic percentage of sodium in natural clinoptilolite was inferior to the one relative to Na-Clino2 sample (0.7% in Clino T.Q versus 6.6% in Na-Clino2). Hence it was hypothesized that an excess Na^+ cations could be deposited in those sites occupied by H_2O molecules otherwise, thus preventing a proper water adsorption. To support this theory FT-IR spectra should be mentioned, where the weak increase of adsorption bands and the net lowering of the expansion ones indicated less affinity with zeolite's water. Additionally, in Na-Clino2 sample the heigh of the bed (h= 7 cm) placed in reactor was higher than the one possessed by ClinoT.Q (h=4.5 cm) and, consequently, preferential paths could be created, thus leading to not negligible pressure losses which reflected

in sample's efficiency. On the other hand, Na-Clino1 sample was characterized by the same bed height as natural clinoptilolite and the sodium content was the half of Na-Clino2, but it didn't seem to show the same inhibition effect since it produced an increase of 7.5°C. However, among all samples considered, 13X showed the best performance. The height of the bed of this synthetic zeolite was 6.5 cm, only 0.5 cm inferior to the one relative to Na-Clino2.Nevertheless, when the test was executed temperature raised from 50°C to 60°C , thereby showing a $\Delta T=10°C$.

Finally, a comparison among all samples was necessary to do some considerations about the kinetics and the efficiency.

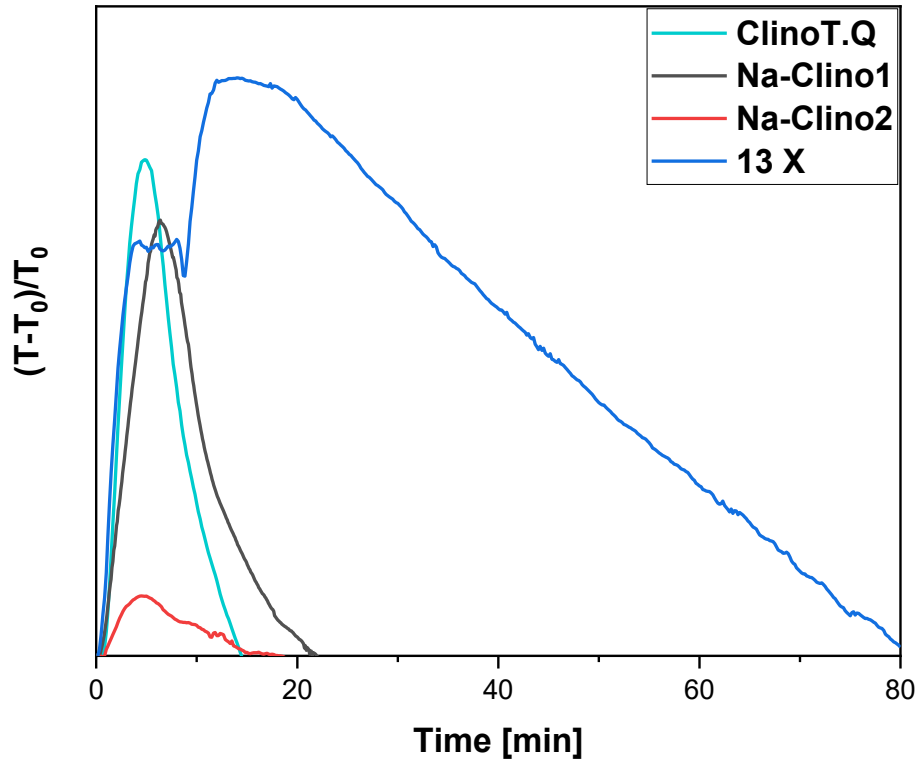

Figure 7.32: Adsorption tests with humid air, comparison among the outcomes of all samples

Table 7.10: Report of adsorption tests with humid air executed at 50°C with 50 ml/min N_2 (RH=10%)

Sample	**Height of bed [cm] (500 mg pellets 212-250 µm)**	**Time [min]**	**ΔT [°C]**
Clino T. Q	4.5	15	9
Na-Clino1	4.5	21	7.5
13X	6.5	19	10
Na-Clino2	7	80	1

What appeared to be evident from figure 7.20 is that, from a kinetic point of view, natural clinoptilolite seemed to present the fastest adsorption kinetic whereas the 13 X resulted to be the slowest. As a matter of fact, the temperature difference of 9 °C was recorded only after 15 minutes in ClinoT.Q and Na-Clino1 sample took 6 minutes longer to show a temperature increase of 7.5 minutes. It was observed that in the same time period of ClinoT.Q performance (approximately 10-15 minutes) 13X showed a rapid temperature enhancement of about 6 °C, and then it seemed to reach a plateau. After this time, temperature began to rise again, peaking it maximum value (T=60°C) and reaching a second plateau which lasted for 10-15minute. Later temperature dropped gradually until returning to 50°C after 40 minutes. Therefore, the whole adsorption test for 13X lasted 80 minutes.

Since ClinoT.Q demonstrated the highest temperature increase among all natural zeolites and its performance was comparable with the one obtained through the commercial 13X, the following sections will be dedicated to further investigation as well as optimization process of this zeolite, thus comparing it with the synthetic one.

7.9 Optimization

During optimization tests, the treatment temperature was decreased from 50°C to 30°C because adsorption is an exothermic process and, consequently, should be favored by lower temperatures. In addition to this, also the mass of the sorbent was modified in order to investigate the influence of the height of the bed, to verify if the latter would be the cause of the formation of preferential paths which negatively affected the adsorption phase. Finally, the influence of porosity was tested by performing some tests with Clino T.Q sample in powder form.

Hence, a first test was performed with 100 mg of ClinoT.Q pellets which resulted in a height of the bed of 0.9 cm, at 50°C. Later a second test was carried out with 500 mg of Clino T.Q pellets (height of bed =4,5 cm) at 30°C.Then, the third and fourth tests were carried out at 100°C and 150°C, respectively, to demonstrate that the increments of temperature decreased with the increase of test temperature because of the exothermic nature of the process. Finally, as previously announced, a test with 100 mg of ClinoT.Q powder (heigh of bed= 0.9 cm) was conducted at 150°C. It should be added that there was also an attempt to perform a test with 500 mg of Clino T.Q powder at 50°C but it came out that it was not possible even to conclude the pre-treatment phase because of the huge pressure drop caused by the scarce porosity of the sorbent bed. Test results are summarized in the following table.

Table 7.11: Optimization test results. The initial test is referred to tests performed in section 7.6.

Test	Mass [mg]	Size/shape	T[°c] treatment	height of bed [cm]	final ΔT [°c]	Time [min]
Initial test	500	pellets	50	4.5	9	15
Test 1	100	pellets	50	0.9	5	16
Test 2	500	pellets	30	4.5	5	55
Test 3	500	pellets	100	4.5	3	17
Test 4	500	pellets	150	4.5	N.S*	35
Test 5	100	powder	150	0.9	2	15

*N. S= not significant

As can be seen, the best performance remained the one related to the initial test, whose results were presented in section 7.6. Moreover, during the third test, even though temperature was set at 100°C the starting temperature was lower, at 93°C and after ΔT increase of approximately 3°C (from 93°C to 96°C) temperature remained constant at 96°C and did not return to its starting value, differently from the other tests performed in this thesis.

Additionally, as it could be imagined, the worst performance was obtained at T=150°C with 500 g of Clino T.Q pellets, thus demonstrating that higher temperatures would obstruct the adsorption process. Finally, it should be emphasized that test 1 and 2 showed the same temperature increase with different kinetics. As a matter of fact, the first test, which was conducted with a sorption bed of 0.9 cm, lasted only 16 minutes and led to a Δt of 16 minutes, differently from the second test which lasted 55 minutes. In other words, considering the same pre-treatment, the same inlet flowrate and the same temperature increase at the end of the process, the main advantages of the first test were the lower amount of sorbent utilized and the faster kinetic of the adsorption while the principal disadvantage was the higher test temperature required whereas for the second test a lower treatment temperature led to the same performance but , as a drawback , the adsorption process resulted slower and a greater amount of sorbent (which results in a higher height of the bed) was necessary.

8 Key performance indicators (KPIs)

Key performance indicators or KPI are considered useful parameters to compare different solutions in a specific field. Their definition is not unambiguous and strictly dependent on the system considered. The most relevant ones for this thesis are(Aghemo *et al.*, 2023):

- Energy storage density.
- Charging temperature
- Thermal conductivity
- Lifetime
- Cost and availability.

Among these ones, the Energy Storage density (ESD) is undoubtedly one of the most important KIPs. The ESD is related to the amount of energy which can be stored in a certain quantity of material. Differently from Energy Storage Capacity (ESC [kJ/kg]), which is related to the amount of energy per unit mass of the sorbent, the ESD is calculated per unit volume of the sorbent itself. These quantities can be correlated though the following expression:

$$ESD = ESC \cdot \rho \tag{8.1}$$

Where ρ is the sorbent's density [kg/m^3].

It should be noted that a high value of ESC for a certain material could correspond to a low value of ESD for the same material. Therefore, the value which should be taken into consideration depends on the specific application, considering that mass influences the average cost of the process whereas volume affects hindrance of the technology (Aghemo *et al.*, 2023).However it is usually preferred having greater mass and lower volume.

Regarding charging temperature instead, it is strictly related to the charging phase of TES system, when the heat source split sorbate from sorbent which remain separated until the discharging step. Since the ideal heat source for this system should be the one coming from solar collectors that may reach up a temperature of 150°C, the ideal charging temperature should be below 150°C.(Aghemo *et al.*, 2023) This is a crucial point during comparison between natural and synthetic zeolites because, as previously mentioned, natural zeolites generally require a charging temperature of 350°C , thus resulting more suitable for waste gas treatment.

Thermal conductivity on the other hand involves heat transfer within the material. In case of zeolites, the optimization of this property can occur through the enhancement of porosity. Indeed, experimental results presented in this thesis demonstrated how a better performance was achieved thanks to the use of pellets, instead of utilizing powder.

Lifetime instead is related to the number of cycles that the material taken into consideration can stand without affecting its efficiency. It has been estimated an ideal lifetime of 20 years, which is abundantly satisfied by zeolites. As a result, lifetime is not a crucial KPI for this study.

Finally cost and availability are considered KPIs as well. To estimate the cost of storage of thermal energy using zeolites it is fundamental to have an idea of the average cost of the raw material. This is valid both for natural and synthetic zeolites.

In this regard, it should be emphasized that synthetic zeolites are relatively expensive in comparison with natural ones since the synthesis of new materials requires the utilization of adequate equipment, clean substrates and energy(Król, 2020). Natural zeolites, on the other hand, represent abundant, low-cost natural minerals although they generally result poor in quality because of impurities and low crystallinity. Nevertheless, it can be adopted both physical and chemical modifications to improve the quality of natural zeolites(Kurniawan *et al.*, 2022).

Among synthetic zeolites, 13 X appears to be the cheapest. It is difficult, however, to estimate the exact price as this varies depending on the supplier and the quantity purchased. According to some market surveys, based on the sale of around 150000-200000 tons in 2015 with a corresponding profit of USD 450-550 (Belviso, 2016; Kouchachvili *et al.*, 2023) the cost of 13 X is around USD 2750-3500/ton (around CAD $3500/ton). Tran et al., on the other hand, estimated the cost of 13 X around CAD$6000/ ton. (Tran *et al.*, 2021).

Basing on another recent study from 2022 instead (de Gennaro *et al.*, 2022b)industrial quantities of 13 X can be purchased monthly by the Chinese industry at a competitive price of around 1300-1800 USD/ ton, with a minimum order of 1-2 tons.

As far as natural zeolites are concerned, costs have been estimated to be far lower, by about an order of magnitude. However, even in this case there is a range of prices and not a specific one. The key parameters to determine the natural zeolites' cost on the market are undoubtedly the size of crystals and purity. Regarding Clinoptilolite, in an article which dates back to 2015 (Jänchen, Herzog and Thrun, 2015) a price of 200-300 €/ ton has been estimated (cost compared with that of 13 X, estimated at around 2000-3000 €/ton).

It should be remembered at this point that the cost is strongly influenced by the adsorption mode that is imposed on the TES material. For example, reducing the water vapour pressure of the inlet stream will result in a lower heat of adsorption and, consequently, a higher storage cost. In other words, the cost also depends fiercely on the temperature and vapour pressure of the evaporating component (Kouchachvili *et al.*, 2023).

This last KPI is usually expressed in terms of price per stored Kwh [€/Kwh]. As it can be imagined, to estimate it an average price of the raw material is necessary. In this thesis the average price for 13 X zeolite will be considered ranging from 2000€/ton to 3000€/ton whereas the cost of natural clinoptilolites will be estimated around 200€/ton to 300€/ton.

A way of expressing this KIP is through the use of the storage capacity cost, also known as SCC [€/kwh], which allows a comparison between different adsorbent categories(Aghemo *et al.*, 2023)

$$SCC = \frac{€/ton}{ESC \cdot 1000} \cdot 3600 \qquad (8.4)$$

Where ESC is the energy storage capacity [kJ/kg]. It is only necessary to know the cost of the materials investigated. This is considered a useful tool to evaluate is the system taken into consideration is technologically feasible and scalable, since an adsorbent which is efficient but expensive could result not suitable for implementation on a large scale. The SCC value for liquid sorbents is lower than the one related to solid sorbents(Aghemo *et al.*, 2023)

As an example, synthetic zeolites, having a market price of 2000-3000€ /ton are not competitive on a economical point of view if compared with other sorbents like bentonite or vermiculite (160€ /ton) and this affect their SCC value(Aghemo *et al.*, 2023).

8.1 Cost analysis

In this section an estimation of the SCC of the investigated samples is reported. It should be noted that this evaluation was based on experimental results obtained during all the analyses performed in this thesis. More precisely, the mass of the sample was the one used during adsorption tests with humid nitrogen (500 mg) and thanks to the same tests' temperature increment was estimated, the mass of water was taken from TGA analysis whereas the sorbent's density was calculated through the following equation:

$$\rho = \frac{m}{V} \tag{8.5}$$

Where m is the sample's mass put in the reactor [kg] and V is the volume of the bed reactor [m^3], strictly dependent on the heigh of the bed of each sample. This density value was multiplied by a corrective factor of 0.6 which took account of material's porosity. To calculate SCC, the first step was to evaluate the Energy density [J], by the means of the equation 8.6 (used by hypothesizing adiabatic conditions):

$$E = \sum_i (m_i cp_i)\Delta T \tag{8.6}$$

Where m_i refers to the mass [kg] of was the species involved in the adsorption process (i.e adsorbent and adsorbate), cp_i[J/Kg/K] refers to the specific heat of all the species (cp of water is equal to 4.186J/g/K) and ΔT is temperature increment[K] from adsorption tests at T=50°C.

After evaluating E, it was possible to estimate the real Energy Density ED (J/m^3) through the following equation:

$$ED = \frac{E}{m_{sample}/\rho_{sample}} \tag{8.7}$$

Where m_{sample} indicated the mass [kg] of the investigated sample and ρ [kg/m^3] is the density of the samples.

However, ED does not correspond to the above mentioned ESD. This latter considers also the enthalpy of water vaporization (41 kJ/mol). However, thanks to the knowledge of ED from equation 8.7 and water uptake(χ) from TGA analysis ESD [kJ/m3] was calculated as follows:

$$ESD = \frac{41\ KJ/mol \cdot \chi}{18} \cdot \rho + ED \tag{8.8}$$

Once estimated ESD, ESC was calculated through equation 8.1 and consequently SCC value was obtained by means of equation 8.4,

Regarding instead the cost of all zeolites which was necessary to calculate SCC, for Clino T.Q it was estimated a cost of 200-300 €/ton , for Na-Clino1 it was considered a 20% higher price since it was considered the cost of the precursor (NaCl) and the energy demand for functionalization process, for Na-Clino 2 on the other hand it was chosen a 40% higher cost, considering all the energetic expenses as well as the price of two different precursors whereas for 13 X it was considered a price of 2000-3000 €/ton.

Therefore, following the KPI definitions explained in the previous paragraphs, the SCC was calculated, as summarized in the following table.

Table 8.1: ESD [kJ/m^3], ESC [kJ/kg], SCC[€/kwh]and SCC^{-1}[kwh/€] of the investigated samples

Sample	ρ[kg/m^3]	Water uptake [g/g]	ESD [kJ/m^3]	ESC [kJ/kg]	SCC range [€/kwh]	SCC^{-1} range [kwh/€]
Clino T. Q	5.31e+02	0.01	2,92e+04	5.51e+01	13-20	7.66e-02
Na-Clino1	5.31e+02	0.005	2.30e+04	4.34e+01	19-27	5.24e-02
Na-Clino2	3.18e+02	0.002	4.63e+03	1.45e+01	69-94	1.44e-02
13X	3.67e+02	0.015	2.38e+04	6.47e+01	111-167	8.99e.03

It was interesting to observe that SCC values for natural zeolites samples resulted in agreement with the ones usually reported in literature for zeolites(Aghemo *et al.*, 2023).

As can be noted, decreasing values of SCC followed the order: 13X>Na-Clino2>Na-Clino1>ClinoT.Q, thus confirming that, although synthetic 13X zeolite is more efficient, it resulted not to be competitive on the market. On the other hand, among all natural zeolites investigated, bare clinoptilolite resulted to be the most convenient solution, considering both economic aspects and energy-related performance.

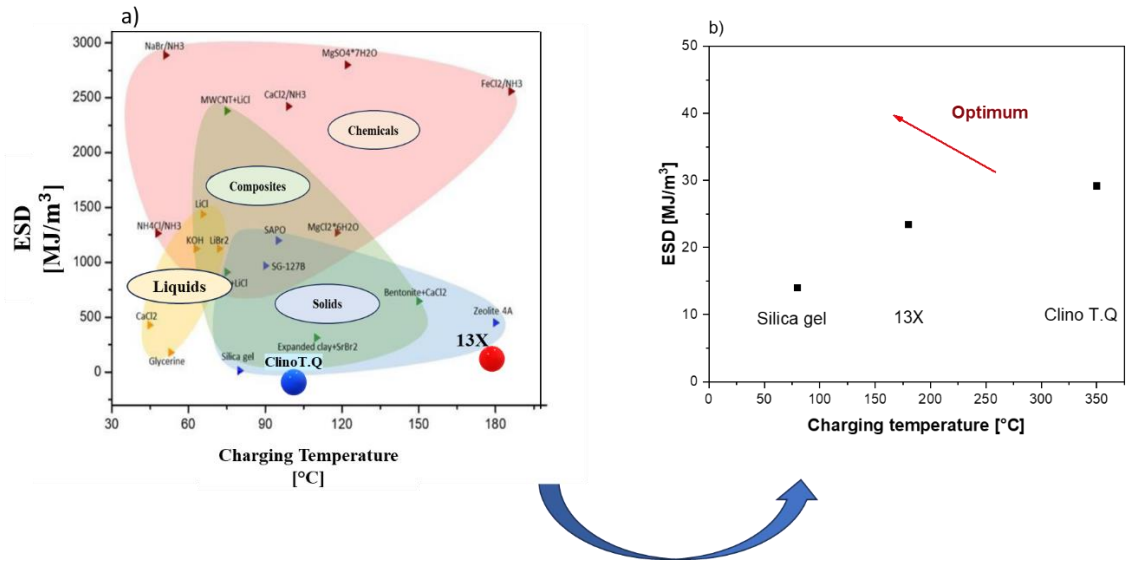

Figure 8.1: a) ESD [MJ/m^3] of various adsorption materials as a function of the charging temperature, and b) magnification of the solid adsorbents region where zeolites are placed. Illustration taken from (Aghemo *et al.*, 2023)with modifications.

Figure 8.1 provides an overview of the ESD of zeolites as a function of charging temperature, (estimated from literature for Clino T.Q and 13X) in comparison to other conventional sorption materials. Indeed KPIs (ESC, ESD, SCC and charging temperature) can be helpful in the choice of the best material for a specific application. A simple procedure to use graphs **8.1** and **8.2** has been suggested by Aghemo et al.(Aghemo *et al.*, 2023). The first step consists in choosing an objective (i.e the minimization of the mass or of the volume or the maximization of the stored

heat). Then constraints must be defined (i.e charging temperature limit at T=150-160°C for domestic applications in TES sorbent materials or limits on volume as well as cost). Constraints allows the elimination of certain areas of the graphs so that, combining this information with objective the optimum region can be easily found. In the graph in figure 8.1 the objective is the minimization of volume per MJ of stored thermal energy whereas the constraint is the charging temperature limit (which should does not exceed 150-160°C to use these adsorbents together with solar collectors). Therefore, the optimum region has been identified in the left upper region, as indicated in figure **8.1.b.**

It is possible to notice that it is necessary to maximize ESD values (or ESC ones) to obtain higher efficiency with a minimization of volume of the adsorption system. From experimental analysis it came out that synthetic 13X zeolites resulted to have a slightly lower ESD value (23.8 MJ/m^3) than Clino T. Q (29.2 MJ/m^3), it also resulted to be more expensive than the natural zeolite and additionally the synthetic 13 X showed a charging temperature of 180°C, in agreement with literature data (Lavagna *et al.*, 2020; Aghemo *et al.*, 2023).As a drawback, 13X zeolite resulted in a higher ESC value (64.7 kJ/kg) than the one found for Clino T.Q (55.1 kJ/kg),and an higher water uptake that justify the slower kinetic of the adsorption process. However, apart from these two KPIs, it is important to consider also the SCC value which also takes into account the cost of the raw material itself. Comparing zeolites performance with the one of the other sorbents it was evident that sorbents for chemisorption resulted the most efficient materials event though their cost is inconvenient. Zeolites as solid sorbents, on the other hand showed greater energy storage density than liquids and silica gel. Hence it is worth to further investigate them as innovative and cost-efficient materials for TES applications in order to make them competitive with chemical sorbents.

In conclusion, thanks to SCC parameter it was possible to compare zeolites performance with the ones of the most conventional sorbent material, as shown in the figure below.

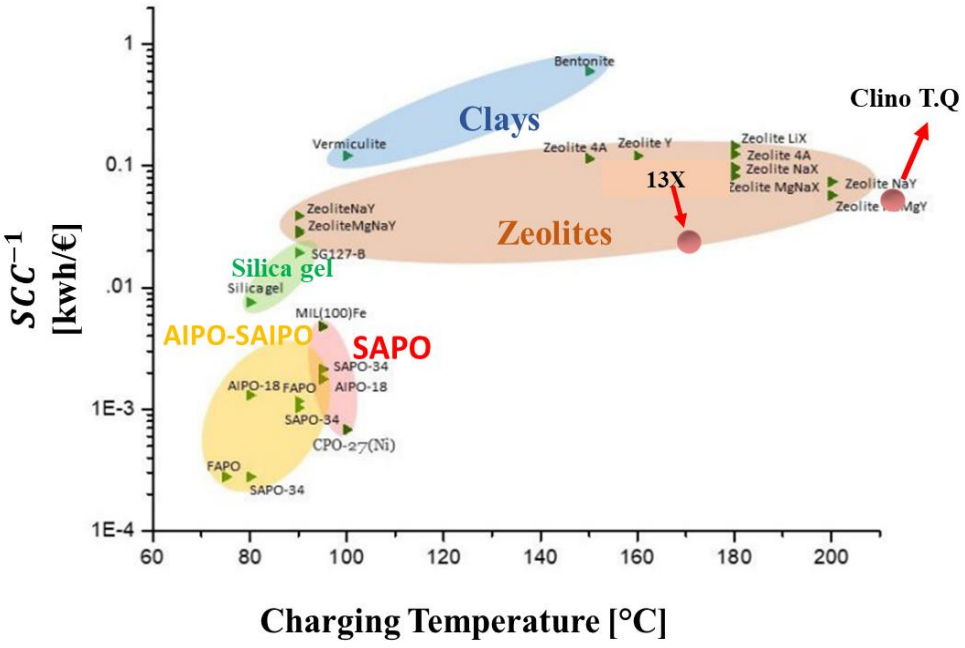

Figure 8.2: Charts reporting SCC^{-1} values of different solid sorption materials as a function of Charging temperature. Illustration taken from(Aghemo *et al.*, 2023) with modifications.

In figure 8.2 the optimum region is located in the upper side of the graph, since the main objective is the minimization of costs per kwh of thermal energy produced (which is equivalent to the maximization of SCC^{-1}value, in kwh/€). Once again, the constraint is constituted by the charging temperature, which should be as lower as possible.

As it can be seen from DTG and DSC curves, Clino T.Q(the most efficient natural sample investigated in this thesis) resulted having a charging temperature of approximately 100°C and a SCC value lower than 13X zeolites (which is equivalent to higher SCC^{-1} value). Synthetic zeolite 13 X on the other hand showed a higher charging temperature (150-180°C, confirmed by literature data (Lavagna *et al.*, 2020; de Gennaro *et al.*, 2022a; Aghemo *et al.*, 2023)) and higher SCC value. The optimum scenario should consist in a compromise between relatively low charging temperatures (150-180°C), suitable for domestic applications of STES systems but high SCC^{-1} value. However, if the charging temperature is too low the water uptake capacity becomes insufficient to store and release thermal energy. After all these considerations, it was possible to draw back to the conclusion that zeolites showed better performances than AIPO and SAPO sorption material and in particular, considering ESD and ESC results, natural clinoptilolite seem to be a promising alternative to synthetic zeolite 13 X for thermal energy storage.

9 Conclusions

In this thesis the role of sodium in the enhancement water adsorption capacity of natural zeolites was investigated. For this purpose, four different samples were analyzed and compared. Among them, two samples consisted in natural clinoptilolite functionalized through ionic exchange following two different procedures. From first procedure which exploited NaCl as a precursor Na-Clino1 was obtained. Since it is known from literature that the presence of NH_4^+ions favor zeolite's exchange capacity, in the second procedure sample was firstly treated with and then $NaNO_3$ as precurs, thus obtaining Na-Clino2.

After analyzing surface area, crystalline and elemental composition through physico-chemical characterizations, it was found out that not only ion exchange occurred properly, but also that sodium content in Na-Clino2 doubled the one present in Na-Clino1 and sixfold the quantity in natural clinoptilolite (ClinoT.Q) sample. Considering also the overall results, both from thermal analysis such as DSC and TGA and from FT-IR spectroscopy it is possible to draw to the conclusion that Na-Clino2 possessed the lowest value of enthalpy, specific heat and from FT-IR spectra it was clear that water was weekly physiosorbed on its surface so that desorption process occurred by gradual expansion, in contrast with other samples for which thermal treatment was required to remove water from their structure. In conclusion Na-Clino2 is the less efficient zeolite and its scarce performance may be due to the excessive quantity of sodium in its framework, which probably causes inhibition as side effect. On the other hand, among natural zeolites, ClinoT.Q showed, the higher enthalpy od dehydration, the higher affinity with water (both at low and high pressures) and consequently higher water adsorption capacity, as well as the higher water uptake during sorption process which led to the greater temperature increase. TGA results showed a mass loss relative to physiosorbed water below 200°C, but then it was not recorded the loss of structural water (related to thermal destruction of the framework) up to 700°C, thereby confirming thermal stability. Considering all the experimental results it was possible to conclude that natural clinoptilolite constituted the best alternative to synthetic zeolites 13X in TES systems. As a matter of fact, natural clinoptilolite is cost effective since its price is tenfold inferior to 13X one (200 €/ton against 2000€/ton), it does not require a synthesis process and its production only requires two non-energy demanding steps, that are an extraction and a purification phase. In addition to this it is thermally stable up to 450-500°C, it has a good

affinity with water and at T=50°C and ambient pressure it is capable of produce a ΔT=9°C in 15 minutes, which is comparable with the one obtained for zeolite 13 X with 80 minutes. Respect to 13 X, natural clinoptilolite showed a faster kinetic and a lower water uptake at ambient pressure and therefore it resulted efficient for those application which requires an immediate huge amount of thermal energy :13 X zeolite on the other hand is capable of maintaining a certain value of constant temperature for a longer period of time, probably due to its higher specific surface area (528 m^2/g)) which lead to greater adsorption capacities. In this regard, further investigations are required to investigate the influence of operative conditions on Clinoptilolite performance.

Finally, it should be mentioned that it has a SCC value of 13-20 €/kwh which is lower than the one found for zeolite 13 X and comparable with the ones generally measured for other zeolites. Finally, clinoptilolite is not dangerous for the environment or for the humankind and its utilization in TES system does not cause CO_2 or PM emissions, thus contributing to reduce mankind's reliance on fossil fuels and critical raw materials.

9.1 Future perspectives

In this thesis experimental tests were carried out at ambient pressure. Additionally, adsorption tests with humid nitrogen were performed without changing the relative humidity (RH=10%). However, it is known from literature that operative conditions (i.e temperature, pressure, moisture, adiabatic conditions…) play a key role in adsorption processes. From experimental tests it was observed that the role of temperature was strictly correlated to the charging temperature of the sample investigated. From FT-IR adsoption tests with water it was discovered that the variation of partial pressure (strictly correlated with pressure of the system and water concentration) could affect affinity toward water. Hence it could be interesting to investigate how pressure influence temperature increase in adsorption tests. Besides, the SCC evaluation, as well as the estimation of the others KPIs may be influenced by the experimental setting or the type of measurement (i.e open cycle, closed cycle, isosteric evaluation or calorimetric evaluation).

As a matter of fact, in section 8 it was mentioned that to properly estimate some KPIs the isosteric heat of adsorption (strictly reliant on temperature and pressure) is required. This parameter could be evaluated through TGA dynamic water vapor sorption analyses (based on the use of DSC vacuum analyzer)(Lavagna *et al.*, 2020) to assess equilibrium sorption isobars in the water uptake-temperature chart and hence to build Clausius -Clapeyron graphs with all the cycles that simulate seasonal and daily cycles. In this way it could be possible to analyze the effect of moisture, temperature and pressure on zeolites in adsorption tests and find the operative conditions which maximize Clinoptilolite's performance.

10 References:

Aghemo, L. *et al.* (2023) 'Comparison of key performance indicators of sorbent materials for thermal energy storage with an economic focus', *Energy Storage Materials*. Elsevier B.V., pp. 130–153. Available at: https://doi.org/10.1016/j.ensm.2022.11.042.

Alberti, A. and Vezzalini, M.G. (1984) 'Topological changes in dehydrated zeolites: breaking of TOT oxygen bridges', in *Proceedings of the Sixth International Zeolite Conference*. Butterworth, pp. 834–841.

Alothman, Z. (2012) 'A Review: Fundamental Aspects of Silicate Mesoporous Materials', *Materials*, 5, pp. 2874–2902. Available at: https://doi.org/10.3390/ma5122874.

Alver, B.E., Sakizci, M. and Yörükoğullari, E. (2010) 'Investigation of clinoptilolite rich natural zeolites from Turkey: A combined XRF, TG/DTG, DTA and DSC study', *Journal of*

Thermal Analysis and Calorimetry, 100(1), pp. 19–26. Available at: https://doi.org/10.1007/s10973-009-0118-0.
Anderson, R. *et al.* (2014) 'Experimental results and modeling of energy storage and recovery in a packed bed of alumina particles', *Applied Energy*, 119, pp. 521–529. Available at: https://doi.org/10.1016/j.apenergy.2014.01.030.
Aprea, P. *et al.* (2016) 'Sr-, Zn- and Cd-exchanged zeolitic materials as water vapor adsorbents for thermal energy storage applications', *Applied Thermal Engineering*, 106, pp. 1217–1224. Available at: https://doi.org/10.1016/j.applthermaleng.2016.06.066.
Armbruster, T. (1993) 'Dehydration mechanism of clinoptilolite and heulandite: Single-crystal X-ray study of Na-poor, Ca-, K-, Mg-rich clinoptilolite at 100 K', *American Mineralogist*, 78(3–4), pp. 260–264.
Bales, C. *et al.* (2008) *Laboratory Tests of Chemical Reactions and Prototype Sorption Storage Units A Report of IEA Solar Heating and Cooling programme-Task 32 Advanced storage concepts for solar and low energy buildings Report B4 of Subtask B*.
Banaei, A. and Zanj, A. (2021a) 'A Review on the Challenges of Using Zeolite 13X as Heat Storage Systems for the Residential Sector', *Energies*, 14(23), p. 8062. Available at: https://doi.org/10.3390/en14238062.
Banaei, A. and Zanj, A. (2021b) 'A Review on the Challenges of Using Zeolite 13X as Heat Storage Systems for the Residential Sector', *Energies*, 14(23). Available at: https://doi.org/10.3390/en14238062.
Bardestani, R., Patience, G.S. and Kaliaguine, S. (2019) 'Experimental methods in chemical engineering: specific surface area and pore size distribution measurements—BET, BJH, and DFT', *Canadian Journal of Chemical Engineering*. Wiley-Liss Inc., pp. 2781–2791. Available at: https://doi.org/10.1002/cjce.23632.
Belviso, C. (2016) *Zeolites*. Rijeka: IntechOpen. Available at: https://doi.org/10.5772/61950.
Berthomieu, C. and Hienerwadel, R. (2009a) 'Fourier transform infrared (FTIR) spectroscopy', *Photosynthesis Research*, pp. 157–170. Available at: https://doi.org/10.1007/s11120-009-9439-x.
Berthomieu, C. and Hienerwadel, R. (2009b) 'Fourier transform infrared (FTIR) spectroscopy', *Photosynthesis Research*, pp. 157–170. Available at: https://doi.org/10.1007/s11120-009-9439-x.
Bilgin, O. (2017) 'Technologic Tests of Turkey-Gordes Zeolite Minerals', *Journal of Minerals and Materials Characterization and Engineering*, 05(05), pp. 252–265. Available at: https://doi.org/10.4236/jmmce.2017.55021.
Bish, D.L. and Carey, J.W. (2001) 'Thermal behavior of natural zeolites', *Reviews in Mineralogy and Geochemistry*, 45, pp. 403–452. Available at: https://doi.org/10.2138/rmg.2001.45.13.
Bısh, D.L. and Carey, J.W. (2001) 'Thermal behavior of natural zeolites, Natural Zeolites: Occurrence, Properties, Applications', *Mineral. Soc. Am. Rev. Mineral. Geochem*, 45, pp. 403–452.
Blengini, G. *et al.* (2020) 'Study on the EU's list of Critical Raw Materials (2020) Final Report'. Available at: https://doi.org/10.2873/11619.
Boles, J.R. (1972) 'Composition, Optical Properties, Cell Dimensions, and Thermal Stability of Some Heulandite Group Zeolites', *American Mineralogist*, 57(9–10), pp. 1463–1493.
Bose, R. *et al.* (2020) 'Adsorption of hydrogen and carbon dioxide in zeolitic imidazolate framework structure with SOD topology: experimental and modelling studies', *Adsorption*, 26. Available at: https://doi.org/10.1007/s10450-020-00219-2.
Breck, D.W. (1974) 'Zeolite Molecular Sieves: Structure, Chemistry and Uses', in. New York,NY, pp. 771–771.

Britannica, T.E. of E. (2023) *X-ray diffraction*, *Encyclopedia Britannica https://www.britannica.com/science/X-ray-diffraction*.
Carotenuto, G and Camerlingo, C. (2020) 'Kinetic investigation of water physisorption on natural clinoptilolite at room temperature', *Microporous and Mesoporous Materials*, 302, p. 110238. Available at: https://doi.org/https://doi.org/10.1016/j.micromeso.2020.110238.
Carotenuto, G. and Camerlingo, C. (2020) 'Kinetic investigation of water physisorption on natural clinoptilolite at room temperature', *Microporous and Mesoporous Materials*, 302. Available at: https://doi.org/10.1016/j.micromeso.2020.110238.
Castaldi, P. *et al.* (2005) 'Thermal and spectroscopic studies of zeolites exchanged with metal cations', *Journal of Molecular Structure*, 734(1–3), pp. 99–105. Available at: https://doi.org/10.1016/j.molstruc.2004.09.009.
Cavallo, M. *et al.* (2023) 'Shaped natural and synthetic zeolites for CO2capture in a wide temperature range', *Journal of CO2 Utilization*, 67. Available at: https://doi.org/10.1016/j.jcou.2022.102335.
Chauhan, A. and Chauhan, P. (2014) 'Powder XRD technique and its applications in science and technology', *J Anal Bioanal Tech*, 5(5), pp. 1–5.
Cocuzza, C. *et al.* (2022) 'Simultaneous CO2 reduction and NADH regeneration using formate and glycerol dehydrogenase enzymes co-immobilized on modified natural zeolite', *RSC Advances*, 12(48), pp. 31142–31155. Available at: https://doi.org/10.1039/d2ra03459j.
Commission, E. (no date) 'Study on the EU's list of Critical Raw Materials (2020) Final Report'. Available at: https://doi.org/10.2873/904613.
Craig, D.Q.M. and Reading, M. (2006) *Thermal Analysis of Pharmaceuticals*. CRC Press. Available at: https://books.google.it/books?id=G2jLBQAAQBAJ.
Davarpanah, E. *et al.* (2020) 'CO2 capture on natural zeolite clinoptilolite: Effect of temperature and role of the adsorption sites', *Journal of Environmental Management*, 275. Available at: https://doi.org/10.1016/j.jenvman.2020.111229.
Davidson, J. and Monteleone, C. (2022) 'The 2021 G20 and Italy: keeping our dreams alive?', *Contemporary Italian Politics*, 14(2), pp. 207–223.
Dicaire, D. and Tezel, F.H. (2011) 'Regeneration and efficiency characterization of hybrid adsorbent for thermal energy storage of excess and solar heat', *Renewable Energy*, 36(3), pp. 986–992. Available at: https://doi.org/10.1016/j.renene.2010.08.031.
Dosa, M. *et al.* (2021) 'Natural zeolites as sustainable materials for environmental processes', in *Nanostructured Catalysts for Environmental Applications*. Springer International Publishing, pp. 367–381. Available at: https://doi.org/10.1007/978-3-030-58934-9_13.
Dosa, M. *et al.* (2022) 'Natural zeolite clinoptilolite application in wastewater treatment: Methylene blue, zinc and cadmium abatement tests and kinetic studies', *Materials*, 15(22), p. 8191.
Dyer, A. (1988) 'An Introduction to Zeolite Molecular Sieves', in Wiley (ed.) *An Introduction to Zeolite Molecular Sieves*. 1st ed. Chichester, UK, pp. 76–83.
Feng, C. *et al.* (2021) 'Key technology and application analysis of zeolite adsorption for energy storage and heat-mass transfer process: A review', *Renewable and Sustainable Energy Reviews*, 144, p. 110954. Available at: https://doi.org/10.1016/j.rser.2021.110954.
Gaeini, M., Zondag, H.A. and Rindt, C.C.M. (2016) 'Effect of kinetics on the thermal performance of a sorption heat storage reactor', *Applied Thermal Engineering*, 102, pp. 520–531. Available at: https://doi.org/10.1016/j.applthermaleng.2016.03.055.
Gao, S. *et al.* (2023) 'Synthesis of zeolites from low-cost feeds and its sustainable environmental applications', *Journal of Environmental Chemical Engineering*, 11(1), p. 108995. Available at: https://doi.org/10.1016/j.jece.2022.108995.

de Gennaro, B. *et al.* (2022a) 'Use of Zeolites in the Capture and Storage of Thermal Energy by Water Desorption—Adsorption Cycles', *Materials*, 15(16). Available at: https://doi.org/10.3390/ma15165574.
de Gennaro, B. *et al.* (2022b) 'Use of Zeolites in the Capture and Storage of Thermal Energy by Water Desorption—Adsorption Cycles', *Materials*, 15(16). Available at: https://doi.org/10.3390/ma15165574.
Gibson, N. *et al.* (2019) 'Volume-specific surface area by gas adsorption analysis with the BET method', in *Characterization of Nanoparticles: Measurement Processes for Nanoparticles*. Elsevier, pp. 265–294. Available at: https://doi.org/10.1016/B978-0-12-814182-3.00017-1.
Gottardi, G. *et al.* (1985) 'Zeolites of the heulandite group', *Natural zeolites*, pp. 256–305.
Guo, Y., Zhang, H. and Liu, Y. (2018) 'Desorption characteristics and kinetic parameters determination of molecular sieve by thermogravimetric analysis/differential thermogravimetric analysis technique', *Adsorption Science & Technology*, 36, p. 026361741877266. Available at: https://doi.org/10.1177/0263617418772665.
Harrington, G. and Santiso, J. (2021) 'Back-to-Basics tutorial: X-ray diffraction of thin films', *Journal of Electroceramics*, 47, pp. 1–23. Available at: https://doi.org/10.1007/s10832-021-00263-6.
Higgins, F.M., de Leeuw, N.H. and Parker, S.C. (2002a) 'Modelling the effect of water on cation exchange in zeolite A', *Journal of Materials Chemistry*, 12(1), pp. 124–131. Available at: https://doi.org/10.1039/b104069n.
Higgins, F.M., de Leeuw, N.H. and Parker, S.C. (2002b) 'Modelling the effect of water on cation exchange in zeolite A', *Journal of Materials Chemistry*, 12(1), pp. 124–131. Available at: https://doi.org/10.1039/b104069n.
INFRARED SPECTROSCOPY (no date).
Intergovernmental Panel on Climate Change. Working Group III and Edenhofer, O. (no date) *Climate change 2014 : mitigation of climate change : Working Group III contribution to the Fifth Assessment Report of the Intergovernmental Panel on Climate Change*.
Jänchen, J. *et al.* (2004) 'Studies of the water adsorption on Zeolites and modified mesoporous materials for seasonal storage of solar heat', *Solar Energy*, 76(1–3), pp. 339–344. Available at: https://doi.org/10.1016/j.solener.2003.07.036.
Jänchen, J., Herzog, T. and Thrun, E. (2015) 'NATURAL ZEOLITES IN THERMAL ADSORPTION STORAGE AND BUILDING MATERIALS FOR SOLAR ENERGY UTILIZATION IN HOUSES', in.
Jentys, A. *et al.* (1989) *Adsorption of Water on ZSM5 Zeolites*, *J. Phys. Chem*. Available at: https://pubs.acs.org/sharingguidelines.
Kadja, G.T.M., Culsum, N.T.U. and Putri, R.M. (2023) 'Recent advances in the utilization of zeolite-based materials for controlled drug delivery', *Results in Chemistry*, 5, p. 100910. Available at: https://doi.org/10.1016/j.rechem.2023.100910.
Kafle, B.P. (2019) *Chemical analysis and material characterization by spectrophotometry*. Elsevier.
Khan, H. *et al.* (2020) 'Experimental methods in chemical engineering: X-ray diffraction spectroscopy—XRD', *The Canadian journal of chemical engineering*, 98(6), pp. 1255–1266.
Koohsaryan, E., Anbia, M. and Maghsoodlu, M. (2020) 'Application of zeolites as non-phosphate detergent builders: A review', *Journal of Environmental Chemical Engineering*, 8(5), p. 104287. Available at: https://doi.org/10.1016/j.jece.2020.104287.
Kouchachvili, L. *et al.* (2023) 'Natural zeolites as host matrices for the development of low-cost and stable thermochemical energy storage materials', *Journal of Porous Materials*, 30(1), pp. 163–173. Available at: https://doi.org/10.1007/s10934-022-01277-3.

Król, M. (2020) ‘Natural vs. Synthetic Zeolites’, *Crystals*, 10(7). Available at: https://doi.org/10.3390/cryst10070622.
Kukobat, R. *et al.* (2022) ‘Thermal and structural stability of microporous natural clinoptilolite zeolite’, *Microporous and Mesoporous Materials*, 341. Available at: https://doi.org/10.1016/j.micromeso.2022.112101.
Kurniawan, T. *et al.* (2022) ‘Catalytic acetalization of glycerol waste over alkali-treated natural clinoptilolite’, *Results in Chemistry*, 4. Available at: https://doi.org/10.1016/j.rechem.2022.100584.
KYOTO PROTOCOL TO THE UNITED NATIONS FRAMEWORK CONVENTION ON CLIMATE CHANGE UNITED NATIONS (1998).
Langella, A. *et al.* (2003) ‘Thermal behavior of natural and cation-exchanged clinoptilolite from Sardinia (Italy)’, *Clays and Clay Minerals*, 51(6), pp. 625–633. Available at: https://doi.org/10.1346/CCMN.2003.0510605.
Lavagna, L. *et al.* (2020) ‘Cementitious composite materials for thermal energy storage applications: a preliminary characterization and theoretical analysis’, *Scientific Reports*, 10(1). Available at: https://doi.org/10.1038/s41598-020-69502-0.
Li, Y., Li, L. and Yu, J. (2017) ‘Applications of Zeolites in Sustainable Chemistry’, *Chem*. Elsevier Inc, pp. 928–949. Available at: https://doi.org/10.1016/j.chempr.2017.10.009.
Mason, B. and Sand, L.B. (1960) ‘Clinoptilolite from Patagonia The relationship between clinoptilolite and heulandite’, *American Mineralogist: Journal of Earth and Planetary Materials*, 45(3–4), pp. 341–350.
Mastinu, A. *et al.* (2019) ‘Zeolite clinoptilolite: Therapeutic virtues of an ancient mineral’, *Molecules*. MDPI AG. Available at: https://doi.org/10.3390/molecules24081517.
McCusker, L.B. and Baerlocher, C. (2001) ‘Chapter 3 Zeolite structures’, in, pp. 37–67. Available at: https://doi.org/10.1016/S0167-2991(01)80244-5.
McCusker, L.B., Liebau, F. and Engelhardt, G. (2001) ‘Nomenclature of structural and compositional characteristics of ordered microporous and mesoporous materials with inorganic hosts(IUPAC Recommendations 2001)’, *Pure and Applied Chemistry*, 73(2), pp. 381–394. Available at: https://doi.org/10.1351/pac200173020381.
MEIER, W.M. and OLSON, D.H. (1974) ‘Zeolite Frameworks’, in, pp. 155–170. Available at: https://doi.org/10.1021/ba-1971-0101.ch014.
Mette, B. *et al.* (2014) ‘Experimental and numerical investigations on the water vapor adsorption isotherms and kinetics of binderless zeolite 13X’, *International Journal of Heat and Mass Transfer*, 71, pp. 555–561. Available at: https://doi.org/10.1016/j.ijheatmasstransfer.2013.12.061.
Mohamed, M.A. *et al.* (2017) ‘Fourier Transform Infrared (FTIR) Spectroscopy’, in *Membrane Characterization*. Elsevier Inc., pp. 3–29. Available at: https://doi.org/10.1016/B978-0-444-63776-5.00001-2.
Mumpton, F.A. (1999) *This paper was presented at National Academy of Sciences colloquium ’ ’Geology, Mineralogy, and Human Welfare*. Available at: www.pnas.org.
Nasruddin *et al.* (2020) ‘Experimental analysis of Indonesian natural zeolites-water pair for closed system adsorption thermal energy storage’, in *AIP Conference Proceedings*. American Institute of Physics Inc. Available at: https://doi.org/10.1063/5.0013934.
Nizami, A.S. *et al.* (2016) ‘The potential of Saudi Arabian natural zeolites in energy recovery technologies’, *Energy*, 108, pp. 162–171. Available at: https://doi.org/https://doi.org/10.1016/j.energy.2015.07.030.
Oktariani, E. *et al.* (2012) ‘Experimental Investigation on the Adsorption Process for Steam Generation Using a Zeolite–Water System’, *JOURNAL OF CHEMICAL ENGINEERING OF JAPAN*, 45(5), pp. 355–362. Available at: https://doi.org/10.1252/jcej.11we128.

Olegario-Sanchez, E., Felizco, J.C. and Mulimbayan, F. (2017) 'Investigation of the thermal behavior of Philippine natural zeolites', in *AIP Conference Proceedings*. American Institute of Physics Inc. Available at: https://doi.org/10.1063/1.5010514.
Ozaydin, S., Kocer, G. and Hepbasli, A. (2006) 'Natural Zeolites in Energy Applications', *Energy Sources, Part A: Recovery, Utilization, and Environmental Effects*, 28(15), pp. 1425–1431. Available at: https://doi.org/10.1080/15567240500400804.
Rehakova, M. *et al.* (2004) 'Agricultural and agrochemical uses of natural zeolite of the clinoptilolite type', *Current Opinion in Solid State and Materials Science*, 8(6), pp. 397–404.
Rodríguez-Iznaga, I., Shelyapina, M.G. and Petranovskii, V. (2022) 'Ion Exchange in Natural Clinoptilolite: Aspects Related to Its Structure and Applications', *Minerals*, 12(12). Available at: https://doi.org/10.3390/min12121628.
Roque-Malherbe, R.M.A. (no date a) *Perspectives of the use of natural zeolites in aquaculture*. Available at: https://www.researchgate.net/publication/259006041.
Roque-Malherbe, R.M.A. (no date b) *Perspectives of the use of natural zeolites in aquaculture*. Available at: https://www.researchgate.net/publication/259006041.
Ruiz-Serrano, D. *et al.* (2010) 'Study by XPS of different conditioning processes to improve the cation exchange in clinoptilolite', *Journal of Molecular Structure*, 980(1–3), pp. 149–155. Available at: https://doi.org/10.1016/j.molstruc.2010.07.007.
Saadatkhah, N. *et al.* (2020) 'Experimental methods in chemical engineering: Thermogravimetric analysis—TGA', *The Canadian Journal of Chemical Engineering*, 98(1), pp. 34–43. Available at: https://doi.org/https://doi.org/10.1002/cjce.23673.
Schick, C. (2009) 'Differential scanning calorimetry (DSC) of semicrystalline polymers', *Analytical and Bioanalytical Chemistry*, 395(6), pp. 1589–1611. Available at: https://doi.org/10.1007/s00216-009-3169-y.
Scrivener, K., Snellings, R. and Lothenbach, B. (2018) *A practical guide to microstructural analysis of cementitious materials*. Crc Press.
Sistema ibrido integrato a zeolite Specifiche tecniche zeoTHERM (2012).
De Souza, V.C. *et al.* (2018) 'Basic Treatment in Natural Clinoptilolite for Improvement of Physicochemical Properties', *Minerals*, 8(12). Available at: https://doi.org/10.3390/min8120595.
Spragg, R.A. (2016) 'IR spectrometers', in *Encyclopedia of Spectroscopy and Spectrometry*. Elsevier, pp. 419–427. Available at: https://doi.org/10.1016/B978-0-12-803224-4.00088-1.
Stagnaro, P., Luciano, G. and Utzeri, R. (no date) *La calorimetria differenziale a scansione e l'analisi termogravimetrica nella caratterizzazione termica dei materiali polimerici*.
Sun, D.-Wen. (2009) *Infrared spectroscopy for food quality analysis and control*. Academic Press/Elsevier.
Tahraoui, Z. *et al.* (2020) 'Influence of the Compensating Cation Nature on the Water Adsorption Properties of Zeolites', *Molecules*, 25(4). Available at: https://doi.org/10.3390/molecules25040944.
Titus, D., James Jebaseelan Samuel, E. and Roopan, S.M. (2018) 'Nanoparticle characterization techniques', in *Green Synthesis, Characterization and Applications of Nanoparticles*. Elsevier, pp. 303–319. Available at: https://doi.org/10.1016/B978-0-08-102579-6.00012-5.
Tran, T.V. *et al.* (2021) 'Developing a techno-economic model to evaluate the cost performance of a zeolite 13X-based space heating system', *Energy Conversion and Management*, 244, p. 114325. Available at: https://doi.org/10.1016/j.enconman.2021.114325.
Treacy, M.M.J. and Higgins, J.B. (no date) *Collection of Simulated XRD Powder Patterns for Zeolites Editors*. Available at: http://www.iza-structure.org/databases/.

Tzia, C. and Zorpas, A.A. (2012a) 'Zeolites in food processing industries', in *Handbook of Natural Zeolites*. Bentham Science Publishers Ltd., pp. 601–651. Available at: https://doi.org/10.2174/978160805261511201010601.
Tzia, C. and Zorpas, A.A. (2012b) 'Zeolites in food processing industries', in *Handbook of Natural Zeolites*. Bentham Science Publishers Ltd., pp. 601–651. Available at: https://doi.org/10.2174/978160805261511201010601.
VALUEVA, G.P. *et al.* (1988) 'Natural chabazite : heats of rehydration and X-ray study in relation to H2O contents at room temperature', in *International conference on the occurrence, properties and utilization of natural zeolites*. Budapest: Akad. kiado, pp. 283–289.
Villa, C.C. *et al.* (2022) 'Zeolites for food applications: A review', *Food Bioscience*, 46, p. 101577. Available at: https://doi.org/10.1016/j.fbio.2022.101577.
Vision Potential Deployment Roadmap Strategic Research Agenda Solar Heating and Cooling for a Sustainable Energy Future in Europe (no date). Available at: www.esttp.org.
Weitkamp, J. (2000) *Zeolites and catalysis*, *Solid State Ionics*. Available at: www.elsevier.com/locate/ssi.
Zhang, Y. and Shi, X. (2021) 'Laboratory evaluation of a sustainable additive for anti-icing asphalt', *Cold Regions Science and Technology*, 189, p. 103338. Available at: https://doi.org/https://doi.org/10.1016/j.coldregions.2021.103338.

11 Acknowledgments

Ringrazio il mio relatore Marco Piumetti per avermi dato la possibilità di lavorare su un argomento che rientra pienamente nell'ambito della sostenibilità e dell'economia circolare, temi a me cari, determinanti nella scelta di intraprendere questo corso di laurea magistrale. Ringrazio inoltre il prof. Matteo Pavese e Luca Lavagna per il supporto fornito nelle analisi calorimetriche.
A questo punto vorrei dedicare qualche riga per esprimere la mia più sincera gratitudine nei confronti di Nadia, non solo la dottoranda che mi ha affiancato durante questo percorso, ma anche una maestra di vita, pronta a motivarmi quando più ne avevo bisogno e a rimproverarmi quando volevo buttare la spugna facendomi sopraffare dall'ansia, sempre disponibile (anche in giorni ed orari improbabili), sempre paziente .E 'stato un privilegio lavorare con lei su un argomento tanto interessante quanto complesso e ricco di sfide e spero che la vita le riservi grandi e meritate soddisfazioni. Farò tesoro di tutti i suoi insegnamenti e sono sicura che questi si riveleranno fondamentali durante il mio futuro percorso lavorativo. Non posso inoltre fare a meno di ringraziare anche Marco, Andrea e tutti gli abitanti del BLUNOX che mi hanno accompagnato e supportato durante la fase sperimentale dello studio.
Questo lavoro di tesi segna la fine non solo di un percorso accademico ma anche di un percorso di vita. Dunque, vorrei spendere qualche ultima parola per ringraziare tutti coloro che ne hanno fatto parte.
Non posso non iniziare col ringraziare i miei genitori, sponde sicure nel mare agitato. Ringrazio mia madre per essere stata non soltanto un'educatrice ma anche un'amica, per aver sempre riposto la totale e cieca fiducia in me, senza alcuna esitazione. Le sono grata per avermi sempre ascoltata e compresa, anche quando per il resto del mondo ero incomprensibile. Ringrazio mio padre per l'incommensurabile stima nei miei confronti e per avermi trasmesso i valori di affidabilità e onestà che sono sempre stati il faro della sua vita. Le sono grata per avermi convinta a venire qui al Politecnico di Torino, credendo ciecamente in me, ritenendomi all'altezza di questo percorso di studi. Sono grata anche al mio fratellino Tommaso perché è il mio gigante buono, il mio "partner in crime", perché grazie a lui imparo ogni giorno a prendere la vita un po' più alla leggera, con filosofia. Nelle nostre diversità ci

completiamo. Sono grata alla mia famiglia per tutti i sacrifici fatti affinché io potessi giungere a questo giorno.
Rivolgo un sentito ringraziamento ad Anna, la mia" cheerleader", perché mi ha insegnato quali sono le che davvero contano nella vita (le famigerate palle di vetro) e che, se hai un obiettivo, nemmeno la condizione più avversa ti può ostacolare.
Dedico inoltre qualche riga di gratitudine nei confronti di Arianna e Greta, che hanno contribuito a rendere questi due anni indimenticabili e che non mi hanno mai fatta sentire sola. Mi sono state vicine sia dentro che fuori l'università, pronte a darmi una mano quando ne avevo bisogno senza esitazione, e con loro ho vissuto momenti che rimarranno indelebili nel mio cuore.
Ci tengo infine a ringraziare tutte le amiche e gli amici più stretti(Federica , Giulia, Matteo, Luigi), i miei compagni di viaggio (Raffaela, Cecilia e tanti altri), l'allegra brigata della Borsellino tutti i miei compagni di corso e di Politecnico (tra cui Martina, Moira, Angela, Mario, Giacomo, Mathis, Elena, Eugenia e Paolo)perché da sola non ce l'avrei mai fatta. Non è assolutamente scontato trovare delle persone con cui studiare e passare al meglio i vari semestri senza impazzire, tra un lavoro di gruppo e un aperitivo, tra un pranzo della domenica e un esame.
Concludo ringraziando mamma Torino che in questi anni mi ha coccolata con i suoi tramonti, con le sue piazze, con il suo foliage in autunno e col suo cioccolato e grazie alla quale ho trovato la mia dimensione e la mia seconda casa. Grazie.